Melodies in space: Neural processing of musical features

A DISSERTATION

SUBMITTED TO THE FACULTY OF THE GRADUATE SCHOOL

OF THE UNIVERSITY OF MINNESOTA

BY

Roger Edward Dumas

IN PARTIAL FULFILLMENT OF THE REQUIREMENTS

FOR THE DEGREE OF

DOCTOR OF PHILOSOPHY

Dr. Apostolos P. Georgopoulos, Adviser

Dr. Scott D. Lipscomb, Co-adviser

March 2013

Table of Contents

List of Tables

List of Figures

List of Equations

Abbreviations

ACPV	auto-correlation processing vector
BA	Brodmann area
BCE	Before the Common Era
BOLD	blood-oxygen level dependency signal
ERAN	early right anterior negativity
D^{MEG}	successive absolute differences in the MEG signal
$D^{1, 2, 3, 4, 5, 6}$	distance vectors in six tonal spaces
E*d*,	Euclidean distance
EEG	electroencephalograph, -y
fMRI	functional magnetic resonance imaging
LH	harmonic space (Longuet-Higgins, 1979)
HZ	Hertz, -log frequency tonal space
KK	probe tone profile tonal space (Krumhansl et al., 1982)
MEG	magnetoencephalograph, -y
MIDI	musical instrument digital interface
MIP	musical interval perplexity
MMN	mismatch negativity
ms	milliseconds
P4h	perfect 4th helix tonal space (Dumas, 2011)
P88	chroma salience profile (Parncutt, 2011)
PI	perplexity index
PPV	pitch-processing vector
SAM	spiral array model (Chew, 2000)
SMA	supplementary motor area in the brain
SOM	self-organizing map
SQUID	super-conducting quantum interference device

Chapter 1. Introduction

Melody & neuro-imaging

With modern digital technology, it is now possible to capture, store, and describe brain data in relation to musical stimuli with some degree of confidence. Increasing financial and material resources are being made available to music-brain researchers and, as a result, the number of music perception and cognition publications is expanding exponentially (Levitin & Tirovolas, 2011). Two paradigmatic threads run through the majority of brain-music studies. First, published brain-imaging studies involving musical stimuli overwhelmingly emphasize brain regions-of-interest (ROI). Studies have shown, for example, that the brain response is strong for pitch in the right hemisphere and for rhythm in the left (Kanno et al., 1996; Limb, Kemeny, Ortigoza, Rouhani, & Braun, 2006; Ono et al., 2011). Second, many investigators favor psycho-acoustical phenomena over higher-level processing. Their attentions rest primarily on the brain's response to isolated events such as unexpected chord progression completions (S.-G. Kim, Kim, & Chung, 2011), out-of-key endnotes (Hashimoto, Hirata, & Kuriki, 2000), fundamental and spectral pitch preference, (Schneider et al., 2005), Huggins pitch (Chait, Poeppel, & Simon, 2006) and melody errors (Yasui, Kaga, & Sakai, 2009).

Among neuro-musicological publications, studies of the brain's response to melodic phrases are comparatively rare. One explanation for the scarcity of such publications is that the predominant brain-scanning method is functional magnetic resonance imaging (fMRI). Users of fMRI have uncovered information about task-related flow of oxygenated blood (blood-oxygen level dependency, or BOLD signal) to specific brain areas. A strong BOLD signal in a brain region-of-interest indicates increased oxygen usage and concomitant neural activity. As it is an *indirect* measure of brain activity, i.e. the measure of a signal indirectly related to synaptic events, fMRI is subsequently challenged by the "…significant temporal and spatial differences between electro-physiological responses and the complex cascade of the hemodynamic responses" (Pouratian, et al. 2003). When compared to the speed of synaptic events (~1k Hz), the development of the blood-oxygen signal captured by fMRI is slow (2 to 5 seconds). As a consequence, fMRI experiments relating brain activity to changes in melodic parameters focus on signals that are acquired at a latency of several seconds, i.e. well after the subject has been exposed to the stimulus. These studies have involved the contrasting of melodies with fixed-pitch sound (Patterson, Uppenkamp, Johnsrude, & Griffiths, 2002), melodic contour discrimination (Lee, Janata, Frost, Hanke, & Granger, 2011), identification of scrambled music (Matsui, Tanaka, Kazai, Tsuzaki, & Katayose, 2013), temporal reversal of a melody (Zatorre, Halpern, & Bouffard, 2009), recognizing heard and imagined melodies (Herholz, Halpern, & Zatorre, 2012) and free improvisation (De Manzano & Ullén, 2012).

In contrast, neuroscientists have used the high temporal resolution of MEG (ms) to relate brain response to specific musical events, e.g. consonant vs. dissonant melodic tones (Kuriki, Isahai, & Ohtsuka, 2005), lyrics and melody deviants (Yasui et al., 2009), omission of one tone out of a musical scale (Nemoto, 2012), melodic contour deviation perception (Fujioka, Trainor, Ross, Kakigi, & Pantev, 2004), different pitch extraction from same tone complexes (Patel & Balaban, 2001) and probability of chord progression (S.-G. Kim et al., 2011).

The MEG signal

MEG features high temporal resolution (~1 ms), reasonable spatial precision (~5mm) and high fidelity, i.e. the clean, direct measurement of undistorted electro-magnetic fluctuations in neural populations (Lounasmaa, Hamalainen, Hari, & Salmelin, 1996). It is the ideal technology for matching synchronous neural interactions (Georgopoulos AP et al, 2007) to the processing of melodies played at normal tempos. It takes approximately 100,000 synaptic events to produce a sufficiently large signal (~50 to 1000 femtoTeslas, or 10^{-15} T) for detection by an MEG sensor, *aka* super-conducting quantum interference device (SQUID). (By comparison, the earth's magnetic field registers at 5×10^{10} fT, or roughly 1 billion times stronger.) Each one of the 248 SQUIDS (Figure 1-1) in the whole-head Magnes 3600WH system (4-D Neuroimaging, San Diego, CA) used in these experiments captures the biomagnetic signal of these dense clusters of tightly-interconnected pyramidal cells in the cerebral cortex to a depth of approximately 4 mm and at a rate of 1017.25 samples-per-second.

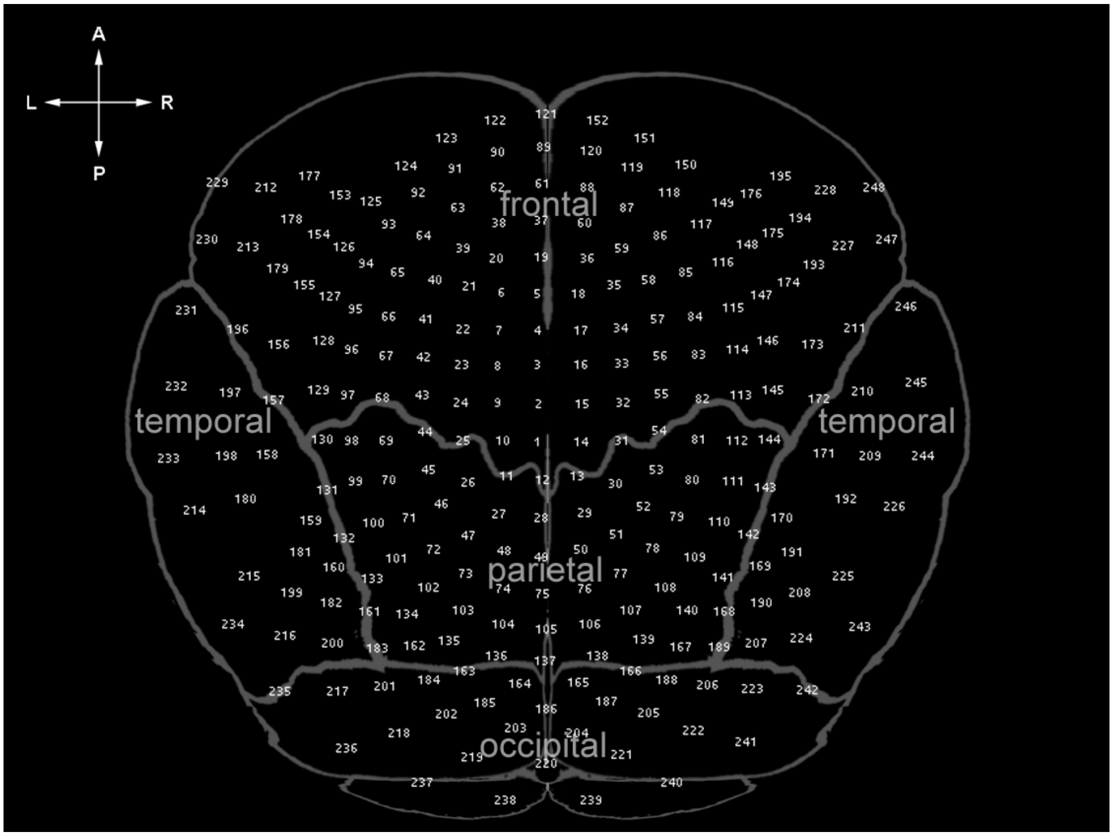

Figure 1-1. MEG sensor plot, flat-brain layout. Arrows indicate anterior (A), posterior (P), left (L) and right (R).

Biomagnetic signals originating in the brain follow the “right-hand rule” mnemonic that determines direction for current flow, magnetic field and magnetic force (Figure 1-2a). In this analogy, the thumb points in the direction of the electric current flow, the fingers curled around the wire represent the curved direction of the generated magnetic field, and the index finger points in the direction of the magnetic force, i.e. the signal-of-interest in MEG studies. Figure 1-2b illustrates the application of the right-hand rule to the biomagnetic activity in and around a cortical fold. If the source of the synchronous neural activity lies along a gyrus, the cancellation of parallel volume and source currents along the cortical surface renders the signal nearly invisible to the

SQUID. If the intra-cellular currents are generated within the two-thirds of the total cortical surface that is found within the sulci, the signal has a force component that is tangential to the surface. As a consequence, cancellation is avoided and the sulcal signal is more easily detected (Lounasmaa et al., 1996). It is this tangential signal arising from aligned pyramidal neuronal populations in the fissural cortex that figures prominently in MEG-based research (Hari, 1990).

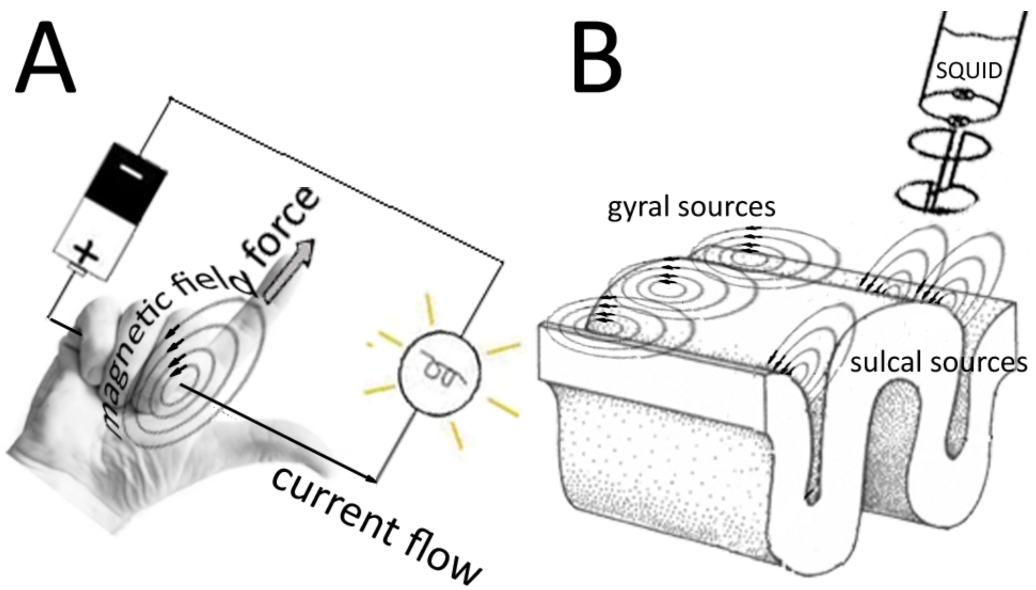

Figure 1-2. Right-hand rule and brain biomagnetics. a) The "right-hand rule" mnemonic illustrates the relative direction of current flow (thumb), magnetic force (index finger) and magnetic field (curled fingers) in an electric conductor. b) Biomagnetics of a cortical fold. The signal from the radial projection of a gyral source (i.e. a source parallel to the cortical surface) is prone to cancellation from its neighbors. The tangential projection of magnetic force from a sulcus is more readily detected by the SQUID.

The experiments described in this dissertation are novel, in that magnetoencephalography (MEG) was used to examine the whole brain in identifying significant relations between dynamic, interacting neural networks and systematically varied musical features of entire melodies. The following chapter serves as an introduction to theories of music cognition related to the melodic features of my stimuli.

Background

Neurophysiological studies of brain lesions and related behavioral deficits have shown that the human brain is a complex functional network comprising specialized neural populations. Although pitch perception has been studied extensively by musicologists, philosophers, psychologists, audiologists, and, lately, neuroscientists (Levitin & Tirovolas, 2011; Purwins & Hardoon, 2009), little is written about cortical sub-networks involved in the processing of melodies. Our approach to this problem is novel, in that we employ magnetoencephalography (MEG) to study four melodic features: pitch, contour, interval and perplexity.

Melodic pitch

Our study of neural processing of pitch is novel in that it examines the brain's response to melodies in their entirety. Researchers mainly focus on brain response to stimuli other than entire melodic passages, e.g. mismatched negativities elicited by final, oddball notes or chords (e.g. Maess et al., 2001; Herholz et al., 2009; Kim et al., 2011). Such explanations fall short of describing the complex neural interactions involved in melody processing. In our study entitled "Experiment A: Neural processing of pitch", we used MEG to discover synchronous neural networks involved in processing melodic stimuli.

Melodic contour

Melodic motion can be *conjunct*, i.e. formed from successive note intervals between consecutive scale degrees, or *disjunct*, i.e. formed from "skips" or "leaps" of intervals of a minor third or larger. Figure 1-3 shows examples of conjunct and disjunct motion in Deutsch's "chromatic illusion" (1987). In this study, melodic stimuli presented to each of the subject's ears were disjunct, but the reported perceptions were often of conjunct motion.

Figure 1-3. Examples of disjunct motion (above) and conjunct motion (below) (Deutsch, 1987).

Brain-imaging studies have produced solid evidence of melodic contour processing (Fujioka et al., 2004; Granier-Deferre, Bassereau, Ribeiro, Jacquet, & DeCasper, 2011; Lee et al., 2011). Core areas for generating melodic phrases were discovered in left Brodmann area (BA) 45, right BA 44, bilateral temporal planum polare, lateral BA 6, and pre-supplementary motor area (SMA) (Brown, Martinez, & Parsons, 2006). To test the idea that our brains can discriminate between conjunct and disjunct melodies, we played pseudo-random melodies to human subjects. The melodies had identical pitch sets/ranges, timbres, loudness and rhythms, but differed in *auto-correlation* (AC), i.e. the cross-correlation of the signal (pitch structure) with itself. Figure 1-4 demonstrates the effect of increasing the level of AC from 0.0 to 0.9 in melodies. The melody with an AC of 0.0 is the least auto-correlated (or most disjunct) in the series. As AC increases to 0.1, large intervals (leaps) become less frequent, until the point at AC 0.9, where the motion is most conjunct.

Figure 1-4. Notated sample stimuli with serial auto-correlations increasing from pseudo-random (AC 0.0) to highly auto-correlated (AC 0.9).

Melodic perplexity

Humans have evolved to anticipate future events, an ability that gives us a distinct advantage in our environment. Although the psychological and physiological consequences are not vital, musical expectations are critical to the aesthetic experience (Narmour, 1990). The generation, confirmation, even the violation of our expectations are essential to understanding the communication of emotion and meaning in music. When we listen to a tune, we expect melodies to follow certain rules, and we identify note groupings, or *phrases*, by identifying local discontinuities in temporal proximity, pitch, duration and dynamics. For example, we expect that a melody in a major key is composed from a set of seven pitch-classes (i.e. *do-re-mi-fa-sol-la-ti/si*)[1].

According to Meyer (1956), violations of our expectations occur in three forms: a) an event expected within a given context is delayed; b) the context fails to generate strong expectations for any particular continuation; and c) the continuation is unexpected or surprising. Neuroscientists working with MEG have discovered an event-related *mismatch negativity* (MMN) that occurs in the brain when a wholly-unexpected note or chord is heard at the end of a sequence (Koelsch, et al. 2001; Leino et al., 2007; Maess et al., 2001; Maess, et al., 2007). Drawing from a Western music corpus, MEG researchers recently reported negative correlations between probabilities for inappropriate chord progressions and elicited brain responses (Kim, Kim, & Chung, 2011). Researchers have also found evidence that expectations in melodic pitch structure can be accurately

[1] These are the syllables in the *Tonic sol-fa* pedagogical technique invented by Sarah Ann Glover (1785-1867). The system is based on *movable do solfège*, whereby every tone is given a name according to its relationship with other tones in the key. Glover changed the seventh syllable *si* to *ti* so that no two syllables would begin with the same letter. *Si* is still used in languages other than English.

modeled as “a process of prediction based on the statistical induction of regularities in various dimensions of the melodic surface” (Pearce & Wiggins, 2006). Their results point to two characteristic brain responses: the early (right) anterior negativity (ERAN) with a latency of 150–280 ms, and a later bilateral or right-lateralized negativity with a latency of 500 ms (Koelsch et al., 2001). The former is considered as a response to the violation of harmonic expectation, while the latter reflects higher processing for integrating unexpected harmonies into the ongoing context (Steinbeis, Koelsch, & Sloboda, 2006).

If one could quantify the level of predictability for melodic intervals, then a *perplexity index* might be created for the purpose of determining note-by-note *expectancy*. To that end, and with incalculable assistance from my colleagues, I have converted each of 10,000 melodies from *A Dictionary of Musical Themes* (Barlow & Morgenstern, 1948)) to Musical Instrument Digital Interface (MIDI) note number format and generated the melodic interval perplexity (MIP) index, i.e. the probability of occurrence throughout the corpus for each unique note-pair. Armed with the MIP index table, I was able to correlate the constantly changing perplexity levels of the stimulus with averaged note-for-note MEG data, linking MIP with the dynamic brain signal underlying the inferred probability of notes following each other throughout a monophonic musical stimulus.

Models of music cognition

Stable and unstable tones

Composers of Western classical music follow conventions for the horizontal (temporal) and vertical (tonal) placement of notes (Jackendoff & Lerdahl, 1983). These conventions lead to music-listener expectations (Larson & McAdams, 2004; Narmour, 1990). Upon hearing a familiar tune, a listener expects the melody to follow a path guided by previous experience and, if the listener is musically-trained, by conventions set down in the genre's canon, e.g. melodies in the Western classical tradition generally comprise a set of 7 pitch-classes (a key) and are written in a either a major or minor mode. The subjective experience of melody has been described as periods of "implication" and "realization" (Narmour, 1990), and "stability conditions" (Lerdahl, 1988, p. 316). Krumhansl explains tonal stability as a "hierarchy" of "structural significance" imposed upon a set of tones by "…a context defining a major or minor key" (1990). Russell's "chord-scale" theory defines a stable tone as a member of a chord-scale, i.e. a set of pitches that best project the sound of a chord. Conversely, an unstable tone is one that is not high in the tonal hierarchy. Unstable tones generate melodic tension (Narmour, 1990) that can ultimately be resolved (relaxed) through melodic movement to a stable tone. In Figure 1-5, the uncircled notes (C, E, G, and B) in the opening measure of "The Christmas Song" (Figure 1-5) are members of a chord-scale (C-major-seventh). As such, they are more stable, (i.e. higher in the tonal hierarchy) than the non-member (unstable) fourth and sixth notes (A and F, circled).

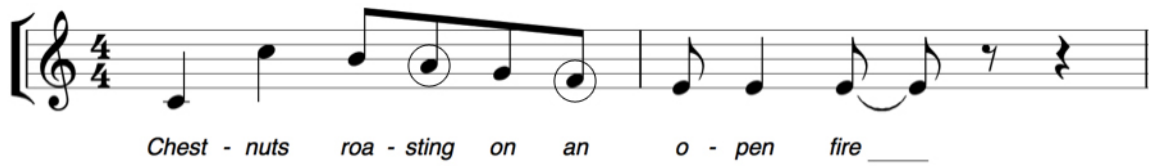

Figure 1-5. “The Christmas Song” (Torme & Wells, 1946). The notes A and F are not members of the chord-scale described by the other notes in this measure (Cmaj7) and are unstable according to Russell’s chord-scale theory (as cited in Larson & McAdams, 2004).

The melodic experience is, therefore, one of transitions between periods of tension and relaxation that coincide with the melody’s progression from one stable tone to the next. Transitions can be swift, as in the opening to J. S. Bach’s “Brandenburg Concerto No. 3” (Figure 1-12a), where stable tones (circled) are frequent. Transitions can be prolonged, as in the opening theme to Claude Debussy’s “Syrinx” (Figure 1-12b). Longer transitions prolong melodic tension by requiring the listener to integrate more information between points of stability.

Figure 1-6. Bridging gaps between points of melodic stability (circled notes). a) The opening phrase of J.S. Bach’s “Brandenburg Concerto No. 3” (1713) presents small gaps between stable tones. b) The opening phrase of Claude Debussy’s “Syrinx” (1913) presents a large gap between stable tones.

Gravity, magnetism & inertia

Evidence of music's origins can be found in the rhythms of human movement (Changizi, 2011) and the emotional vocalizations of primates (Hauser, 2000). The intonations of *motherese* – the soothing voice a mother uses when speaking to her baby – has also been suggested as a possible progenitor for music (Parncutt, 2009). These natural phenomena find corollaries in Larson's *physical force* analogies to *gravity, magnetism* and *inertia* (2002) as depicted in Figure 1-7. In this theory, melodic patterns repeating without much deviation (rectangles) exhibit inertia, unstable tones (circled) are magnetically drawn to neighboring stable tones, and melodies resolve (gravitate) to the tonic (arrow).

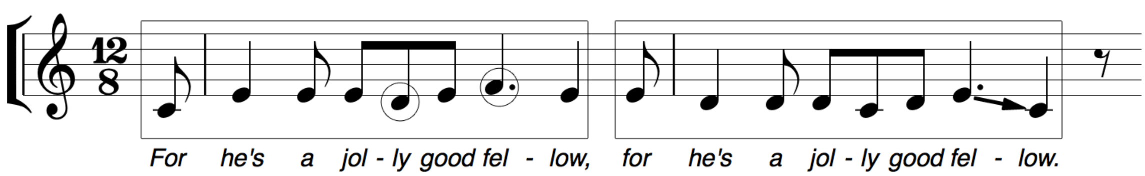

Figure 1-7. "For He's A Jolly Good Fellow" (French folk tune, 1709) demonstrating Larson's three physical force analogies for melodic motion (2002), namely *inertia* (rectangles), *magnetism* (circles), and *gravity* (arrow).

We can reframe Larson's three musical forces as probabilities: *gravity* (the probability that a note heard as up-in-the-air will descend), *magnetism* (the probability that an unstable note will move to the nearest stable one), and *inertia* (the probability that a pattern of musical motion will continue in the same fashion). Larson's theory suggests that, even though melodies do not actually *move* through space, music listeners infer a metaphorical, physical action. The act of *hearing as* enables the listener to attach meaning in a way that mirrors the witnessing of a purposeful act in the physical universe.

Tonal space

Although tonal spaces are often the models of choice for the investigation of broader musical cognition phenomena such as tonal-deviance tracking, key-finding, and expectation, my goal was to discover possible relations between neurological signals and measures of note-to-note distance as calculated in six different spaces. Drawing inspiration from these models, I designed an MEG experiment to test the idea that the human brain tracks melodies in a manner analogous to movement within and across a multi-dimensional tonality surface.

From a Eurocentric point-of-view, the internal organization and categorization of pitches that allow us to share in an appreciation of the concepts of consonance, dissonance, key, melody and harmony are grounded in exposure to music formed from the Western 12-tone scale. The melody is the "figure", the harmony the "ground", and it suits music cognition researchers to place the whole within "pitch space" (Brower, 2008; Chew, 2003; Ellis et al., 2012; Larson & McAdams, 2004; Lerdahl, 2001; Minor, 1978; Parncutt, 2011; Teki et al., 2012). Music theoreticians throughout the ages have proposed dimensional models of the hierarchical structure of music. The following a brief history of the development of tonal space, beginning with the physical properties of pitched tones as set down by Pythagoras and ending with a description of the perfect 4th helix, a novel tonal space.

The Circle of Fifths

Upon hearing a simultaneous presentation of two or more pitches (a chord), we quickly form an opinion as to whether the notes are mutually consonant or dissonant. Pitches presented sequentially are also judged on their relative *melodic* merits, or how well they fit together to build a musical phrase. The twin concepts of *interval* and *scale* can be traced to the school of Pythagoras around 500 BCE (Gibson & Johnston, 2002). Pythagoras built a 12-tone (chromatic) scale around frequency ratios of 2:1 (the octave) and 3:2 (the perfect 5^{th})[2], reducing each number by half (octaves) until it was less than an octave above the fundamental. The resulting scale-tone ratios can be seen in Figure 1-8. The circle of fifths moves clockwise from C. The shaded notes outline the 7-note diatonic C major scale, and are represented by the white keys of a piano. The un-shaded notes complete the 12-tone scale and denote the black keys. The numbers indicate the ratio of the frequency of each note with that of the fundamental (Gibson & Johnston, 2002).

[2] The term *perfect fifth* refers to the fifth note (e.g. "G") from the tonic ("C") in an ascending diatonic scale. It exhibits "perfect consonance", as opposed to the medieval "imperfect consonance" of the interval of a third or a sixth. With the modern exception of the perfect fourth, all other intervals within a octave from the tonic are considered to be dissonant. (Rushton, 2004)

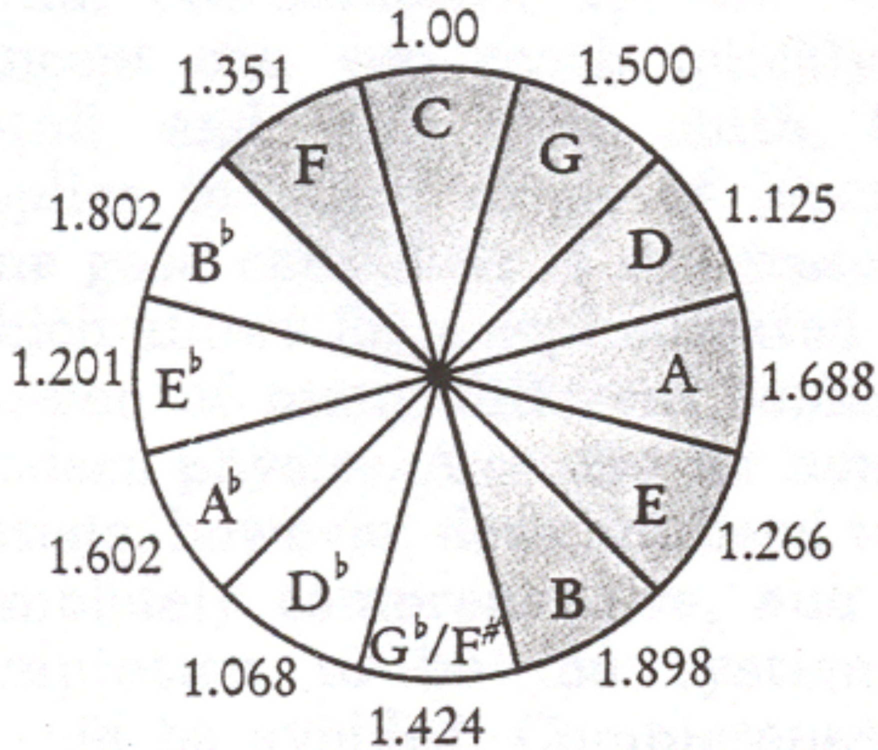

Figure 1-8. Pythagoras' chromatic scale (Gibson & Johnston, 2002). Adapted with permission from Gibson, G. N., & Johnston, I. D. (2002). New Themes and Audiences for the Physics of Music. Physics Today, 55(1), 42

The diatonic scale

The Greek philosopher Pythagoras devised a system of tuning based solely upon the interval of a 5^{th}. His system can be replicated by successively multiplying pitch proportions by 3/2 to achieve ascending fifths and by 2/3 to reach descending fifths, as in the following example. The method yields the pitch classes C, D, E, F, G, A, B arranged in D Dorian mode (Figure 1-9).

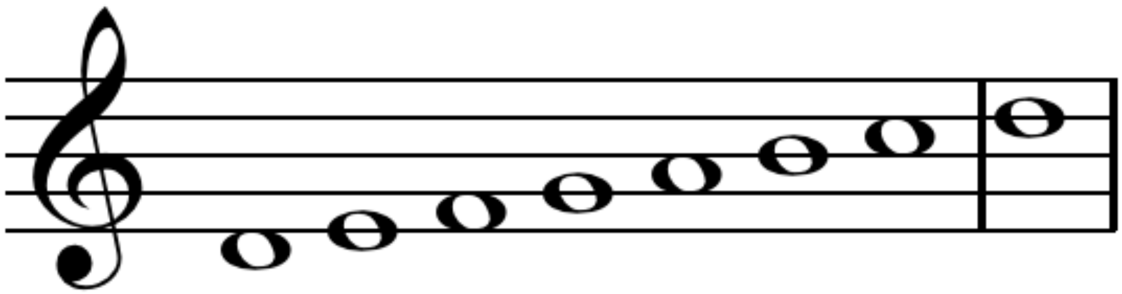

Figure 1-9. Pitches of the D Dorian mode: D, E, F, G, A, B, C, D'

1. Tune two strings to an octave: D D'
2. To add A and G, tune 2 new strings to the 5th above D and the 5th below D'.

   D A G D'
3. To add C and E, tune 2 new strings to the 5th above A and the 5th below G:

   D C A G E D'
4. To add B and F, tune 2 new strings to the 5th above E and the 5th below C, then collapse (retune) the pitch range to within 1 octave. (Unspaced letters denote semitone steps.): D BC A G EF D'

Repeating the tuning 5 more times (tuning to fifths above B and below F) will produce the chromatic pitch classes (F#, C#, G#, D#, A#), completing the Western 12-tone chromatic scale.

Diletski's circle of fifths' (1679)

The 17th-century composer Nicolay Diletski's composition treatise, *Grammatika musikiyskago peniya* (A Grammar of Musical Singing), introduced the first-known description of the "Circle of Fifths" (Figure 1-10), preceding Western examples by decades (Jensen, 1992). With the exception of the interval between pitches 12 and 1, Diletsky's bass clef notation in Figure 1-10 displays the evenly spaced perfect fifth intervals of *equal temperament*. All modern fixed-pitch instruments (e.g. electronic keyboards) are tuned to equal temperament, and it is this tuning system that forms the basis for the tonal spaces described in this dissertation.

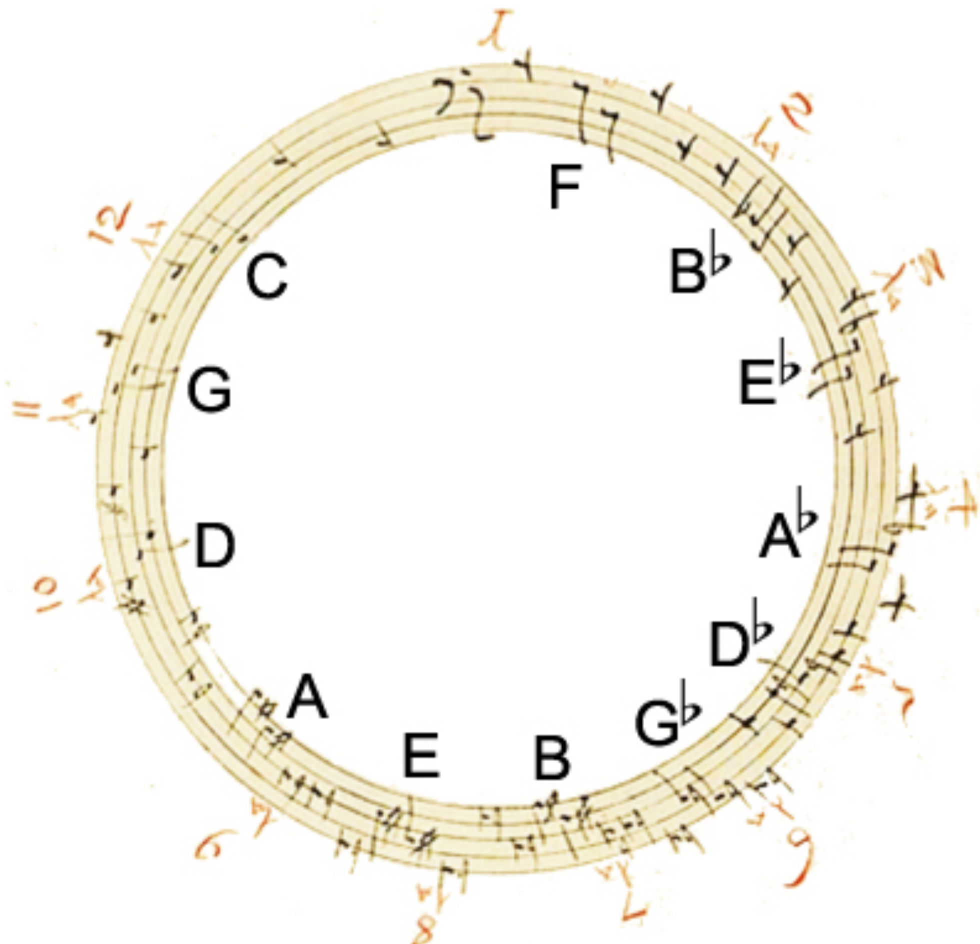

Figure 1-10. Diletski's musical notation of the Circle of Fifths. Pitch names added by the author (Jensen, 1992).

Euler's tonnetz (1739)

The Swiss mathematician Leonhard Euler discovered the *tonnetz*, a geometrical array of the 12 keys based upon both the circle of fifths and major 3rd relationships (Figure 1-11)[3]. Euler designed his tonal surface with axes of fifths and thirds. The tonnetz places harmonically related keys in close proximity, e.g. C, G, F and E. The keys most distantly related, F# and B, form the relatively dissonant tritone interval.

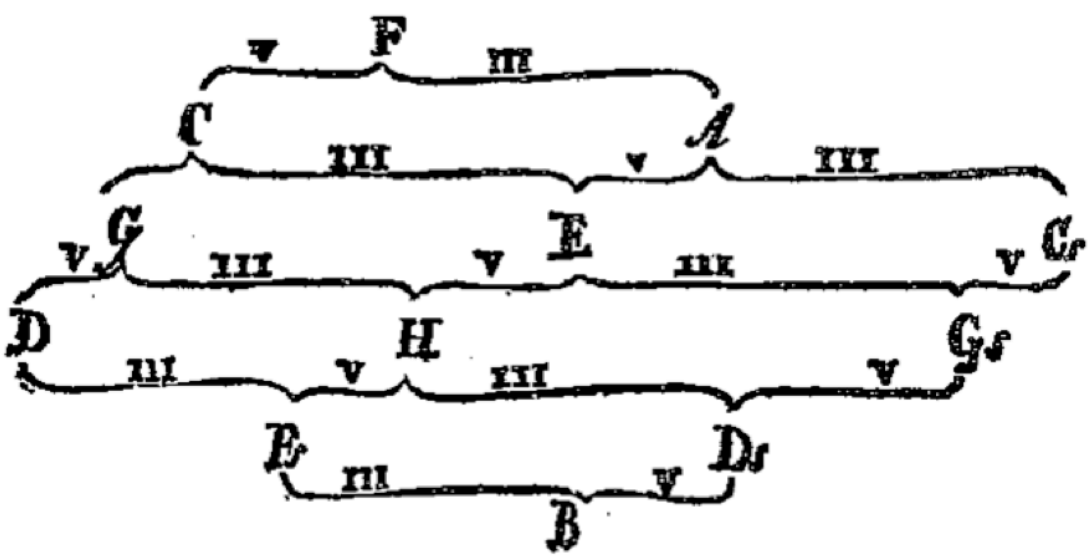

Figure 1-11. Euler's tonnetz was based on orthogonal axes of fifths and thirds (1739). Retrieved from http://en.wikipedia.org/wiki/File:Eulers_tonnetz.png

Riemann's tonnetz (1880)

Hugo Riemann transformed Euler's tonal lattice into a pitch space model for Just Intonation (Figure 1-12), with horizontal alignment of perfect fifths criss-crossed with diagonals of major and minor thirds (Hyer, 1995). The outlined area in the center

---

[3] Pitch class names follow the convention of the day: H = B, Es = $E^{\#}$(F), Cs = $C^{\#}$, etc.

encompasses the base pitches for the key of C major (D-D’, as described in Pythagoras’ tuning process above). Riemann allowed for enharmonic equivalents by expanding sharper tunings octaves above (*Oberterzen:* $\underline{cis}$, $\underline{\underline{cis}}$, $\underline{\underline{\underline{cisis}}}$) and flatter tunings octaves below (*Unterterzen*: $\bar{c}$, $\overline{\overline{ces}}$, $\overline{\overline{\overline{ceses}}}$). With these innovations, the triangular configuration of major and minor triads began to take shape.

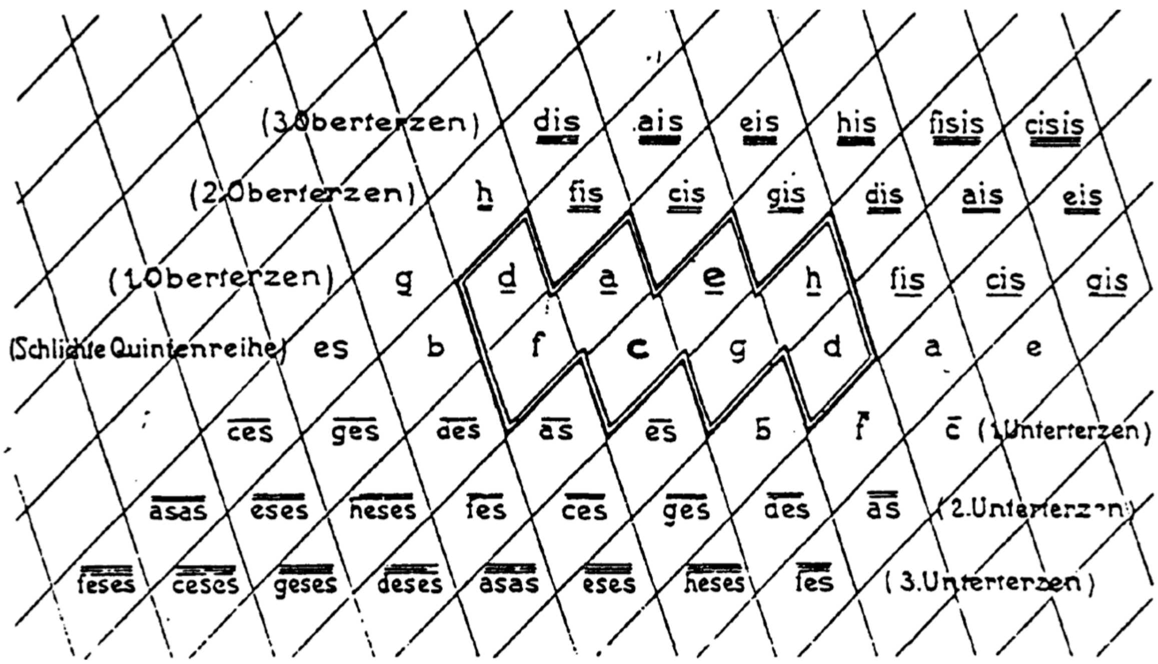

Figure 1-12. Riemann’s Just Intonation tonnetz (Hyer, 1995). Adapted with permission from Hyer, B. (1995). Reimag(in)ing Riemann. Journal of Music Theory, 39(1), pp. 101–138.

Traditional tonnetz

The relations between keys in the tonnetz were further formalized in the 19th century with the adoption of uniform distances between perfect fifths, major and minor thirds (Gollin, 2011).

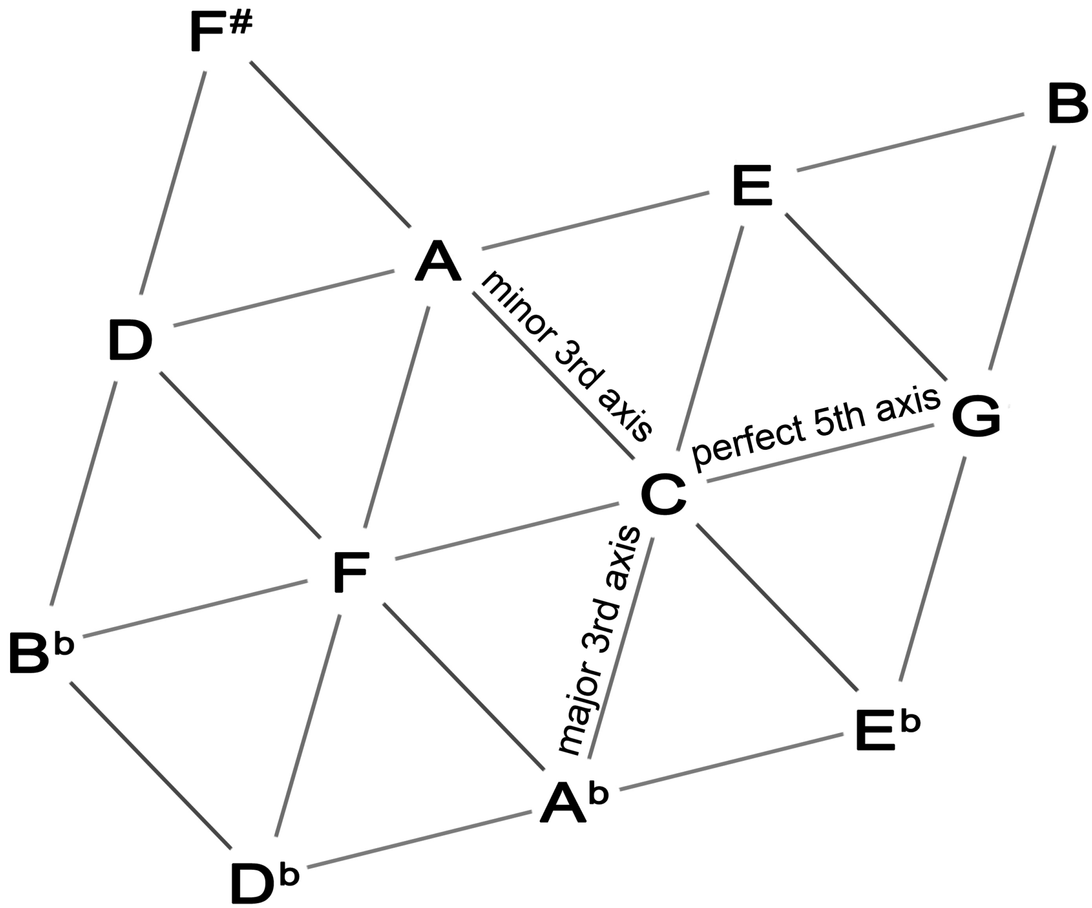

Figure 1-13. Traditional tonnetz for the extended key of C major (as cited in Gollin, 2011). The 12 pitch classes of the chromatic scale are arranged along 3 axes of perfect 5ths, major 3rds, and minor 3rds.

Longuet-Higgins Harmonic space (1962)

> "Longuet-Higgins recognized that musical intervals are in effect vectors in a three-dimensional space of discrete cells, and the remoteness of an interval from one note to another is the magnitude of this vector." (Johnson-Laird, et al. 2012)

Models of relative consonance and dissonance moved into three dimensions in the tonality theories of H. C. Longuet-Higgins. Diverging from the frequency ratios of Helmholtz, Longuet-Higgins chose to create a geometric solution to the problem of conceptualizing the perceived distance between two notes (1962). He showed that the intervals of Western classical music can be created from just three intervals – the octave, 5th and major 3rd (1962). For example, an octave (12 steps) minus a 5th (7 steps) produces a 4th (5 steps), a 4th plus a major 3rd (4 steps) makes a major 6th (9 steps), and so on. He created a two-dimensional *harmonic space* by stacking identical progressions, but shifting them so that the interval between vertical neighbors is a major 3rd, or 4 semitones (Figure 1-14a). Longuet-Higgins completes the spatial analogy through the addition of a vertical axis to represent octave shifts. His 3-dimensional *lattice* (Figure 1-14b) displays perpendicular axes for the octave (top-bottom), perfect 5th (left-right) and major 3rd (front-back).

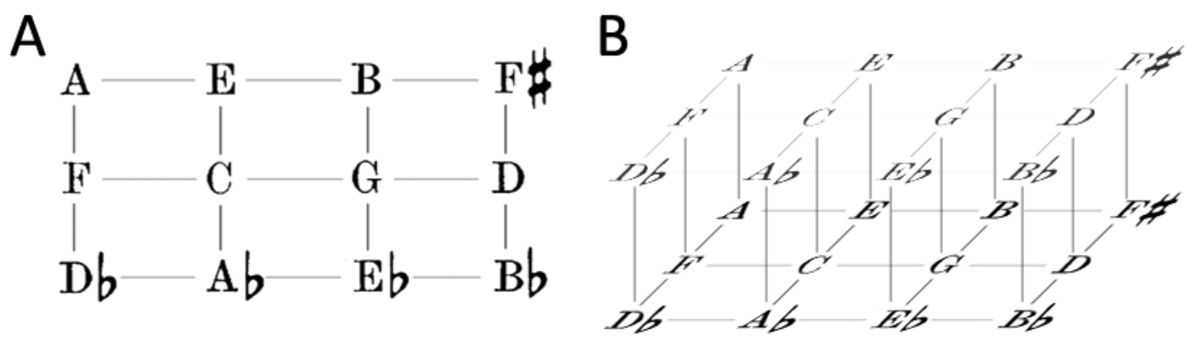

Figure 1-14. Longuet-Higgins' model of consonance/dissonance in two and three dimensions. a) 2-dimensional "harmonic space" encompassing the "extended" keys of C major and C minor, plus F♯ and D♭. c. The 3-dimensional lattice features the addition of an octave dimension along a vertical axis (Longuet-Higgins, 1962a).

Lubin's toroidal tonal space

According to Cohn (1998), Lubin (1974) was the first to recognize a toroidal tonal surface. His *modulatory space* (Figure 1-15) describes routes a composer might take to modulate between keys. Lubin's torus was based on a equal temperament rectangular grid and is a useful graphic for understanding 18th-century European music, suggesting that composers of that era shared a common, evolving harmonic space through which their various, connected musical routes could be traced.

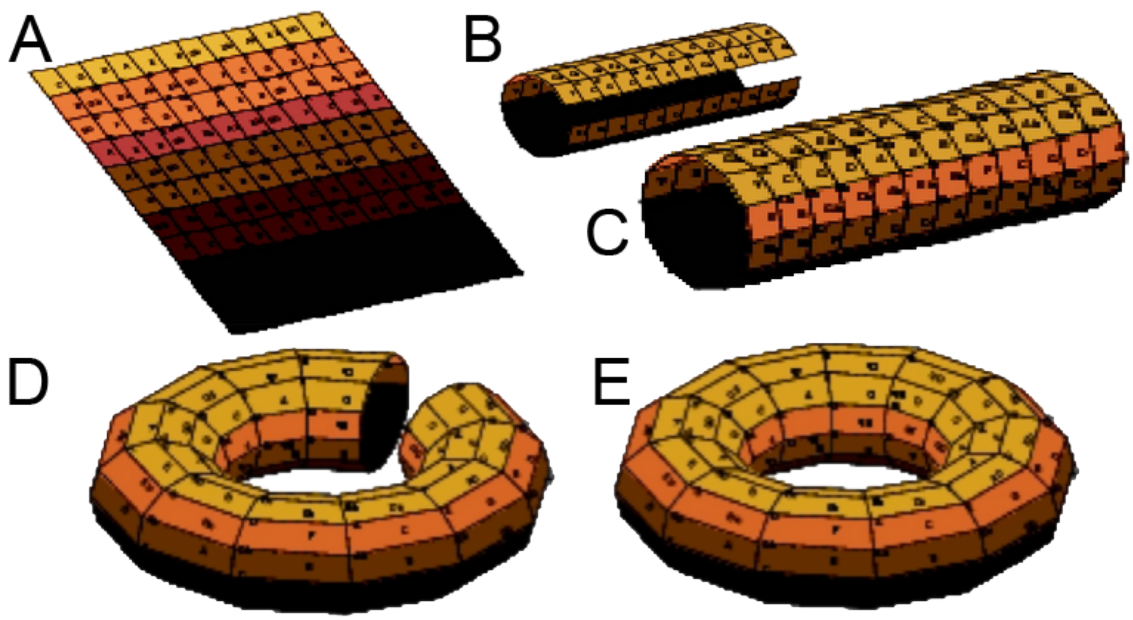

Figure 1-15. Steps in the transformation of the traditional tonnetz into a two-dimensional closed surface (Lubin, 1974). Adapted pending permission from Lubin, S. (1974). Techniques for the Analysis of Development in Middle-Period Beethoven. New York University. Retrieved from http://tonnetz.zxq.net/surfaceForm.html.

The probe tone profile, key-finding torus and self-organizing map

Two recent studies of internal representations of musical space have yielded complementary results. Workers at Cornell have established a neural network model of tonality which they call a "self-organizing map" (SOM), an artificial neural network that simulates the formulation of ordered feature maps (Toiviainen & Krumhansl, 2003), while researchers at the Dartmouth Brain Imaging Center have identified "tonality-specific responses" in the cerebral cortex that correlate closely with the Cornell SOM (Janata et al., 2002).

One part of the Cornell study focused on the "psychological reality of theoretical descriptions of music" (Zatorre & Krumhansl, 2002). Toiviainen and Krumhansl reasoned that, even without formal music training, the understanding of tonal, harmonic, and melodic patterns identified in music theory influences a listener's organization and memory of music. In their experiment, they used the *probe tone* method in which subjects listened to a MIDI file, J. S. Bach's *Duetto* for organ (BWV 805), during which a probe tone of the chromatic scale was heard to play continuously. Subject judgments of probe tone "degree of fit" and "tension" were measured, and the results correlated with those of concurrent probe-tone data and distance away from the predominant key, respectively. A projection of the judgment measures onto a toroidal SOM (Figure 1-16) trained with Krumhansl and Kessler's 24 probe-tone profiles (1982) revealed a close match with the researchers' models of pitch class distribution and tone-transition distribution.

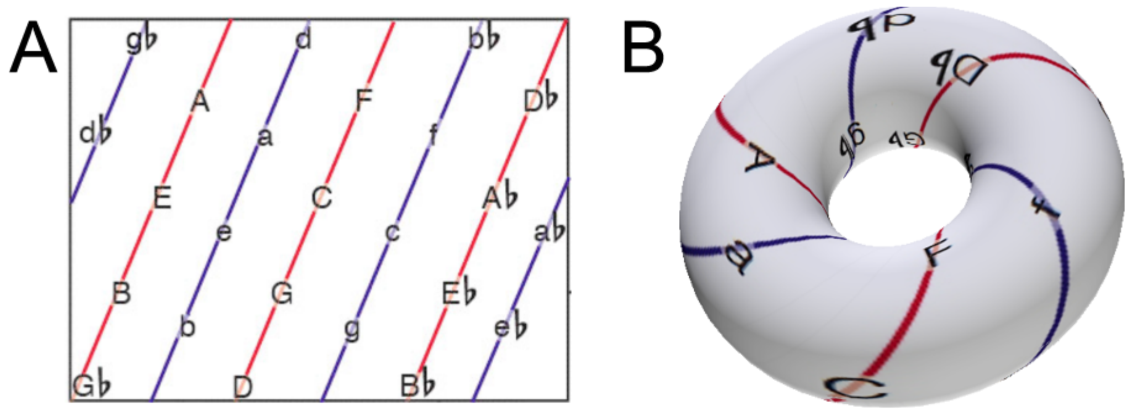

Figure 1-16. Krumhansl and Kessler's self-organizing map (SOM) depicts "inter-key distance" results from behavioral experiments in which subjects were asked to judge degree-of-fit for probe tones heard at the end of major and minor scales (1982). a) Unfolded SOM (Toiviainen & Krumhansl, 2003). Lines indicate circle of fifths for major keys (red) and minor keys (blue). b) Top/bottom and left/right edges of the SOM are joined to form a torus. Adapted with permission from Toiviainen, P., & Krumhansl, C. L. (2003). Measuring and modeling real-time responses to music: the dynamics of tonality induction. Perception, 32(6), 741–766.

Janata employed Krumhansl's probe tone profiles in an analysis of fMRI data to identify a brain region (rostromedial prefrontal cortex) involved in tracking the keys of abstract patterns of Western tonal music stimuli (Janata et al., 2002). In this study, eight "musically experienced" subjects were asked to listen to a repeated melody and perform "go/no-go" tasks during fMRI scanning sessions. During each of three weekly sessions, the melody was played to each subject 24 times as it modulated through all 12 major and minor keys. Workers used a regression analysis on the results of the fMRI scans to distinguish task effects from tonality surface tracking and were able to construct average "tonality surfaces" for each of the 24 keys (Figure 1-17). A 24 x 24 correlation matrix was generated to display the similarity of tonal hierarchy of each key to every other key. In other words, the more stable (high vector) notes that two keys shared, the more closely correlated they were (Figure 1-17a). When the key correlation map is wrapped into a 3-dimensional solution (Figure 1-17b), every major key appears in close proximity to both its parallel minor (e.g. C major and A minor) and relative minor (e.g. C major and C minor.

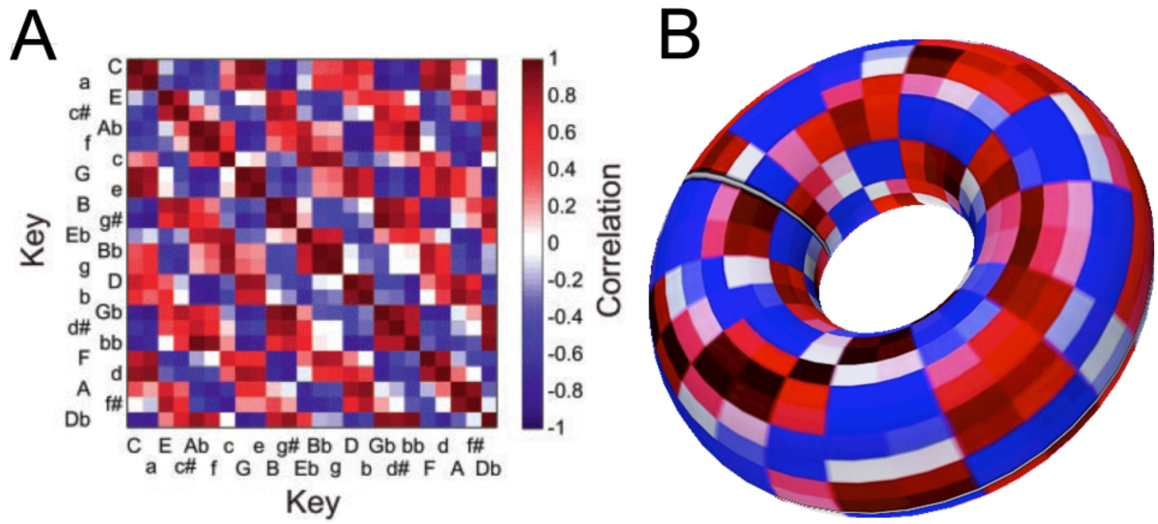

Figure 1-17. A toroid model of tonal space. a) An unfolded, two-dimensional map of key correlations (Janata et al., 2002). Opposite edges connect to each other to form a continuous, wrapping surface. Major scales and their relative minors share the same 7-note scale and are positively correlated (dark red). b) Toroidal representation the key correlation map. Adapted with permission from Janata, P., et al. (2002). The Cortical Topography of Tonal structures Underlying Western Music. Science, 298(5601), 2167.

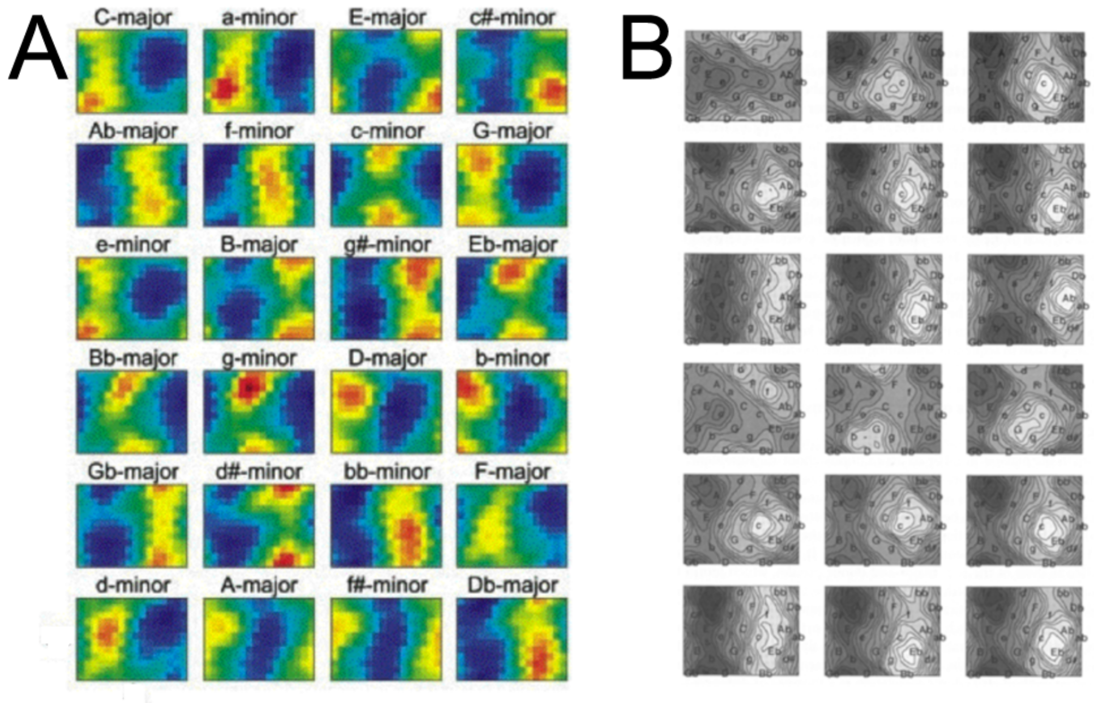

Figure 1-18. Properties of the tonality surface. a. Panels show the average tonality surface for tonality-tracking voxels for each of the 24 keys in the original melody. The surface represents an unfolded torus: the top and bottom edges of each rectangle wrap around to each other, as do the left and right edges. The activation peak in each panel (red = strongest) reflects the melody's progression through all of the keys. b. Distributed mappings of tonality on the self-organizing map (SOM). Each set of 9 panels depicts the areas of highest activation (key focus) after every chord played in a 9-chord key-changing sequence that consisted of the chords D minor diminished, G, C minor, A♭, F, D♭, B♭ minor, E♭, A♭, and modulated from C minor to A♭ major. The top set shows the subjective probe tone judgments, while the bottom set shows the mapping of the key-finding algorithm. Adapted with permission from Janata et al., (2002). The Cortical Topography of Tonal structures Underlying Western Music. Science, 298(5601), 2167.

The team identified cortical sites that were consistently and systematically sensitive to key changes (Figure 1-18a), i.e. their regression analysis revealed correlations between the moment-to-moment activity of neural populations and the calculated harmonic motion across a theoretical tonality surface, a 3D map of the distances among major and minor keys projected onto the doughnut-shape of a torus (Krumhansl & Kessler, 1982). Reviewers suggested that this tonal space model might reflect more general processes of remembering and comparing tones. (Zatorre & Krumhansl, 2002).

Remarkably similar plots came out of Krumhansl & Toiviainen's probe tone experiments at Cornell. To study how the sense of key develops and changes over time, workers played 10 different melodic sequences of 9 chords each to musically trained subjects. As the sequences modulated from one key to another (e.g. from C major to D minor), the listeners did the probe tone task after each chord was played. The same researchers trained their SOM neural network with the 24 K-K profiles, then used a "key-finding" algorithm to process the input from the key-changing sequence stimuli. The behavior of the algorithm followed the same patterns of modulations found by the musically trained experts**Error! Reference source not found.** (Figure 1-18b).

Helical tonal surfaces

Roger Shepard (1982) is credited with the first instantiation of tonal space that departed from unidimensional scales (such as the *mel*) in favor of a *contextual* arrangement in which musical relations (intervals) between pitches were invariant, i.e. a perfect 5^{th} equalled a perfect 5^{th}, regardless of its position on the scale. He began with the a line of the 12 pitch classes (and their octaves) arranged in consecutive semitones, then collapsed the line so that equilateral triangles were formed from adjacent semitones and two parallel lines of whole tone scales emerged (Figure 1-19). Giving the strip a twist produced a double helix and a further twisting arranged the pitch classes in 12 vertical columns. As a result, invariance for interval class distances was maintained.

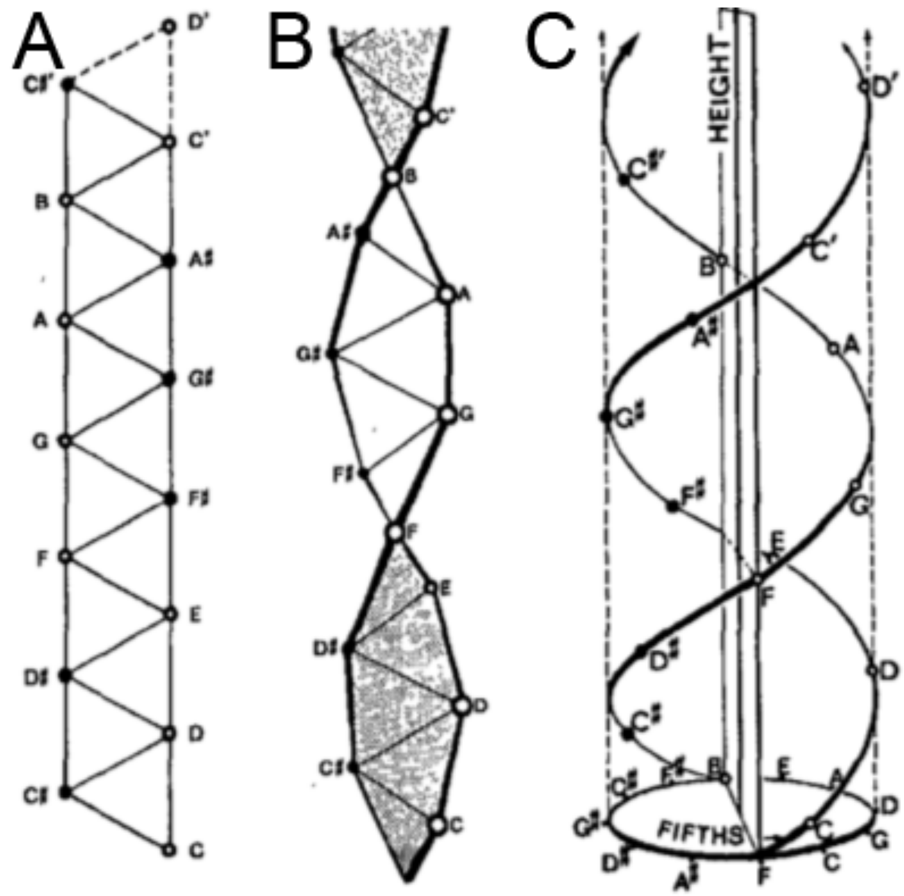

Figure 1-19. Stages in the construction of a double helix of musical pitch: (a) the flat strip of equilateral triangles, b) the strip of triangles given one complete twist per octave, and (c) the resulting double helix shown as wound around a cylinder (Shepard, 1982). Adapted with permission from Krumhansl, Carol L. (2005). The Geometry of Musical Structure : A Brief Introduction and History. Computers in Entertainment, 3(4), 1–14. Retrieved from http://dl.acm.org/citation.cfm?id=1095542

Chew spiral array model (2000)

More a cylindrical helix than a spiral, the spiral array model (SAM) is a 3-dimensional configuration of the *harmonic network* spatial representation of the relations perceived between pitches, intervals, chords and keys in which distance corresponds to perceived musical *closeness*. Originating from Longuet-Higgins harmonic space, it is a *generative* model, in that larger structures (keys, scales, chords) spring from the proximity of their component pitches. As are all tonal spaces in this thesis, the SAM is based on the notion of the circle of fifths, where each pitch on the spiral sits between two pitches at the interval of a perfect 5th (Figure 1-20). Pitches spaced at a 3rd are closer than are pitches at a second interval. Major intervals are closer than minors, i.e. a major 3rd is shorter than a minor 3rd.

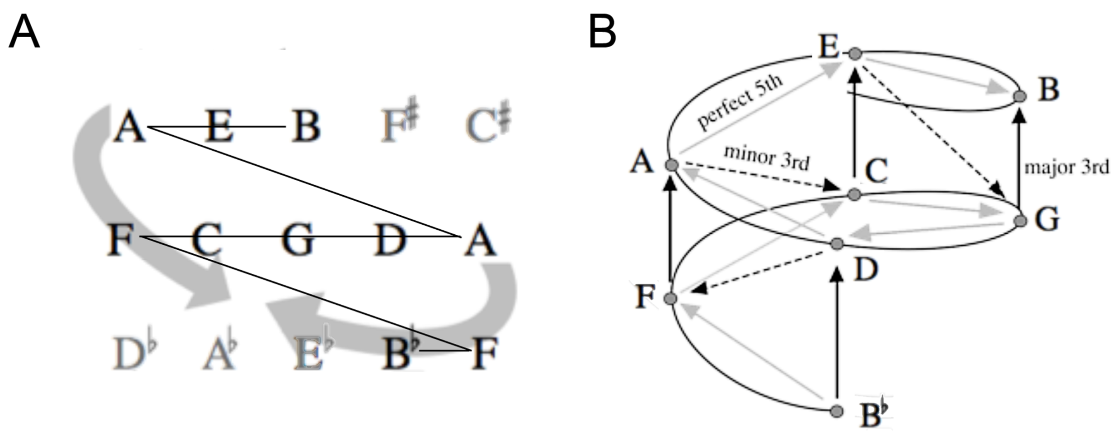

Figure 1-20. Wrapping harmonic space to form the SAM. A) Longuet-Higgins harmonic space centered on C (range: B$^{\flat}$ to B) is curved in upon itself until the pitches A and F meet, forming b) a cylindrical helix wherein the Euclidean distance for all interval classes is invariant (Chew & Chen, 2005). The vertical orientation of the four major 3rd axes is maintained. Adapted with permission from Chew, E. (2003). Thinking Out of the Grid and Inside the Spiral – Geometric Interpretations of and Comparisons with the Spiral Array Model. *Network*. Retrieved from http://lit.gfax.ch/Interpretations of and Comparisons with the Spiral Array Model.pdf.

Dumas perfect 4th helix (P4h)

I have designed the perfect 4th helix (P4h) as a model of melody processing. The P4h is a plot of the relative positions for the pitches of any given melody, each pitch having a node in 4D space, i.e. width, height, depth and octave. The P4h is based upon the three equivalent axes of the traditional tonnetz, i.e. P5, M3 and m3. As shown in Figure 1-21, a P4h for a melody in the key of *C* can be created through the simple expediency of folding the left and right edges of an equilateral tonnetz toward each other. Further folding of the top and bottom edges of the tonnetz to form a torus *ala* Krumhansl et al. would upset the delicate balance of consistent Euclidean distances for interval classes that is at the heart of my thesis, and so I have resisted this temptation.

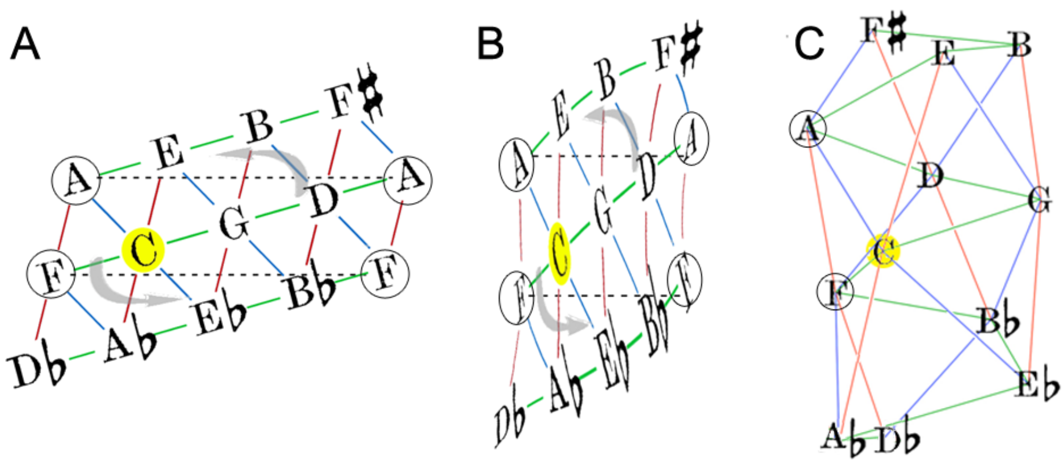

Figure 1-21. Creating a P4h for a melody in the key of *C*. a) Start with a traditional equilateral tonnetz centered on C (yellow) with redundant pitches *A* and *F*. b) Fold the left and right edges behind the figure, maintaining all pitch-connection distances. c) Join *A* to *A* and *F* to *F* to complete a structure comprising 1 P4h (green), 3 minor 3rd helices (blue), and 4 major 3rd helices (red).

Figure 1-22 displays several ways of plotting the P4h, each of which retains the original pitch coordinates. The *geodesic* P4h variation is the most accurate display of the theoretical Euclidean distances for P4, M3 and m3 intervals (Figure 1-22a). The *cylindrical* version (Figure 1-22b) highlights the P4 helix itself and enables a comparison with the Chew SAM. The *vector* version (Figure 1-22c) places the tonic C at the center of the network and clearly demonstrates the 4 interval class distances for all intervals smaller than P5, namely 1 (P4, M3, m3); 1.362 (M2); 1.652 (m2) and 1.841 (tritone). Interestingly, there is a P4h doppelgänger in the chain of amino acids known as the α-helix (Figure 1-22d), in which carbon-oxygen (C=O) groups appear at approximately the same coordinates as the pitch-classes on the P4h.

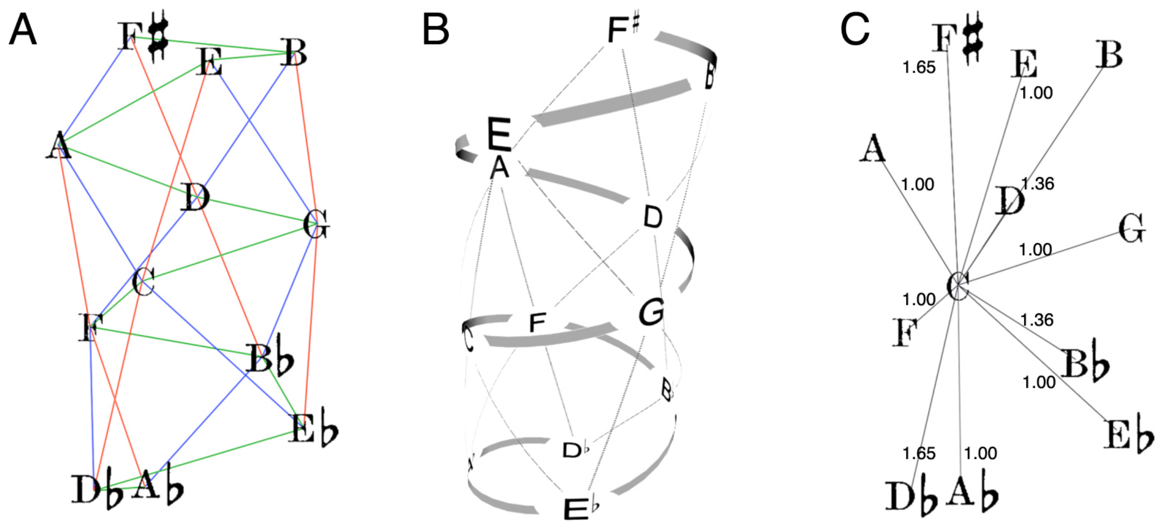

Figure 1-22. P4h variations, key of C. a) geodesic, b) cylindrical, c) vector, showing relative distances from the tonic C.

After wrapping the traditional tonnetz into a cylinder, I calculated values for the helix parameters that would produce equal Euclidean distances for P4, M3 *and* m3: radius (*r)*: 0.645, step height (h): 0.235, step range: -5 to 6, step vertical angle : 20° and step horizontal angle : 97.74° (Table 1-1). The formulae in Table 1-2**Error! Reference source not found.** produced coordinates in 3 dimensions for the 12 pitches within the octave centered on middle C. Table 1-3 shows the coordinates for the pitches within 3 octaves above middle C. The fourth coordinate *w* represents octaves in a fourth dimension.

Interestingly, there is a naturally-occurring P4h doppelgänger in Pauling and Corey's molecular model of the chain of amino acids known as the *α*-helix (Stryer, 1995), in which carbon-oxygen (C=O) groups appear at approximately the same coordinates as the pitch-classes on the P4h (Figure 1-23).

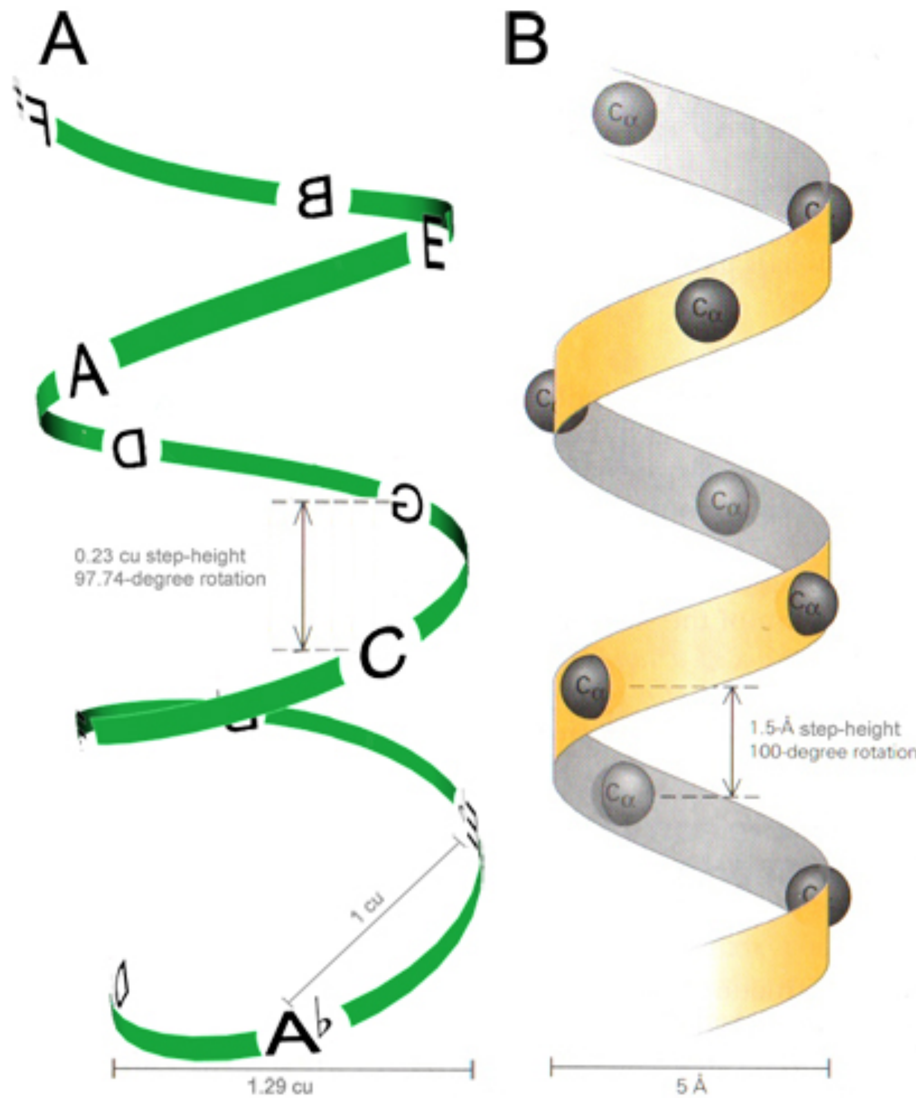

Figure 1-23. Comparing the P4h with Pauling and Corey's α-helix. a) With a step-height of 0.23 *consonance units* (*cu*, the vector distance for every P4, M3 and m3 interval in the model), the P4h has a step-rotation of 97.74° and step-height/radius ratio (*h/r)* of 0.356. b) The α-helix protein

structure has a similar step-rotation (100°), but an elongated *h/r* of 0.60. Adapted with permission from Stryer, L. (1995). Biochemistry (4th ed., pp. 27–30). New York: W. H. Freeman & Company.

Parameter	Description	Value (radians)
cu	Consonance unit distance (P4:M3:m3)	1 *cu*
r	helix radius	0.645 *cu*
h	step height	0.235 *cu*
D	Diameter	1.29 *cu*
h/r	Step-height/radius ratio	.364
P4 step	perfect 4^{th} interval step along the helix relative to tonic (e.g. C = 0)	Range = -5 : 6
$\angle xy$	horizontal angle between steps (relative to origin 0°).	97.74° (1.705)
$\angle$xz	vertical angle (helix slope) between steps.	20° (0.349)

Table 1-1. P4h parameter descriptions and values.

Dimension	Formulae	range
w	integer, number of octaves above/below origin (0)	-3:8 for full MIDI set of 128 integers
x	$r * \cos(\angle xy * p)$	-0.62:0.65
y	$r * \sin(\angle xy * p)$	-0.64:0.64
z	$r * \tan(\angle xz) * p$	-1.17:1.41

Table 1-2. P4h dimensions and formulae.

Pitch	P4 step	∠*xy* (°)	∠*xy* radians	*w*	*x*	*y*	*z*	*cu* (rel. to C)
F#	6	586.44	10.24	0	-0.44	-0.47	1.41	1.84
B	5	488.7	8.53	0	-0.4	0.5	1.17	1.65
E	4	390.96	6.82	0	0.55	0.33	0.94	1.00
A	3	293.22	5.12	0	0.25	-0.59	0.7	1.00
D	2	195.48	3.41	0	-0.62	-0.17	0.47	1.36
G	1	97.74	1.71	0	-0.09	0.64	0.23	1.00
C	0	0	0	0	0.65	0	0	0.00
F	-1	-97.74	-1.71	0	-0.09	-0.64	-0.23	1.00
Bb	-2	-195.48	-3.41	0	-0.62	0.17	-0.47	1.36
Eb	-3	-293.22	-5.12	0	0.25	0.59	-0.7	1.00
Ab	-4	-390.96	-6.82	0	0.55	-0.33	-0.94	1.00
Db	-5	-488.7	-8.53	0	-0.4	-0.5	-1.17	1.65

Table 1-3. P4h, key of C. Pitches, P4 steps, angles, coordinates and consonance units for pitches within the octave centered on the origin (middle C). Columns: a) P4 pitch class; b) P4 step relative to origin C (0); P4 step angle (∠*xy*) in degrees; P4 step angle (∠*xy*) in radians;

MIDI pitch name	MIDI #	x	y	z	w (octave)
C3	60	0.645	0	0	0
Db3	61	-0.403281513	-0.503377613	-1.173804006	0
D3	62	-0.621601772	-0.172151783	0.469521602	0
Eb3	63	0.254299457	0.592753563	-0.704282403	0
E3	64	0.553104693	0.331813499	0.939043204	0
F3	65	-0.086867303	-0.639123675	-0.234760801	0
F#3	66	-0.444478406	-0.467401269	1.408564807	0
G3	67	-0.086867303	0.639123675	0.234760801	1
Ab3	68	0.553104693	-0.331813499	-0.939043204	1
A3	69	0.254299457	-0.592753563	0.704282403	1
Bb3	70	-0.621601772	0.172151783	-0.469521602	1
B3	71	-0.403281513	0.503377613	1.173804006	1
C4	72	0.645	0	0	1
Db4	73	-0.403281513	-0.503377613	-1.173804006	1
D4	74	-0.621601772	-0.172151783	0.469521602	1
Eb4	75	0.254299457	0.592753563	-0.704282403	1
E4	76	0.553104693	0.331813499	0.939043204	1
F4	77	-0.086867303	-0.639123675	-0.234760801	1
F#4	78	-0.444478406	-0.467401269	1.408564807	1
G4	79	-0.086867303	0.639123675	0.234760801	2
Ab4	80	0.553104693	-0.331813499	-0.939043204	2
A4	81	0.254299457	-0.592753563	0.704282403	2
Bb4	82	-0.621601772	0.172151783	-0.469521602	2
B4	83	-0.403281513	0.503377613	1.173804006	2
C5	84	0.645	0	0	2
Db5	85	-0.403281513	-0.503377613	-1.173804006	2
D5	86	-0.621601772	-0.172151783	0.469521602	2
Eb5	87	0.254299457	0.592753563	-0.704282403	2
E5	88	0.553104693	0.331813499	0.939043204	2
F5	89	-0.086867303	-0.639123675	-0.234760801	2
F#5	90	-0.444478406	-0.467401269	1.408564807	2
G5	91	-0.086867303	0.639123675	0.234760801	3
Ab5	92	0.553104693	-0.331813499	-0.939043204	3
A5	93	0.254299457	-0.592753563	0.704282403	3
Bb5	94	-0.621601772	0.172151783	-0.469521602	3
B5	95	-0.403281513	0.503377613	1.173804006	3
C5	96	0.645	0	0	3

Table 1-4. 4D coordinates for the pitches within 3 octaves above middle C. The octave coordinate *w* breaks between F♯ and G, reflecting both the C-centric organization and the fact all intervals within the first 3 dimensions (*xyz*) are smaller than a perfect 5th.

Chapter 2. Materials and Methods

Subjects

Experiment A: Neural processing of pitch

10 healthy, right-handed subjects, ages 25-37 y, (5M:5F, non-musicians).

Experiment B: Neural processing of auto-correlation, Experiment C: Neural processing of interval distance, Experiment D: Neural processing of next-note probability

10 healthy, right-handed subjects, ages 27-47 y, (7M:3F, non-musicians).

Stimuli

Rather than using familiar tunes, we used novel, computer-generated, pseudo-random melodies to (a) more precisely control potential cues (e.g., rhythm) that are not of present interest, (b) eliminate unison intervals that cannot be transformed appropriately, and (c) provide a direct analysis of the nature of the musical feature under investigation.

Experiment A

The stimulus was an audio file of 288 s total duration. An entire stimulus sequence consisted of 576 pure tones segregated into 24 contiguous segments (Figure 2-1), where each segment comprised a random permutation (Figure 2-2) of 24 pure tones (2-octave range: freq. 261.6 Hz - 987.86 Hz; MIDI #60-83; piano; C3 - B4) . The overall loudness level was set at 76 db, as referenced to a 1046 Hz test tone, whereas loudness levels for individual tones were adjusted to conform with the international standard equal loudness contour specifications from ISO 226:2003 - Acoustics (2005). Each tone was 0.5 s long, including the beginning and ending ramped amplitudes, 0 to peak in 20 ms (Figure 2-3). The “fade-in” and “fade-out” ramps were used to diminish the effects of “edge” artifacts, i.e. noise generated when a sound is abruptly turned on or off.

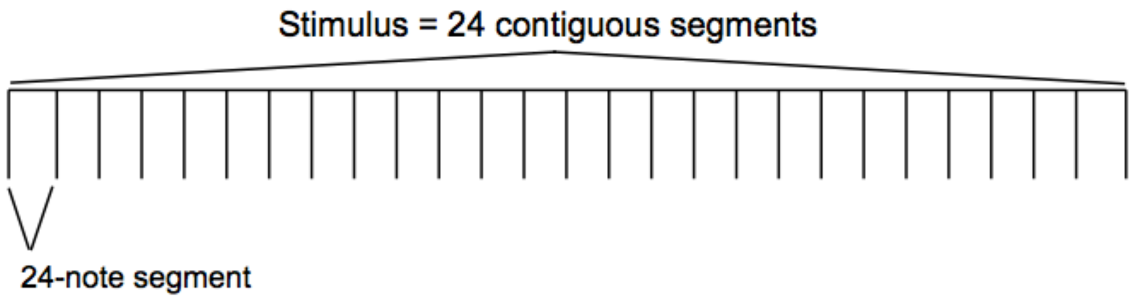

Figure 2-1. Block diagram of Random notes stimulus showing 24 contiguous 24-note segments.

Figure 2-2. Example 24-note quasi-random stimulus segment.

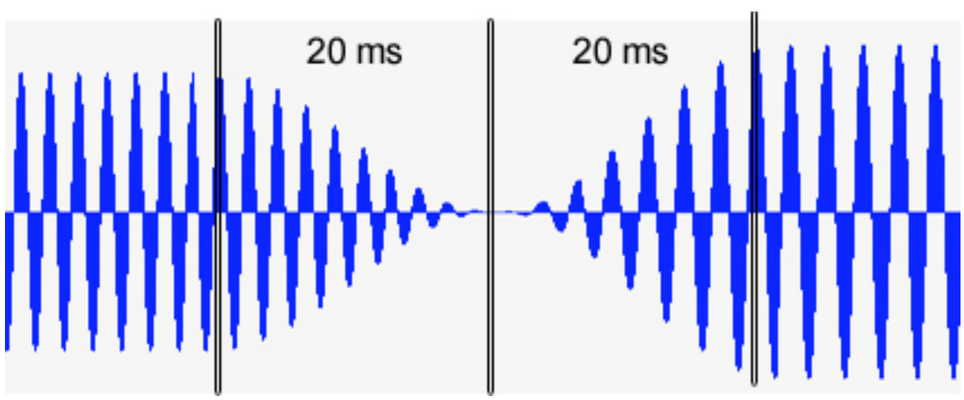

Figure 2-3. Example of the 20ms amplitude fade-in and fade-out at each tone junction. Amplitudes were ramped between 0db and the adjusted peak amplitude.

Random Notes stimulus pitches		
MIDI Pitch name	MIDI Note	Frequency
C3	60	261.63
Db3	61	277.18
D3	62	293.66
Eb3	63	311.13
E3	64	329.63
F3	65	349.23
F#3	66	369.99
G3	67	392.00
Ab3	68	415.30
A3	69	440.00
Bb3	70	466.16
B3	71	493.88
C4	72	523.25
Db4	73	554.37
D4	74	587.33
Eb4	75	622.25
E4	76	659.26
F4	77	698.46
F#4	78	739.99
G4	79	783.99
Ab4	80	830.61
A4	81	880.00
Bb4	82	932.33
B4	83	987.77

Table 2-1. Set of 24 pitches used to produce the quasi-random pure-tone stimuli.

Experiments B, C, and D

Each tone sequence stimulus comprised a random permutation of 240 pure tones (0.25 s each) selected from a set of pitches in the key of C major (or A natural minor, 2-octave range: freq. 261.6 Hz - 987.86 Hz, note names C4 - B5, MIDI #60 - 83) (Figure 2-4). We used a customized MATLAB© program to generate ten 10-sequence sets. Each set comprised ten sequences having serial correlations ranging from 0.0 to 0.9 over 5 lags (Figure 2-5), and each subject heard a unique, randomly ordered set.

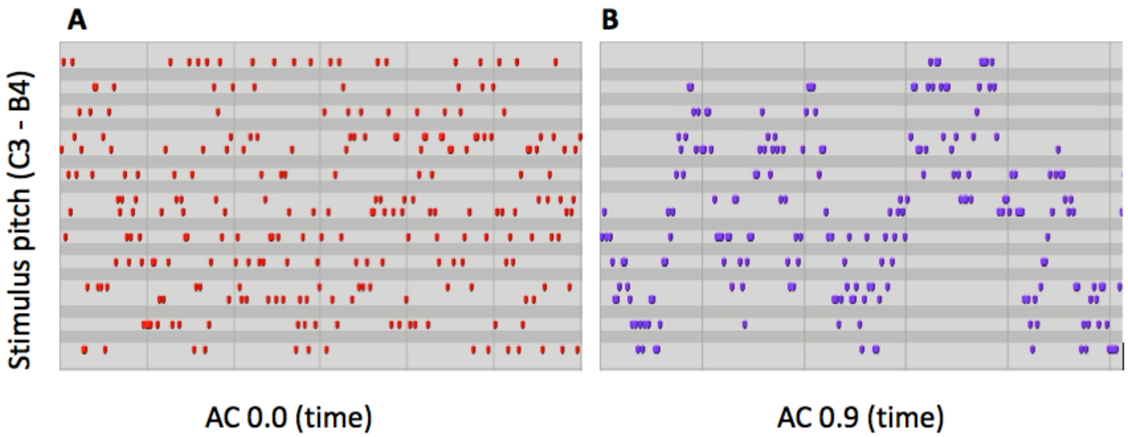

Figure 2-4. Piano-roll representation of stimulus model. a) Sequence with a serial auto-correlation of 0.0. b) Sequence with a serial auto-correlation of 0.9.

Figure 2-5. Notated sample stimuli with serial auto-correlations increasing from pseudo-random (AC 0.0) to highly auto-correlated (AC 0.9).

Task

All Experiments

Subjects lay supine on a bed wearing pneumatic earphones with protective foam ends. Subjects were asked to stay still with their eyes closed while listening to a sequence of tones lasting approximately 5 minutes (Experiment A) or 11 minutes (Experiments B, C, and D).

Data acquisition

All Experiments

Neural recordings. Magnetic field activity of the brain was recorded using 248 axial gradiometers (Magnes 3600WH, 4-D Neuroimaging, San Diego, CA) at a sampling rate of 1017 Hz (bandpass: 0.1- 400 Hz). Given a stimulus of 666 s, and the sampling rate above, the data generated for each subject consisted of 248 matrices (one per sensor), each containing approximately 288,000 measurements (Experiment A) or 677,000 measurements (Experiments B, C, and D).

Chapter 3. Data Analyses

Experiment A

Pitch-processing vectors. First, means for each of the 24 tones (across subjects and repetitions) were computed to obtain a stimulus-response curve, or pitch-processing vector (PPV), for each of the 248 MEG sensors. Next, all pairwise correlation coefficients were calculated (N = 30,628) between sensor PPVs to quantify the similarity of pitch processing between sensors: positive correlations would indicate similar PPVs, i.e. a similar way of processing pitch information, and vice versa for negative correlations (Figure 3-1).

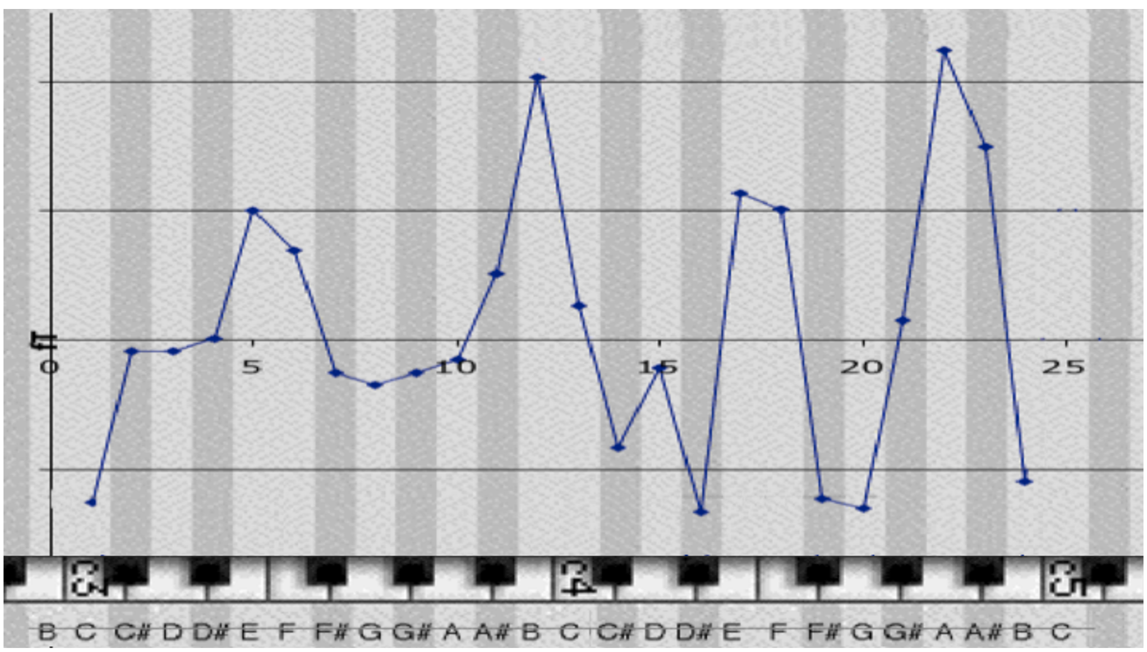

Figure 3-1. Example of an MEG sensor pitch-processing vector (PPV) showing the mean neural activity across subjects (ordinal: femtoTesla) for each of the 24 stimulus pitch-classes (abscissa: piano keyboard range C3-B4) for sensor #154.

Experiment B

We computed the mean MEG signal acquired by each of the 248 sensors (Figure 3-2) during the presentation of each of the 240 stimulus notes. The mean signal was computed across subjects for each of the 10 sequences to obtain a stimulus-response curve, or auto-correlation-processing vector (ACPV). We then calculated all pairwise correlation coefficients (N = 30,628) between sensor ACPVs to quantify the similarity of AC processing between sensors: positive correlations between sensors would indicate similar ACPVs (Figure 3-3), i.e. a similar way of processing AC information, and vice versa for negative correlations.

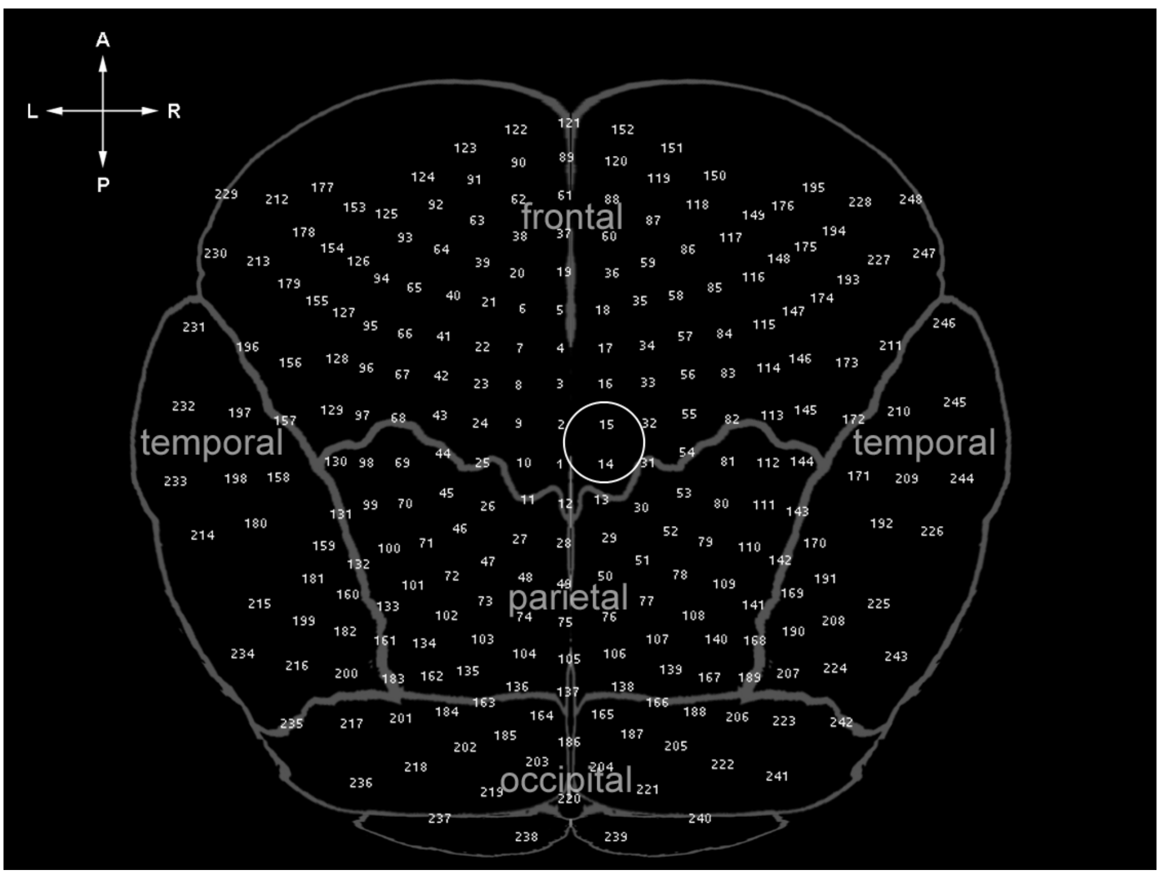

Figure 3-2. Flat-brain MEG sensor map showing location of Sensors #14 and #15 (circled).

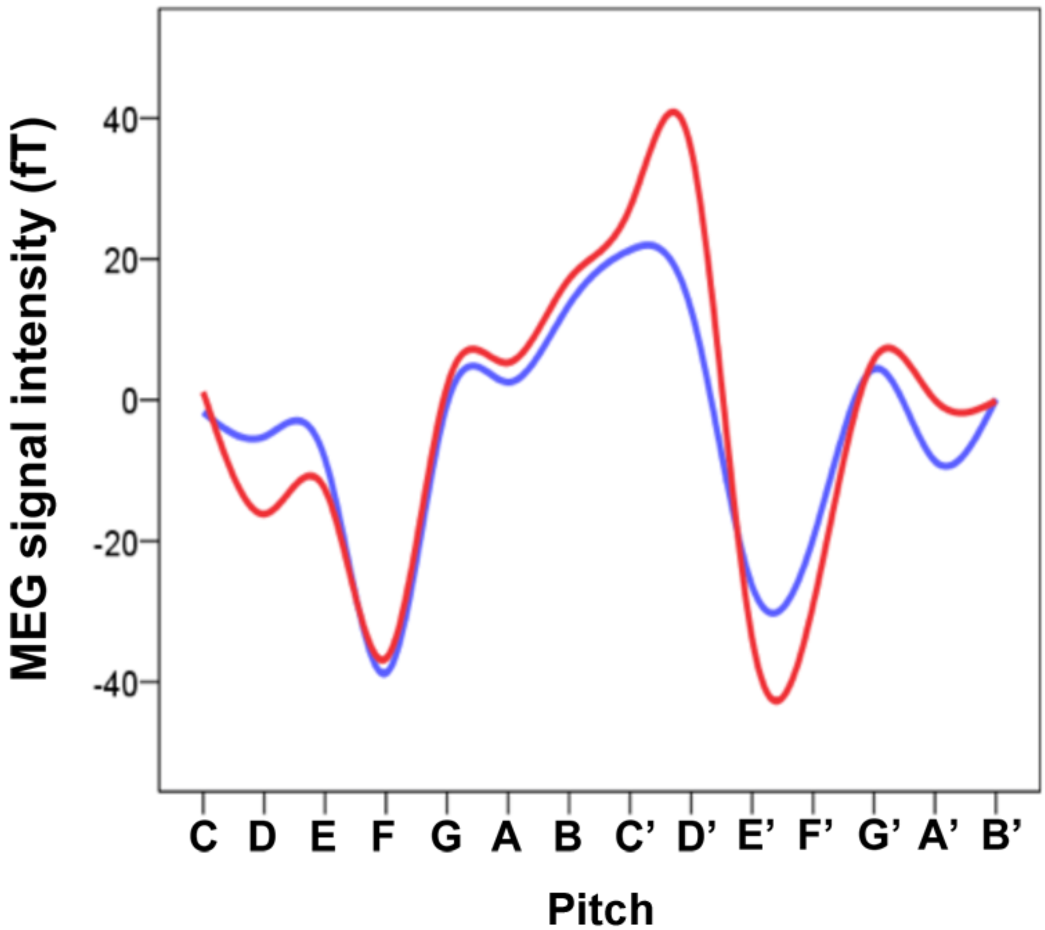

Figure 3-3. Example comparison of auto-correlation-processing vector (ACPV) for two sensors: S14 (blue) & S15 (red). Ordinal axis: Mean MEG signal intensity (MMSI) per pitch across subjects.

Experiment C

For each of the 100 stimuli in this study (i.e. 10 subjects X 10 auto-correlations), Euclidean distance (*D*) was calculated for every note-pair from coordinates in six tonal spaces

(

Pitch	MIDI	Frequency		LH			P4H			KK	P88	CH		
		Hz	log	x	y	z	x	y	z			x	y	z
C4	60	261.63	2.42	0.00	0.00	0.00	0.65	0.00	0.00	6.35	18	0.65	0.00	0.00
D4	62	293.66	2.47	2.00	0.00	0.00	-0.62	-0.17	0.47	3.48	3	-0.65	0.00	0.47
E4	64	329.63	2.52	0.00	1.00	0.00	0.55	0.33	0.94	4.38	10	0.65	0.00	0.94
F4	65	349.23	2.54	-1.00	0.00	0.00	-0.09	-0.64	-0.23	4.09	6	0.00	-0.65	-0.23
G4	67	392.00	2.59	1.00	0.00	1.00	-0.09	0.64	0.23	5.19	10	0.00	0.65	0.23
A4	69	440.00	2.64	-1.00	1.00	1.00	0.25	-0.59	0.70	3.66	7	0.00	-0.65	0.70
B4	71	493.88	2.69	1.00	1.00	1.00	-0.40	0.50	1.17	2.88	0	0.00	0.65	1.17
C5	72	523.25	2.72	0.00	0.00	1.00	0.65	0.00	0.00	6.35	18	0.65	0.00	0.00
D5	74	587.33	2.77	2.00	0.00	1.00	-0.62	-0.17	0.47	3.48	3	-0.65	0.00	0.47
E5	76	659.26	2.82	0.00	1.00	1.00	0.55	0.33	0.94	4.38	10	0.65	0.00	0.94
F5	77	698.46	2.84	-1.00	0.00	1.00	-0.09	-0.64	-0.23	4.09	6	0.00	-0.65	-0.23
G5	79	783.99	2.89	1.00	0.00	2.00	-0.09	0.64	0.23	5.19	10	0.00	0.65	0.23
A5	81	880.00	2.94	-1.00	1.00	2.00	0.25	-0.59	0.70	3.66	7	0.00	-0.65	0.70
B5	83	987.77	2.99	1.00	1.00	2.00	-0.40	0.50	1.17	2.88	0	0.00	0.65	1.17

Table 3-1). An octave dimension "*w*" was included in calculations for Tonal Spaces 2-6 to account for stimulus pitches in the octave above B4.

Pitch	MIDI	Frequency		LH			P4H			KK	P88	CH		
		Hz	log	x	y	z	x	y	z			x	y	z
C4	60	261.63	2.42	0.00	0.00	0.00	0.65	0.00	0.00	6.35	18	0.65	0.00	0.00
D4	62	293.66	2.47	2.00	0.00	0.00	-0.62	-0.17	0.47	3.48	3	-0.65	0.00	0.47
E4	64	329.63	2.52	0.00	1.00	0.00	0.55	0.33	0.94	4.38	10	0.65	0.00	0.94
F4	65	349.23	2.54	-1.00	0.00	0.00	-0.09	-0.64	-0.23	4.09	6	0.00	-0.65	-0.23
G4	67	392.00	2.59	1.00	0.00	1.00	-0.09	0.64	0.23	5.19	10	0.00	0.65	0.23
A4	69	440.00	2.64	-1.00	1.00	1.00	0.25	-0.59	0.70	3.66	7	0.00	-0.65	0.70
B4	71	493.88	2.69	1.00	1.00	1.00	-0.40	0.50	1.17	2.88	0	0.00	0.65	1.17
C5	72	523.25	2.72	0.00	0.00	1.00	0.65	0.00	0.00	6.35	18	0.65	0.00	0.00
D5	74	587.33	2.77	2.00	0.00	1.00	-0.62	-0.17	0.47	3.48	3	-0.65	0.00	0.47
E5	76	659.26	2.82	0.00	1.00	1.00	0.55	0.33	0.94	4.38	10	0.65	0.00	0.94
F5	77	698.46	2.84	-1.00	0.00	1.00	-0.09	-0.64	-0.23	4.09	6	0.00	-0.65	-0.23
G5	79	783.99	2.89	1.00	0.00	2.00	-0.09	0.64	0.23	5.19	10	0.00	0.65	0.23
A5	81	880.00	2.94	-1.00	1.00	2.00	0.25	-0.59	0.70	3.66	7	0.00	-0.65	0.70
B5	83	987.77	2.99	1.00	1.00	2.00	-0.40	0.50	1.17	2.88	0	0.00	0.65	1.17

Table 3-1. 14-note stimulus set with coordinate values for 6 tonal mappings ($D^{1\text{-}6}$). D^1: Frequency, D^2: Longuet-Higgins' harmonic space, D^3: Dumas' P4h, D^4: Krumhansl & Kessler's probe tone profile, D^5: Parncutt's chroma salience profile, D^6: Chew's spiral array model.

Euclidean distance (E*d*)

We used six measures of distance in tonal space as independent variables in our analysis. For the first measure, we calculated the log frequency ratio of each note-pair. For each of the other 5 measures, we calculated Euclidean distances (E*d*) between adjacent notes from coordinates in that particular space.

E*d* - Tonal Space #1: Frequency ratio

Stimulus interval distances in this tonal space equalled the absolute value for the log of the frequency ratio (Equation 1) for notes {t, t-1}, where *t* is a stimulus note and *t-1* is the preceding note (Figure 3-4):

Equation 1 $$D^1 = \left|\ln \frac{F_{t-1}}{F_t}\right| = \left|\ln(F_{t-1}) - \ln(F_t)\right|$$

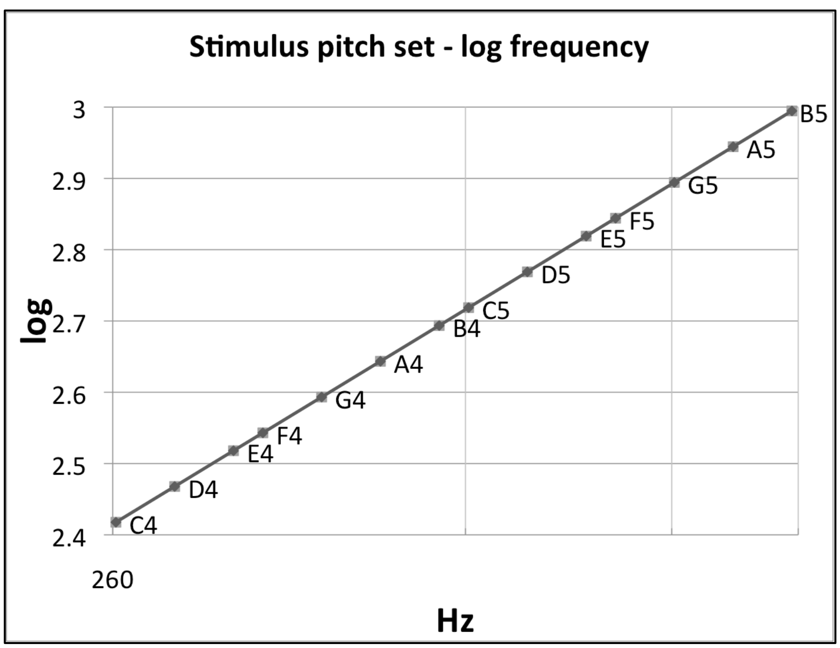

Figure 3-4. Plot of log frequency (Hz) for stimulus pitches.

E*d* - Tonal Space #2: Longuet-Higgins (LH) harmonic space (1962a)

Interval distances in LH space (Figure 3-5) were calculated using Equation 2 and pitch coordinate values from 3 axes: P5, M3 and octave.

Equation 2
$$D^2 = \sqrt{a+b+c}$$
$$a = (P5_t - P5_{t-1})^2, b = (M3_t - M3_{t-1})^2, c = (P8_t - P8_{t-1})^2$$

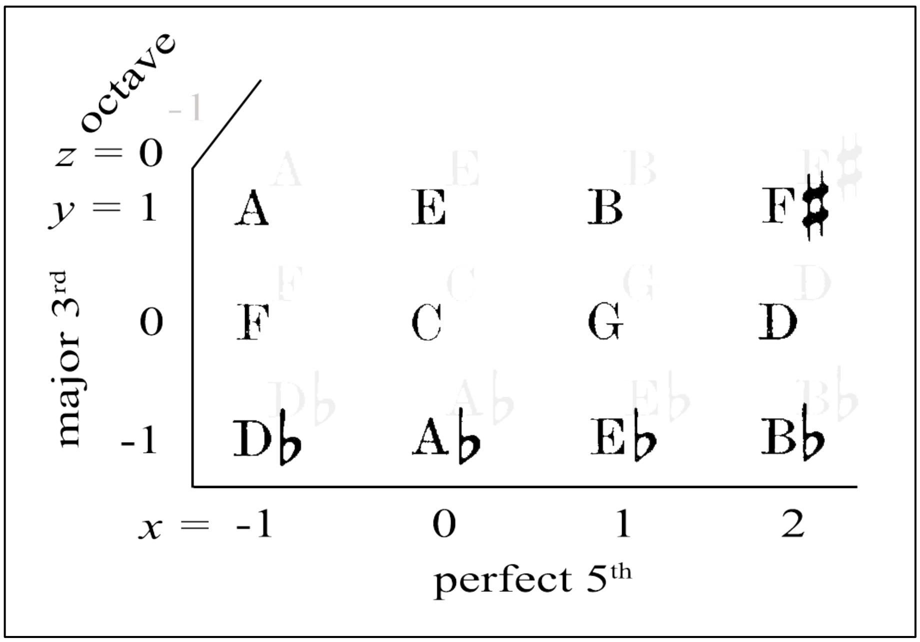

Figure 3-5. Longuet-Higgins' (1962a) harmonic space for the key of C major. abscissa: perfect 5th, ordinal: major 3rd, z-axis: octave.

E*d* - Tonal Space #3 Krumhansl and Kessler (KK) major key probe tone profile (1982).

Interval distances in KK space were calculated using Equation 3 and pitch coordinate values from 2 axes: probe tone profile values and octave (Figure 3-6).

Equation 3
$$D^3 = \sqrt{a+b}$$
$$a = (KK_t - KK_{t-1})^2,\ b = (P8_t - P8_{t-1})^2$$

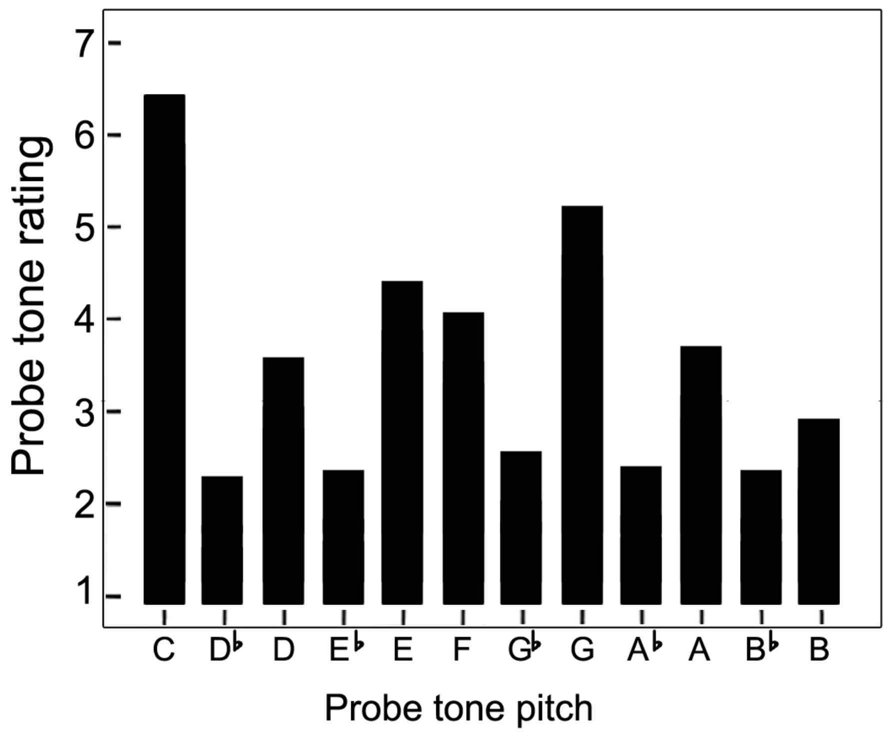

Figure 3-6. Krumhansl & Kessler's (1982) major key probe tone profile for the key of C major.

E*d* - Tonal Space 4: Parncutt (P88) major key chroma salience profile (2011).

Interval distances in P88 space were calculated using Equation 4 and pitch coordinate values from 2 axes: chroma salience values and octave (Figure 3-7).

Equation 4
$$D^4 = \sqrt{a+b}$$
$$a = (P88_t - P88_{t-1})^2, b = (P8_t - P8_{t-1})^2$$

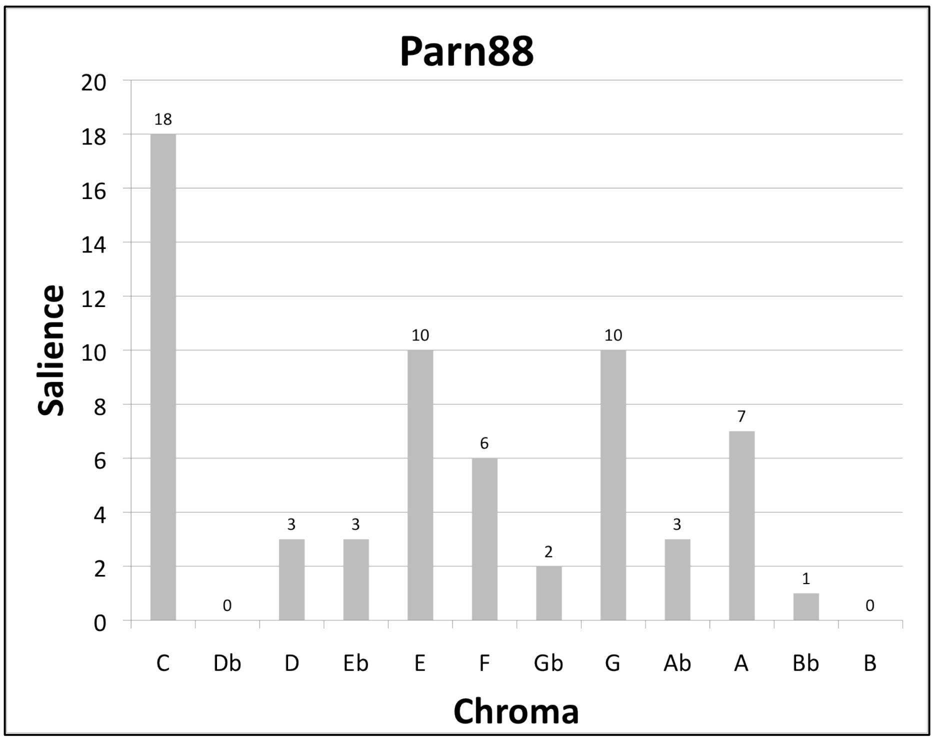

Figure 3-7. Parncutt's (2001) chroma salience profile adds weighted root supports to Krumhansl's probe tone profile.

E*d* - Tonal space #5: Chew (CH) Spiral array model (2000).

Interval distances in CH space were calculated using Equation 5 and pitch coordinate values from 4 axes:). *x, y*, *z* and octave (Figure 3-8).

Equation 5
$$D^5 = \sqrt{a+b+c+d}$$
$$a = (x_t - x_{t-1})^2, b = (y_t - y_{t-1})^2, c = (z_t - z_{t-1})^2, d = (P8_t - P8_{t-1})^2$$

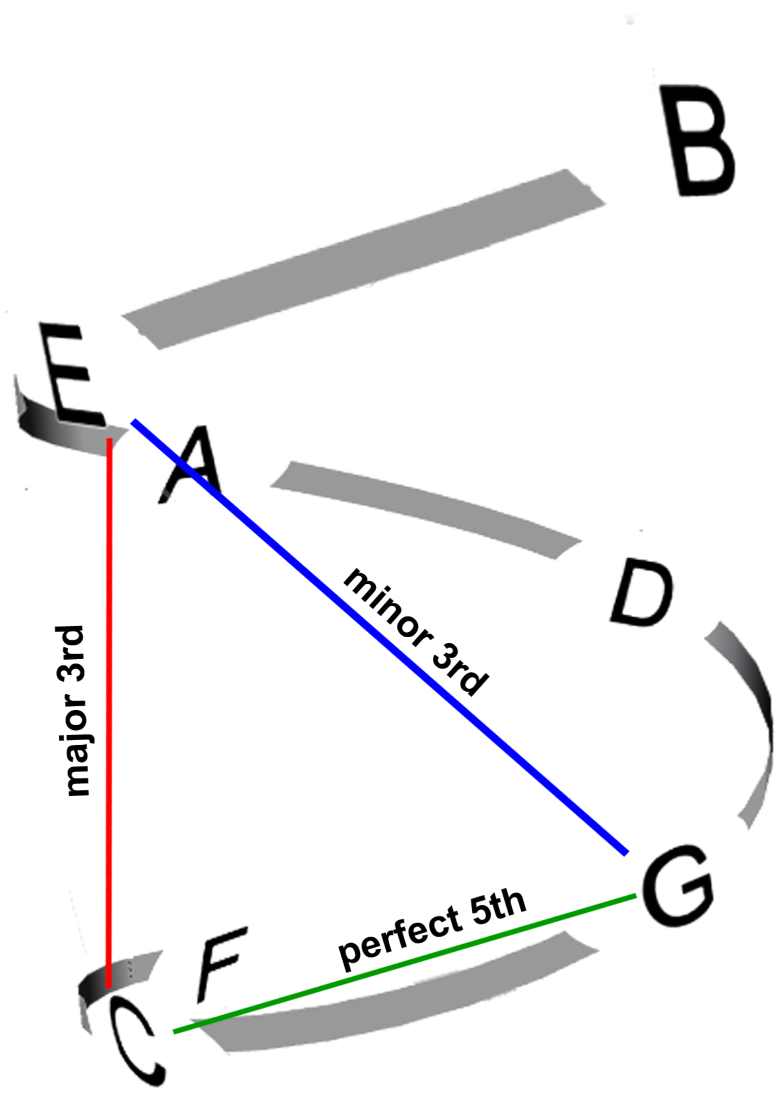

Figure 3-8 Chew (2000) Spiral array model, key of C major.

E*d* - Tonal Space #6: Dumas perfect fourth helix (P4h) (2012).

Interval distances in P4h space were calculated using Equation 6 and pitch coordinate values from 4 axes: *x, y*, *z* and octave (Figure 3-9).

Equation 6 $$D^6 = \sqrt{a+b+c+d}$$

$a = (x_t - x_{t-1})^2, b = (y_t - y_{t-1})^2, c = (z_t - z_{t-1})^2, d = (P8_t - P8_{t-1})^2$

x, y & *z* = coordinate values in 3D, *w* = octave index (range 0:2)

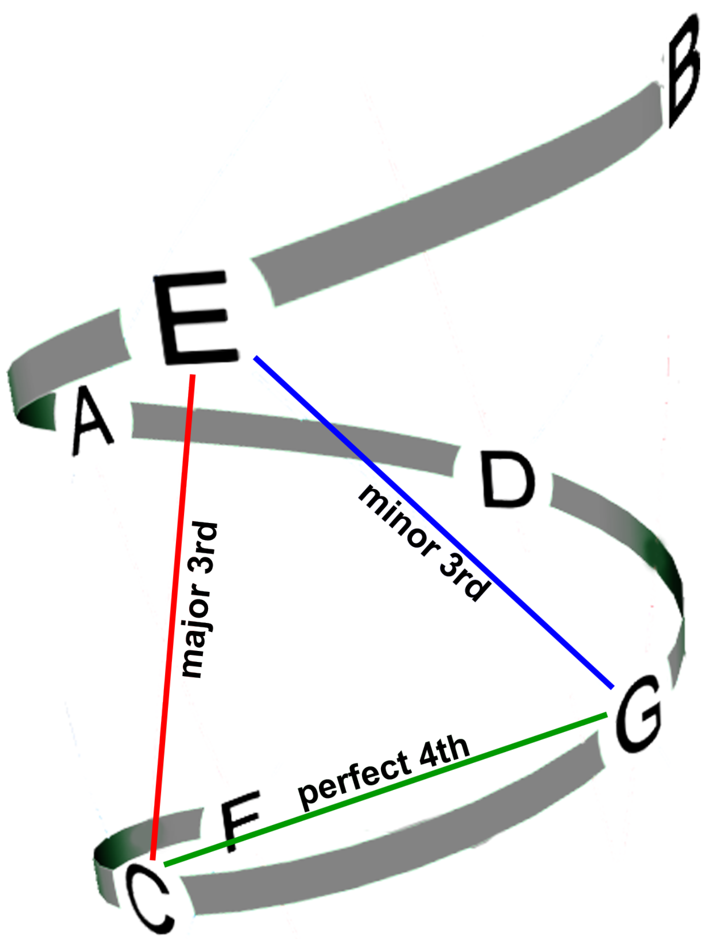

Figure 3-9. Dumas' perfect fourths helix (P4h) for the key of C major.

Auto-regression analysis. With respect to the neural signal, successive absolute differences in the MEG signal (D^{MEG}) were calculated between successive note means for each of 248 sensors. With respect to the notes, E*d* $D^{1, 2, 3, 4, 5, 6}$ were calculated between successive note coordinates. we wanted to assess the relations between changes in neural activity to tone changes in each one of the six different tonal spaces. For that purpose, we carried out an autoregression analysis (to account for possibly correlated errors), where the dependent variable was $\mathrm{D}^{\mathrm{MEG}}$ and the independent variables were $D^{1, 2, 3, 4, 5, 6}$ in six separate regressions.

Experiment D

Melodic Interval Probability (MIP). Almost 10,000 melodies from "A Dictionary of Musical Themes" (Barlow and Morgenstern, 1948) were converted to MIDI note number format to form a corpus of melodic intervals (note-pairs). The relative frequency of occurrence within the corpus for every note-pair (i.e. CC, CC#, CD, etc.) over a 3-octave range (C3-B5) was calculated. To calculate MIP, each associated note-pair-frequency value was divided by the total number of intervals in the corpus. With respect to the stimulus, MIP was calculated between all note-pairs (Table 3-2).

	C3	D3	E3	F3	G3	A3	B3	C4
C3	0.003230	0.005778	0.004137	0.000573	0.001692	0.000354	0.000161	0.000592
D3	0.006170	0.004407	0.013859	0.003178	0.002020	0.001306	0.000270	0.000354
E3	0.003121	0.013235	0.011581	0.018639	0.009091	0.004246	0.002007	0.001750
F3	0.001248	0.002432	0.017237	0.004568	0.015834	0.003159	0.000457	0.000888
G3	0.001570	0.002439	0.008647	0.013550	0.016748	0.025768	0.005559	0.008628
A3	0.000631	0.001017	0.006286	0.002722	0.022777	0.014187	0.028355	0.011800
B3	0.000116	0.000637	0.001171	0.000476	0.003442	0.027621	0.008248	0.041686
C4	0.000779	0.000380	0.002046	0.000676	0.013151	0.010610	0.036809	0.017996

Table 3-2. Melodic interval probabilities (MIP) for stimulus intervals within the octave C3-C4. Ordinal: interval first note. Abscissa: interval second note.

Perplexity Index (PI). We applied a -log transformation to all MIP values to get a PI value for each melodic interval presented to the subject. For example, the interval BC' produces the highest probability (0.041686) and the lowest PI (1.380007308). Thus, the PI vector for our stimulus shows higher values for less-probable intervals (Figure 3-10).

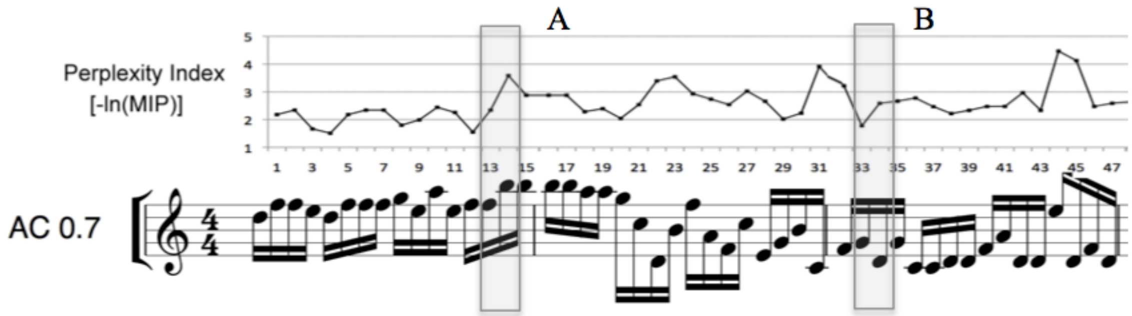

Figure 3-10. Excerpt from sample stimulus AC 0.7. a) The tritone F4-B4 has a high PI. b) The perfect 4th G3-D3 has a low PI. Both intervals have the same scalar distance (4 steps).

MEG data - We calculated successive absolute differences in MEG signal (DMEG) and correlated these with the stimulus PI vector using an auto-regression analysis (correcting for multiple comparisons).

Chapter 4. Results

Experiment A

Statistically significant positive correlations (Figure 4-1) and negative correlations (Figure 4-2) between sensor PPVs are plotted (nominal p<0.01, actual p<0.0000001 = 0.01/30628; corrected for multiple comparisons).

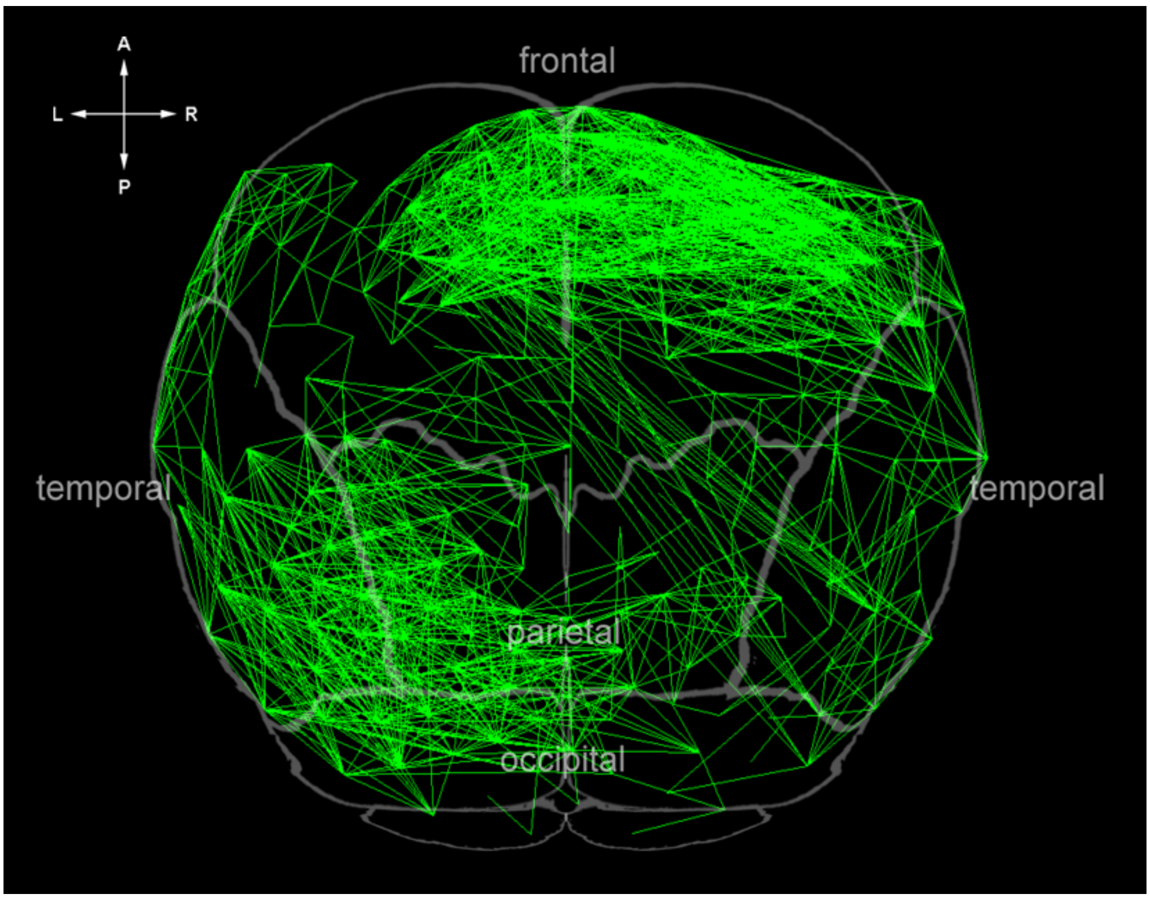

Figure 4-1. MEG sensor plots of correlations between sensor PPVs. Sensors with positively correlated PPVs. These occurred ~4x more frequently than negative correlations and were clustered in the frontal (bilateral) and left temporo-occipital regions.

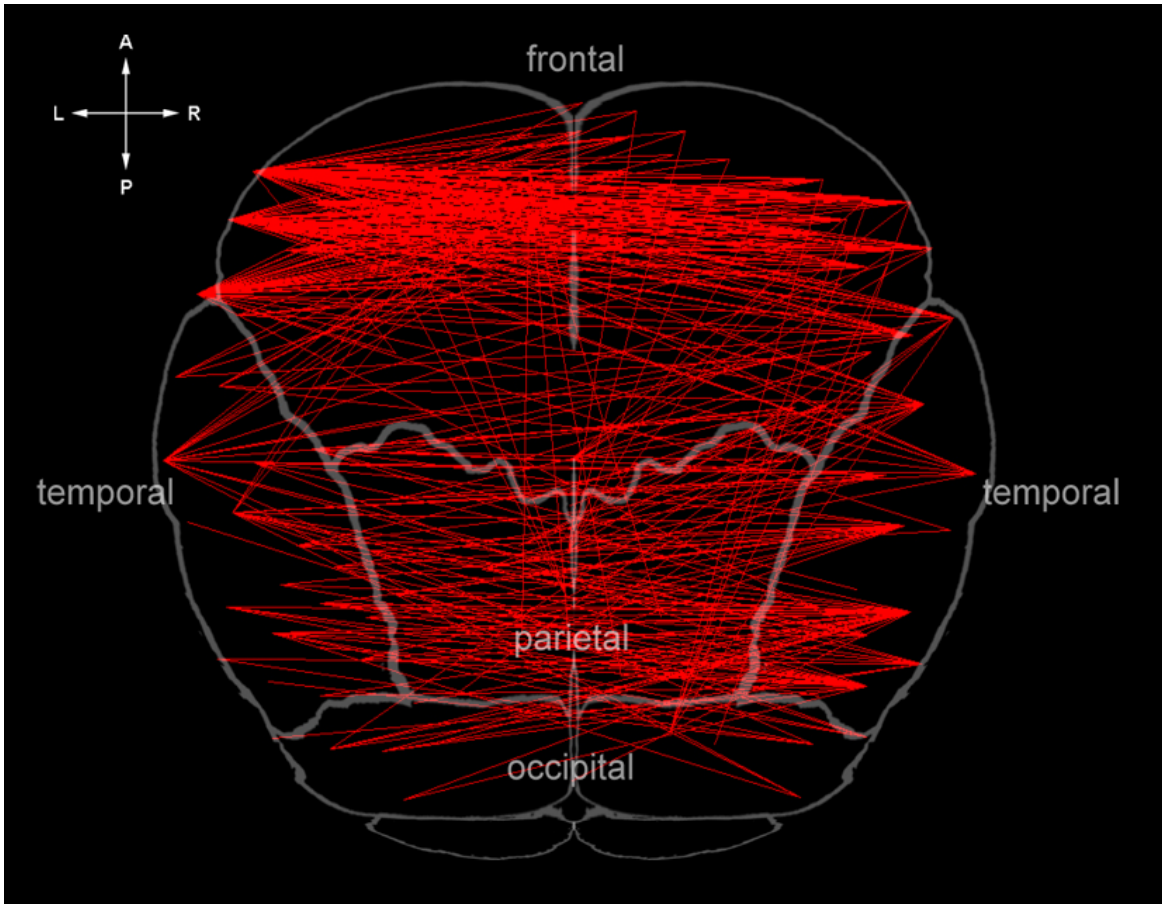

Figure 4-2. MEG sensor plots of correlations between sensor PPVs. Sensors with negatively correlated PPVs were found in opposite hemispheres, mostly in frontal and less so in posterior regions.

Experiment B

We found highly significant positive and negative correlations between sensors, across subjects (Figure 4-3). Positive correlations occurred more frequently than negative correlations. Pairs of sensors with positive correlations clustered in frontal brain areas. Finally, this clustering varied systematically with the degree of serial correlation in the sequence presented. See Appendix A for the complete set of sensor plots.

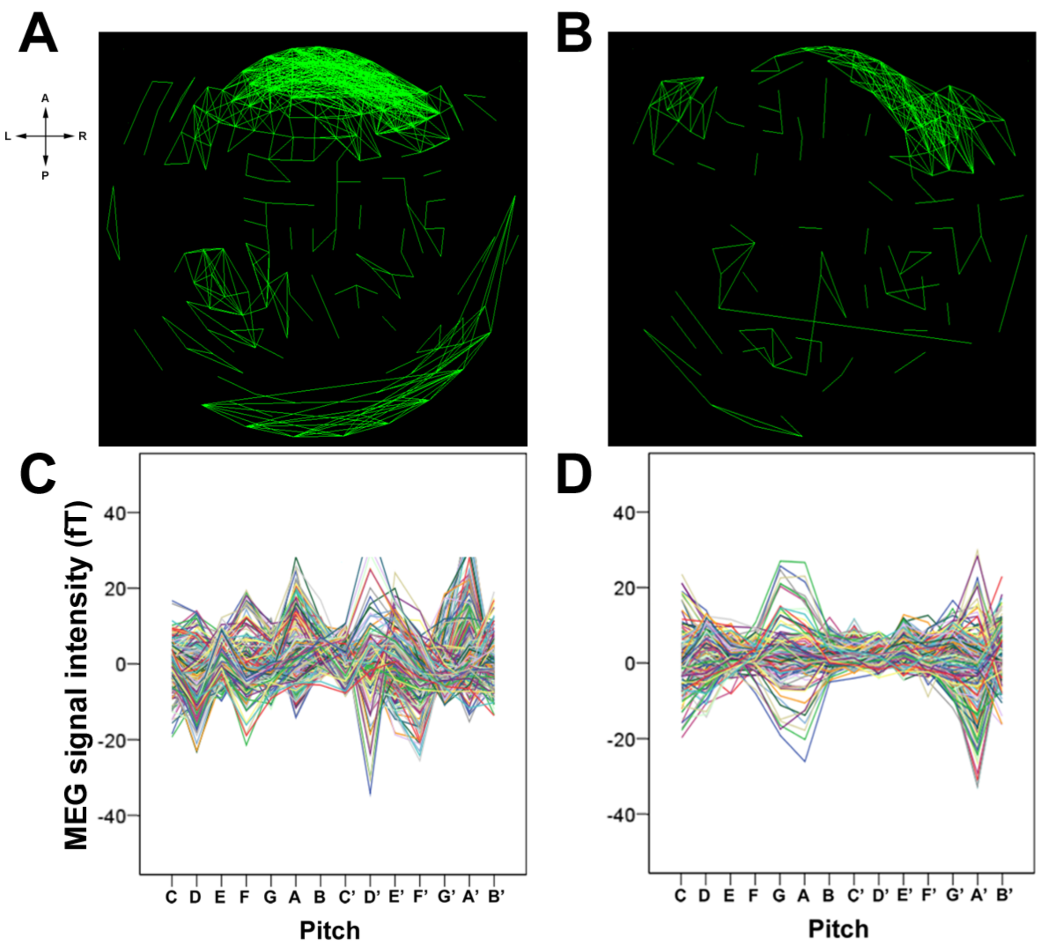

Figure 4-3. (a-b) Plots of all positively correlated MEG sensors/AC (across subjects) a) AC 0.0, b) AC 0.9. (c-d) Plots of ACPV for all sensors (across subjects) c) AC 0.0, d) AC 0.9. Relations

for pseudo-random stimuli were stronger and more numerous than for more-highly auto-correlated stimuli, especially in frontal regions. (See Appendix A for all plots.)

Experiment C

The analyses yielded six neural-tonal maps corresponding to the independent variables. We found dense clusters of systematic (positive and negative coefficients) and statistically significant ($p < 0.05$) relations between MEG data and each one of the 6 tonal maps. Brain patterns included nodes in bilateral superior temporal (positive), bilateral temporo-parietal (positive) and right parieto-occipital (negative) areas. (See Appendix B for individual plots.). These patterns varied systematically with tonal space. Temporal nodes were more prominent with the Hz, LH and P4H spaces and least prominent with P88 space. Right parieto-occipital (negative) nodes were most prominent with Hz and P4H. Four positive clusters in plots HZ, LH and P4H were similar to each other in significance and location. Plots KK, P88 and SAM showed positive clusters with lower significance.

Experiment D

We found highly significant, positive relations ($p < .0001$) between the neural activity for each melodic interval and the -log of the probability of that interval's occurrence in the corpus. Signs of melodic perplexity processing cropped up in bilateral prefrontal, midline, superior parietal and occipital cortex, sparing posterior lateral cortical areas (including primary auditory cortex). Previous studies also implicate prefrontal cortex in melody discrimination (Brown & Martinez, 2007), pitch identification (Bermudez &

Zatorre, 2005), representations of auditory Gestalten (Koelsch, 2011), and passive music listening (Ohnishi et al., 2001).

These results suggest that music appreciation involves prediction. When an unexpected note arrives, the brain taps a “perplexity sub-network” to deal with it. Different analyses (MIP and SAC) of the same data show strong relations in the bilateral frontal and prefrontal areas. Although their measures of melodic complexity were different, namely *level of melody serial auto-correlation* and *melodic interval probability*, both analyses produce quite similar sub-networks. The absence of anterior temporal activity is most notable, especially in light of the role played by this region in processing movement through tonal space.

Chapter 5. Discussion

Experiment A revealed the existence of brain sub-networks processing pitch information in a similar fashion. Sensors with positively correlated PPVs occurred ~4x more frequently than negative correlations and were clustered in the frontal (bilateral) and left temporo-occipital regions. Sensors with negatively correlated PPVs were found in opposite hemispheres, mostly in frontal and less so in posterior regions.

Experiment B provided strong evidence of brain sub-networks processing serial correlation information in a similar fashion. Positive correlations occurred more frequently than negative correlations. Pairs of sensors with positive correlations clustered in various brain areas. The systematic modulation of these networks seems to depend on the degree of serial correlation in the tone sequence presented.

Experiment C yielded significant and systematic relations (positive and negative) between MEG data and each one of the six tonal maps, demonstrating that brain activation data to a series of tones can be differentially interpreted when referred to distinct tonal mappings encoding the stimulus tones. The neural sub-networks discovered are similar to those found in Patel and Balaban's 2001 MEG study of brain response to interval direction (Figure 5-1). In the plots from both studies, significant relations are shown in bilateral frontal and temporo-parietal areas, including a strong relations in right parietal.

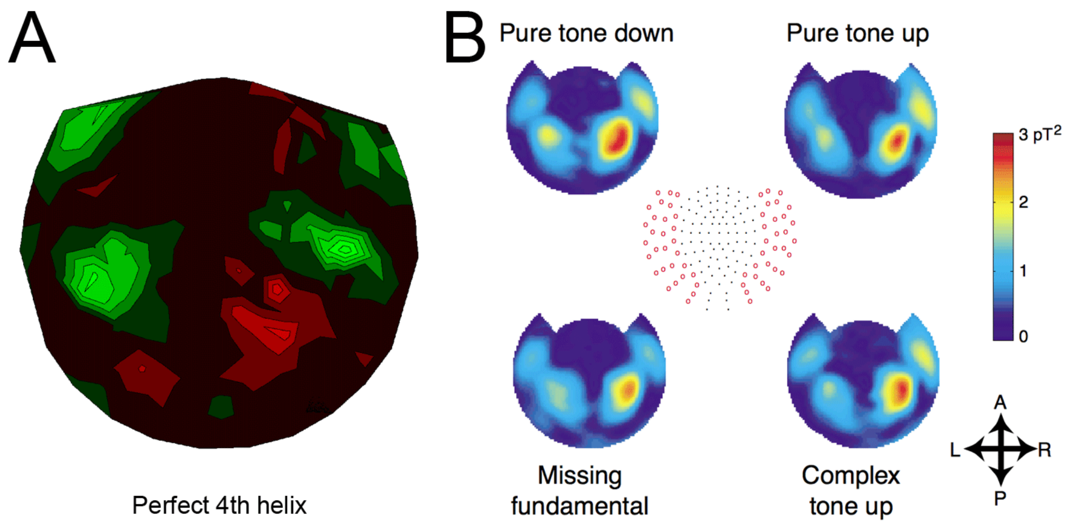

Figure 5-1. Comparison of results from two MEG music studies. a) Clusters of brain activation related to processing of interval distance as measured in Tonal space #6 (Dumas perfect 4th helix). Green = positive relations, red = negative. b) Power and spatial distribution of the aSSR in each of the four conditions (grand average across subjects) Adapted with permission from Patel, A. D., & Balaban, E. (2001). Human pitch perception is reflected in the timing of stimulus-related cortical activity. Nature neuroscience, 4(8), 839-844.

The results from Experiment C demonstrate that brain activation data to a series of tones can be differentially interpreted when referred to distinct tonal spaces encoding the stimulus tones (Figure 5-2). Conversely, these different neural-tonal maps indicate that distinct features of the tonal maps are differentially represented in dynamic brain mechanisms.

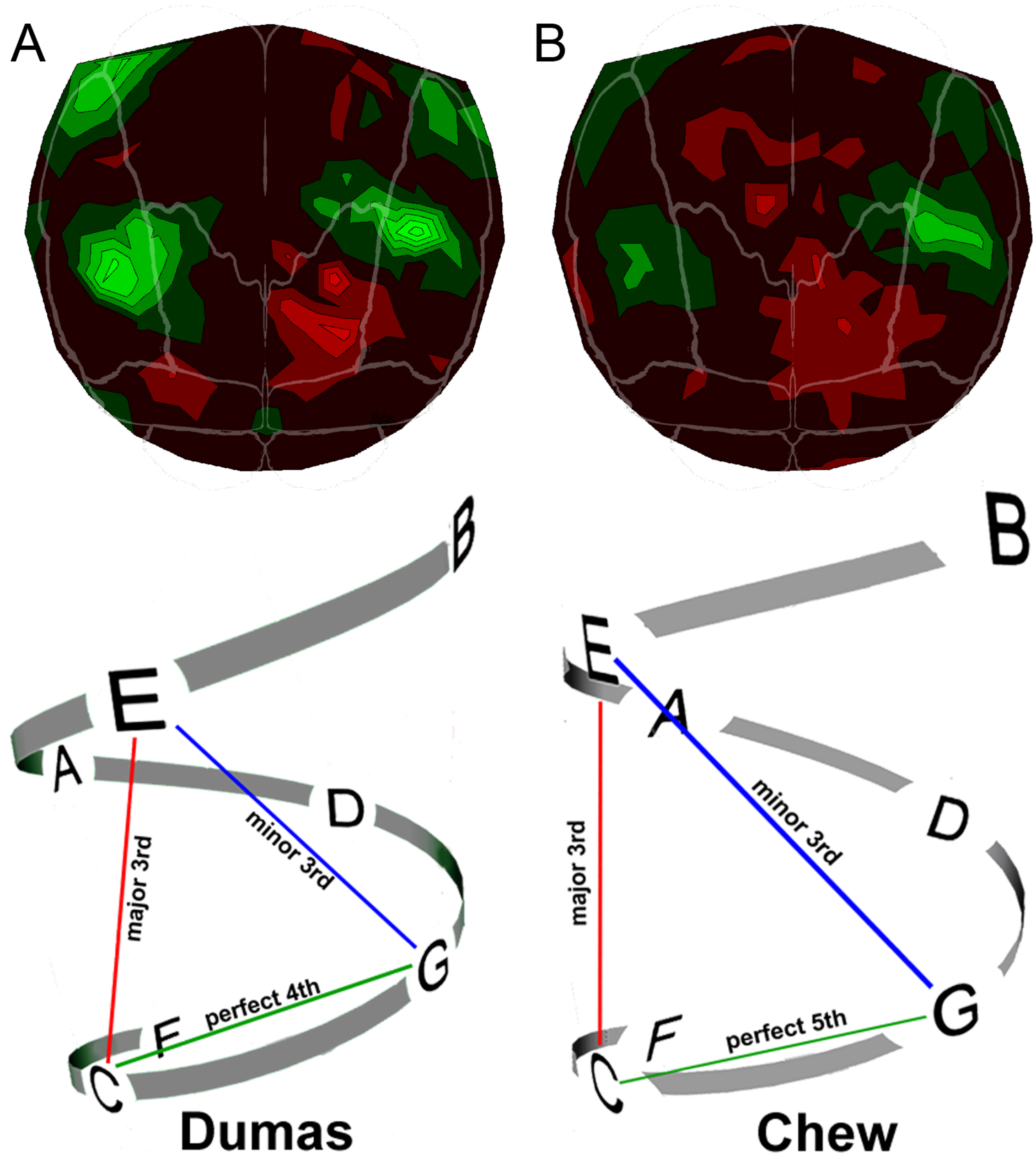

Figure 5-2. MEG sensor plots of relations between brain activity and stimulus melodic interval distance in two models of diatonic tonal space. a) Dumas P4h. b) Chew SAM. The strength and number of both positively- and negatively-correlated brain signals are larger for the P4h plot.

Experiment D produced highly significant, positive relations ($p < .0001$) between the neural activity for each melodic interval and the -log of the probability of that interval's occurrence in the corpus. Signs of melodic perplexity processing appeared in bilateral prefrontal, midline, superior parietal and occipital cortex, sparing posterior lateral cortical areas (including primary auditory cortex). Previous studies also implicate prefrontal cortex in melody discrimination (Brown & Martinez, 2007), pitch identification (Bermudez & Zatorre, 2005), representations of auditory Gestalten (Koelsch, 2011), and passive music listening (Ohnishi et al., 2001).

These results suggest that music appreciation involves prediction. When an unexpected note arrives, the brain taps a “perplexity sub-network” to deal with it. Different analyses (MIP and SAC) of the same data show strong relations in the bilateral frontal and prefrontal areas. Although their measures of melodic complexity were different, namely auto-correlation and melodic interval probability, both analyses produced similar sub-networks. The absence of anterior temporal activity is most notable, especially in light of the role played by this region in processing movement through tonal space.

Chapter 6. Concluding remarks and future directions

The ability relate cortical activity to distinct features of a musical stimulus may prove fruitful in understanding the human brain in health as well as illness. Through extensive cross-correlation analysis, we have demonstrated that the music listener's brain responds to systematic, quantifiable variation in melodic pitch, contour, interval distance and perplexity. We have also demonstrated that neural sub-networks involved in processing these features are found in both hemispheres, but primarily in frontal regions for pitch, contour and perplexity.

Further analysis of the MEG data from the auto-correlation stimulus trials should provide more information about how the brain responds to different melodic contours. In addition, data from trials in which composed melodies were played to subjects has yet to be examined. Our analysis of this data could lead to better understanding of musical expectation, if not to an innovative new field of music cognition. *Melody prediction* research could be the path leading to the development of a real-time, brain-to-music interface. As well as increasing our knowledge of the human mind, it is my hope that this methodology will prove useful as both an aid in the diagnosis and treatment of mental illness, and as a facilitator of non-verbal communication and self-expression.

Bibliography

Bach, J. S. (1713). Brandenburg Concerto No. 3 in G.

Barlow, H., & Morgenstern, S. (1948). *A Dictionary of Musical Themes*. (H. Barlow & S. Morgenstern, Eds.) (Sixth., p. 642). New York: Crown.

Bermudez, P., & Zatorre, R. J. (2005). Conditional associative memory for musical stimuli in nonmusicians: implications for absolute pitch. *The Journal of neuroscience : the official journal of the Society for Neuroscience*, *25*(34), 7718–7723.

Brower, C. (2008). Paradoxes of Pitch Space. *Music Analysis*, *27*(1), 51–106. doi:10.1111/j.1468-2249.2008.00268.x

Brown, S., & Martinez, M. J. (2007). Activation of premotor vocal areas during musical discrimination. *Brain and cognition*, *63*(1), 59–69.

Brown, S., Martinez, M. J., & Parsons, L. M. (2006). Music and language side by side in the brain: a PET study of the generation of melodies and sentences. *The European journal of neuroscience*, *23*(10), 2791–803. doi:10.1111/j.1460-9568.2006.04785.x

Chait, M., Poeppel, D., & Simon, J. Z. (2006). Neural response correlates of detection of monaurally and binaurally created pitches in humans. *Cerebral cortex (New York, N.Y. : 1991)*, *16*(6), 835–848. doi:10.1093/cercor/bhj027

Changizi, M. (2011). *Harnessed: How Language and Music Mimicked Nature and Transformed Ape to Man* (p. 242). BenBella Books, Inc. Retrieved from http://changizi.wordpress.com/book-harnessed/

Chew, E. (2000). Towards a Mathematical Model of Tonality.

Chew, E. (2003). Thinking Out of the Grid and Inside the Spiral – Geometric Interpretations of and Comparisons with the Spiral Array Model. *Network*. Retrieved from http://lit.gfax.ch/Interpretations of and Comparisons with the Spiral Array Model.pdf

Cohn, R. (1998). Neo-Riemannian Tonal Theory: A Survey and a Historical Perspective. *Journal of Music Theory*, *42*(2), 167–180. Retrieved from http://www.jstor.org/stable/10.2307/843871

De Manzano, O., & Ullén, F. (2012). Activation and connectivity patterns of the presupplementary and dorsal premotor areas during free improvisation of melodies and rhythms. *NeuroImage*, *63*(1), 272–280. Retrieved from http://www.ncbi.nlm.nih.gov/pubmed/22732560

Debussy, C. (1913). Syrinx.

Deutsch, D. (1987). Illusions For Stereo Headphones. *Audio*, (March), 36–48.

Ellis, R. J., Norton, A. C., Overy, K., Winner, E., Alsop, D. C., & Schlaug, G. (2012). Differentiating maturational and training influences on fMRI activation during music processing. *NeuroImage*, 1–11. doi:10.1016/j.neuroimage.2012.01.138

Fujioka, T., Trainor, L. J., Ross, B., Kakigi, R., & Pantev, C. (2004). Musical training enhances automatic encoding of melodic contour and interval structure. *Journal of cognitive neuroscience*, *16*(6), 1010–1021. doi:10.1162/0898929041502706

Georgopoulos, A. P., Karageorgiou, E., Leuthold, A. C., Lewis, S. M., Lynch, J. K., Alonso, A., Aslam, Z., et al. (2007). Synchronous neural interactions assessed by magnetoencephalography: a functional biomarker for brain disorders. *J.Neural Eng.*, *4*(4), 349. doi:doi:10.1088/1741-2560/4/4/001

Gibson, G. N., & Johnston, I. D. (2002). New Themes and Audiences for the Physics of Music. *Physics Today*, *55*(1), 42. doi:10.1063/1.1457264

Gollin, E. (2011). Three-Dimensional Tonnetze. *Journal of Music Theory*, *42*(2), 195–206. Retrieved from http://www.jstor.org/stable/10.2307/843873

Granier-Deferre, C., Bassereau, S., Ribeiro, A., Jacquet, A.-Y., & DeCasper, A. J. (2011). A Melodic Contour Repeatedly Experienced by Human Near-Term Fetuses Elicits a Profound Cardiac Reaction One Month after Birth. (G. Chapouthier, Ed.)*PLoS ONE*, *6*(2), 10. Retrieved from http://www.pubmedcentral.nih.gov/articlerender.fcgi?artid=3044162&tool=pmcentrez&rendertype=abstract

Hari, R. (1990). The Neuromagnetic method in the study of the human auditory cortex. In F. Grandori, M. Hoke, & G. L. Romani (Eds.), *Auditory evoked magnetic fields and electric potentials* (vol 6., pp. 222–282). Basel: Advanced Audiology.

Hashimoto, T., Hirata, Y., & Kuriki, S. (2000). Auditory cortex responds in 100 ms to incongruity of melody. *Neuroreport*, *11*(12), 2799–2801. Retrieved from http://www.ncbi.nlm.nih.gov/pubmed/10976966

Hauser, M. D. (2000). The sound and the fury: Primate vocalizations as reflections of emotion and thought. In N. L. Wallin & B. Merker (Eds.), *The origins of music* (pp. 77–102). MIT Press.

Herholz, S. C., Halpern, A. R., & Zatorre, R. J. (2012). Neuronal correlates of perception, imagery, and memory for familiar tunes. *Journal of cognitive neuroscience*, *24*(6), 1382–97. Retrieved from http://www.ncbi.nlm.nih.gov/pubmed/22360595

Hyer, B. (1995). Reimag(in)ing Riemann. *Journal of Music Theory*, *39*(1), pp. 101–138. Retrieved from http://www.jstor.org/stable/843900

Janata, P., Birk, J. L., Horn, J. D. Van, Léman, M., Tillmann, B., Bharucha, J. J., Van Horn, J. D., et al. (2002). The Cortical Topography of Tonal structures Underlying Western Music. *Science*, *298*(5601), 2167. doi:10.1126/science.1076262

Jensen, C. R. (1992). A Theoretical Work Of Late Seventeenth-Century Muscovy: Nikolai Diletskii's "Grammatika" And The Earliest Circle Of Fifths. *Journal of the American Musicological Society*, *45*(2), 305. Retrieved from http://en.wikipedia.org/wiki/Nikolay_Diletsky

Johnson-Laird, P., Kang, O., & Chang Leong, Y. (2012). On Musical Dissonance. *Music Perception*, *30*(1), 19–35. Retrieved from http://www.jstor.org.ezp1.lib.umn.edu/stable/10.1525/mp.2012.30.1.19

Kanno, A., Nakasato, N., Fujita, S., Seki, K., Kawamura, T., Ohtomo, S., Fujiwara, S., et al. (1996). Right hemispheric dominance in the auditory evoked magnetic fields for pure-tone stimuli. *Electroencephalography and clinical neurophysiology. Supplement*, *47*, 129–132.

Kim, S. G., Kim, J. S., & Chung, C. K. (2011). The Effect of Conditional Probability of Chord Progression on Brain Response: An MEG Study. *PloS one*, *6*(2), e17337.

Kim, S.-G., Kim, J. S., & Chung, C. K. (2011). The effect of conditional probability of chord progression on brain response: an MEG study. *PloS one*, *6*(2), e17337. Retrieved from http://www.pubmedcentral.nih.gov/articlerender.fcgi?artid=3045443&tool=pmcentrez&rendertype=abstract

Koelsch, S. (2011). Toward a neural basis of music perception - a review and updated model. *Frontiers in psychology*, *2*(June), 110. doi:10.3389/fpsyg.2011.00110

Koelsch, S., Maess, B., Gunter, T. C., & Friederici, A. D. (2001). Neapolitan chords activate the area of Broca. A magnetoencephalographic study. *Annals of the New York Academy of Sciences*, *930*, 420–421.

Krumhansl, C. L. (1990). *Cognitive Foundations of Musical Pitch* (p. 307). New York: Oxford University Press.

Krumhansl, C. L., & Kessler, E. J. (1982). Tracing the dynamic changes in perceived tonal organization in a spatial representation of musical keys. *Psychological review*, *89*(4), 334–368.

Kuriki, S., Isahai, N., & Ohtsuka, A. (2005). Spatiotemporal characteristics of the neural activities processing consonant/dissonant tones in melody. *Experimental brain research Experimentelle Hirnforschung Expérimentation cérébrale*, *162*(1), 46–55. doi:10.1007/s00221-004-2114-8

Larson, S., & McAdams, S. (2004). Musical Forces and Melodic Expectations: Comparing Computer Models and Experimental Results. *Music Perception: An Interdisciplinary Journal*, *21*(4), pp. 457–498. Retrieved from http://www.jstor.org/stable/10.1525/mp.2004.21.4.457

Lee, Y.-S. S., Janata, P., Frost, C., Hanke, M., & Granger, R. (2011). Investigation of melodic contour processing in the brain using multivariate pattern-based fMRI. *NeuroImage*, *57*(1), 293–300. doi:10.1016/j.neuroimage.2011.02.006

Lerdahl, F. (1988). Tonal Pitch Space. *Music Perception*, *5*(3), 315–349.

Lerdahl, F. (2001). *Tonal pitch space* (p. 411). New York: Oxford University Press.

Levitin, D. J., & Tirovolas, A. K. (2011). Twenty-six years of Music Perception: Trends in the field. *Society for Music Perception & Cognition meeting*.

Limb, C. J., Kemeny, S., Ortigoza, E. B., Rouhani, S., & Braun, A. R. (2006). Left hemispheric lateralization of brain activity during passive rhythm perception in musicians. *The anatomical record.Part A, Discoveries in molecular, cellular, and evolutionary biology*, *288*(4), 382–389.

Longuet-Higgins, H C. (1962). Quantum mechanics and biology. *Biophysical journal*, *2*(2 Pt 2), 207–215.

Longuet-Higgins, H. C. (1962). Letter to a musical friend. *Music Review*, *23*, 244–248.

Lounasmaa, O. V, Hamalainen, M., Hari, R., & Salmelin, R. (1996). Information processing in the human brain: magnetoencephalographic approach. *Proceedings of the National Academy of Sciences of the United States of America*, *93*(17), 8809–8815.

Lubin, S. (New Y. U. (1974). *Techniques for the Analysis of Development in Middle-Period Beethoven*. Retrieved from http://tonnetz.zxq.net/surfaceForm.html

Maess, B., Jacobsen, T., Schroger, E., & Friederici, A. D. (2007). Localizing pre-attentive auditory memory-based comparison: magnetic mismatch negativity to pitch change. *NeuroImage*, *37*(2), 561–571.

Maess, B., Koelsch, S., Gunter, T. C., & Friederici, A. D. (2001). Musical syntax is processed in Broca's area: an MEG study. *Nature neuroscience*, *4*(5), 540–545.

Matsui, T., Tanaka, S., Kazai, K., Tsuzaki, M., & Katayose, H. (2013). Activation of the left superior temporal gyrus of musicians by music-derived sounds. *Neuroreport*, *24*(1), 41–5. doi:10.1097/WNR.0b013e32835c1e02

Meyer, L. (1956). *Emotion and meaning in music*. Chicago: University of Chicago Press.

Minor, N. (1978). Harmony , Structure & Expectancy : Music Theory pitch (space) — > time — >. *Music Perception*, 1–5.

Narmour, E. (1990). *The analysis and cognition of basic melodic structures : the implication-realization model* (p. 485). Chicago: University of Chicago Press.

Nemoto, I. (2012). Evoked magnetoencephalographic responses to omission of a tone in a musical scale. *The Journal of the Acoustical Society of America*, *131*(6), 4770–84. Retrieved from http://www.ncbi.nlm.nih.gov/pubmed/22712949

Normal equal-loudness-level contours - ISO 226 : 2003 Acoustics International Organization for Standardization (ISO) 2nd edition. (2005).*International Organization*, 2005–2005.

Ohnishi, T., Matsuda, H., Asada, T., Aruga, M., Hirakata, M., Nishikawa, M., Katoh, A., et al. (2001). Functional anatomy of musical perception in musicians. *Cerebral cortex (New York, N.Y. : 1991)*, *11*(8), 754–60. Retrieved from http://www.ncbi.nlm.nih.gov/pubmed/11459765

Ono, K., Nakamura, A., Yoshiyama, K., Kinkori, T., Bundo, M., Kato, T., & Ito, K. (2011). The effect of musical experience on hemispheric lateralization in musical feature processing. *Neuroscience letters*, *496*(2), 141–5. Retrieved from http://www.ncbi.nlm.nih.gov/pubmed/21513771

Parncutt, R. (2009). Prenatal and infant conditioning, the mother schema, and the origins of music and religion. *Musicae Scientiae*, *13*(2 Suppl), 119–150. doi:10.1177/1029864909013002071

Parncutt, R. (2011). The Tonic as Triad: Key Profiles as Pitch Salience Profiles of Tonic Triads. *Music Perception: An Interdisciplinary Journal*, *28*(4), pp. 333–366. doi:10.1525/mp.2011.28.4.333

Patel, A. D., & Balaban, E. (2001). Human pitch perception is reflected in the timing of stimulus-related cortical activity. *Nature neuroscience*, *4*(8), 839–844. doi:10.1038/90557

Patterson, R. D., Uppenkamp, S., Johnsrude, I. S., & Griffiths, T. D. (2002). The processing of temporal pitch and melody information in auditory cortex. *Neuron*, *36*(4), 767–776. Retrieved from http://www.ncbi.nlm.nih.gov/pubmed/12441063

Pearce, M. T., & Wiggins, G. A. (2006). Expectation in Melody: The Influence of Context and Learning. *Music Perception*, *23*(5), 377–405. Retrieved from http://www.jstor.org/stable/40285982

Purwins, H., & Hardoon, D. R. (2009). Trends and perspectives in music cognition research and technology. *Connection Science*, *21*(2-3), 85–88. doi:10.1080/09540090902734549

Rushton, J. (2004). Perfect Consonance. Retrieved April 30, 2004, from <http://www.grovemusic.com>

Schneider, P., Sluming, V., Roberts, N., Scherg, M., Goebel, R., Specht, H. J., Dosch, H. G., et al. (2005). Structural and functional asymmetry of lateral Heschl's gyrus reflects pitch perception preference. *Nature neuroscience*, *8*(9), 1241–1247. doi:10.1038/nn1530

Shepard, R. N. (1982). Geometrical approximations to the structure of musical pitch. (D. Deutsch, Ed.)*Psychological Review*, *89*(4), 335–353. Retrieved from http://psycnet.apa.orgjournals/rev/89/4/305

Steinbeis, N., Koelsch, S., & Sloboda, J. A. (2006). The role of harmonic expectancy violations in musical emotions: evidence from subjective, physiological, and neural responses. *Journal of cognitive neuroscience*, *18*(8), 1380–1393.

Stryer, L. (1995). *Biochemistry* (4th ed., pp. 27–30). New York: W. H. Freeman & Company.

Teki, S., Kumar, S., Kriegstein, K. Von, Stewart, L., Lyness, C. R., Moore, B. C. J., Capleton, B., et al. (2012). Navigating the Auditory Scene : An Expert Role for the Hippocampus, *32*(35), 12251–12257. doi:10.1523/JNEUROSCI.0082

Toiviainen, P., & Krumhansl, C. L. (2003). Measuring and modeling real-time responses to music: the dynamics of tonality induction. *Perception*, *32*(6), 741–766. doi:10.1068/p3312

Yasui, T., Kaga, K., & Sakai, K. L. (2009). Language and music: differential hemispheric dominance in detecting unexpected errors in the lyrics and melody of memorized songs. *Human Brain Mapping*, *30*(2), 588–601. doi:10.1002/hbm.20529

Zatorre, R. J., Halpern, A. R., & Bouffard, M. (2009). Mental Reversal of Imagined Melodies: A Role for the Posterior Parietal Cortex. *Journal of cognitive neuroscience*, *22*(4), 775–89. doi:10.1162/jocn.2009.21239

Zatorre, R. J., & Krumhansl, C. L. (2002). Mental Models and Musical Minds. *Science*, *298*(5601), 2138. Retrieved from http://search.epnet.com/login.aspx?direct=true&db=aph&an=8908926

Appendix A – Experiment B plots

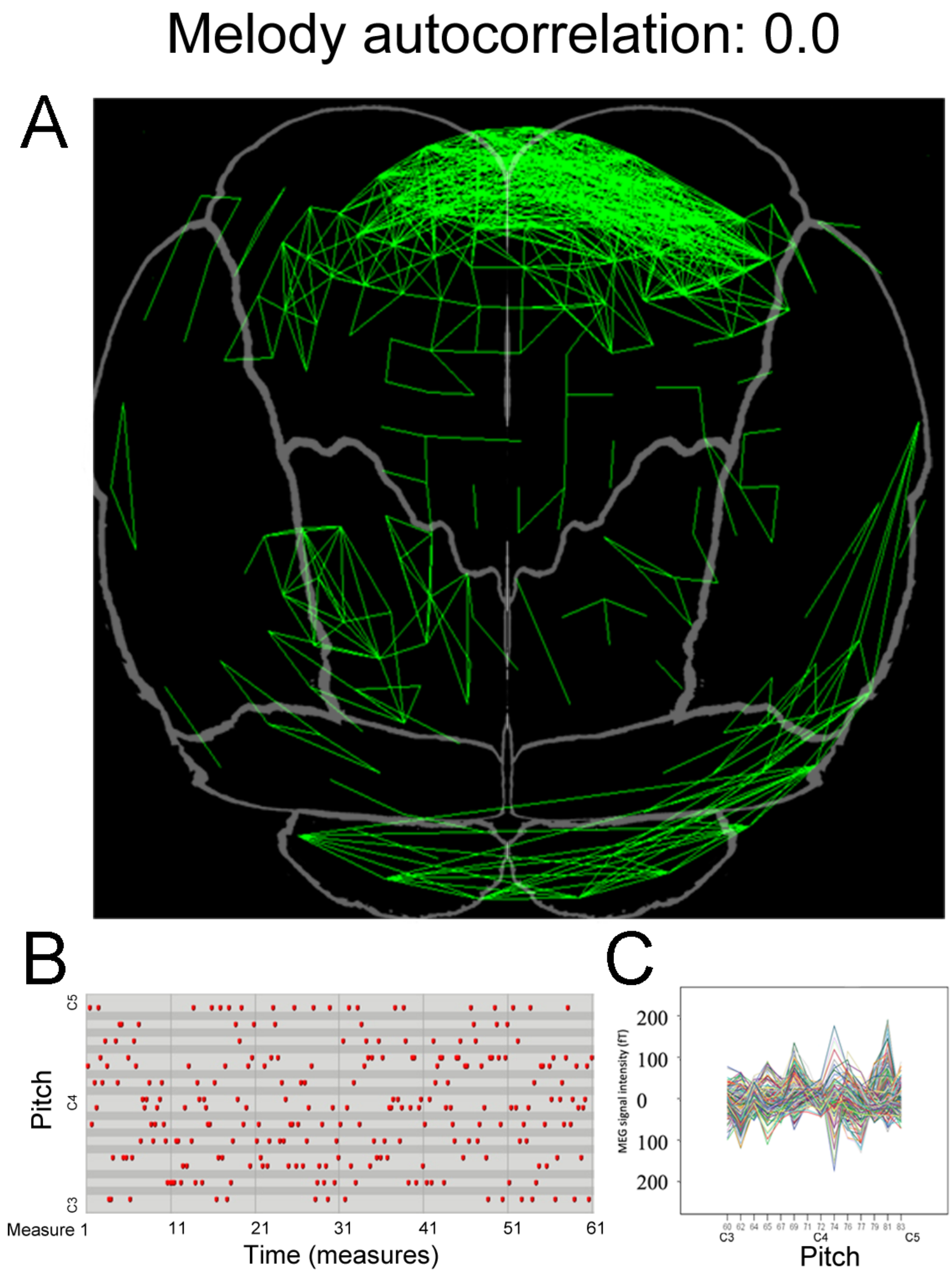

Figure 6-1. Plots for melody autocorrelation of 0.0. a) Positively correlated MEG sensors/AC across subjects. b) Piano-roll representation of sample stimulus. c) Average ACPVs across subjects for all sensors.

Melody autocorrelation: 0.1

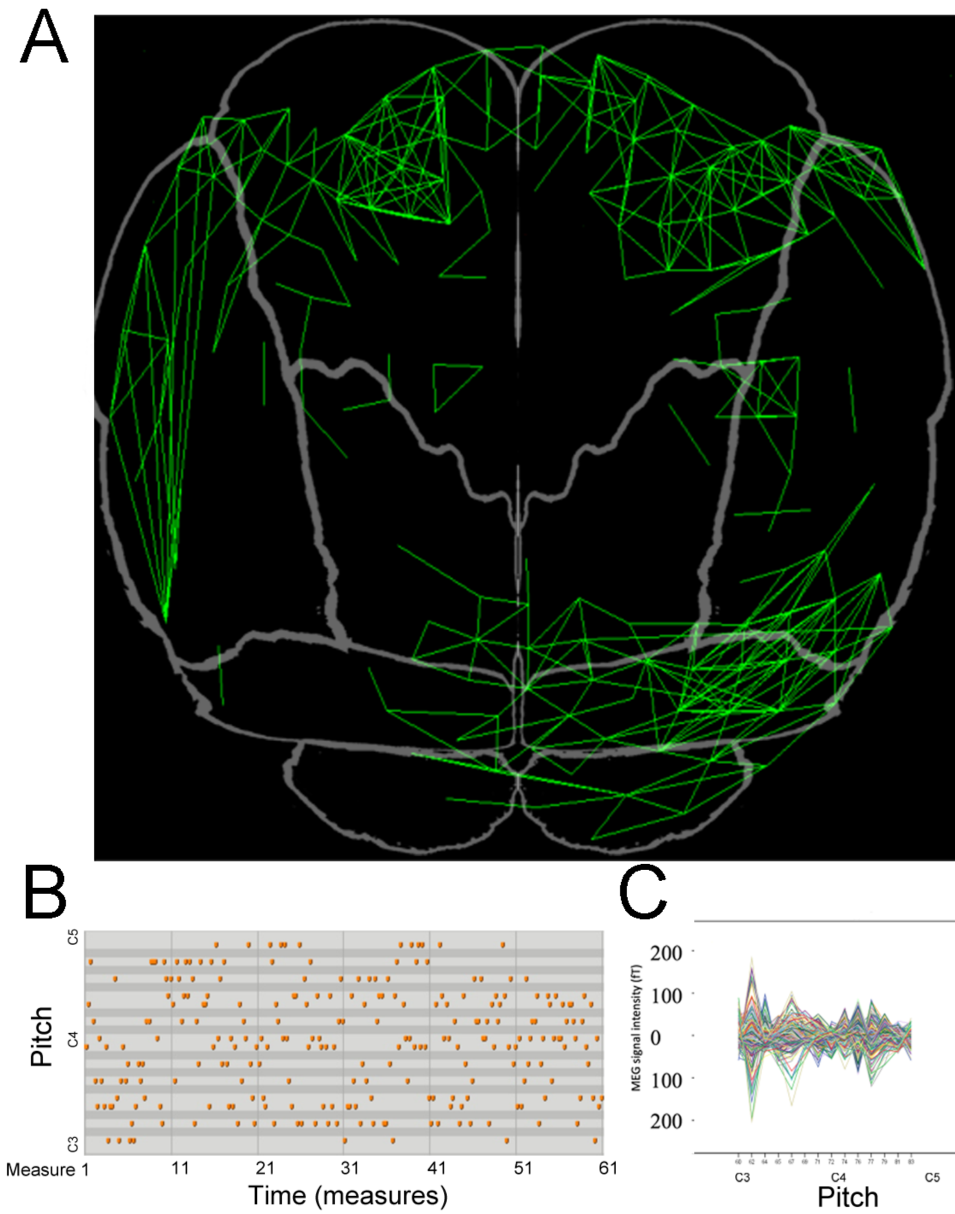

Figure 6-2. Plots for melody autocorrelation of 0.1. a) Positively correlated MEG sensors/AC across subjects. b) Piano-roll representation of sample stimulus. c) Average ACPVs across subjects for all sensors.

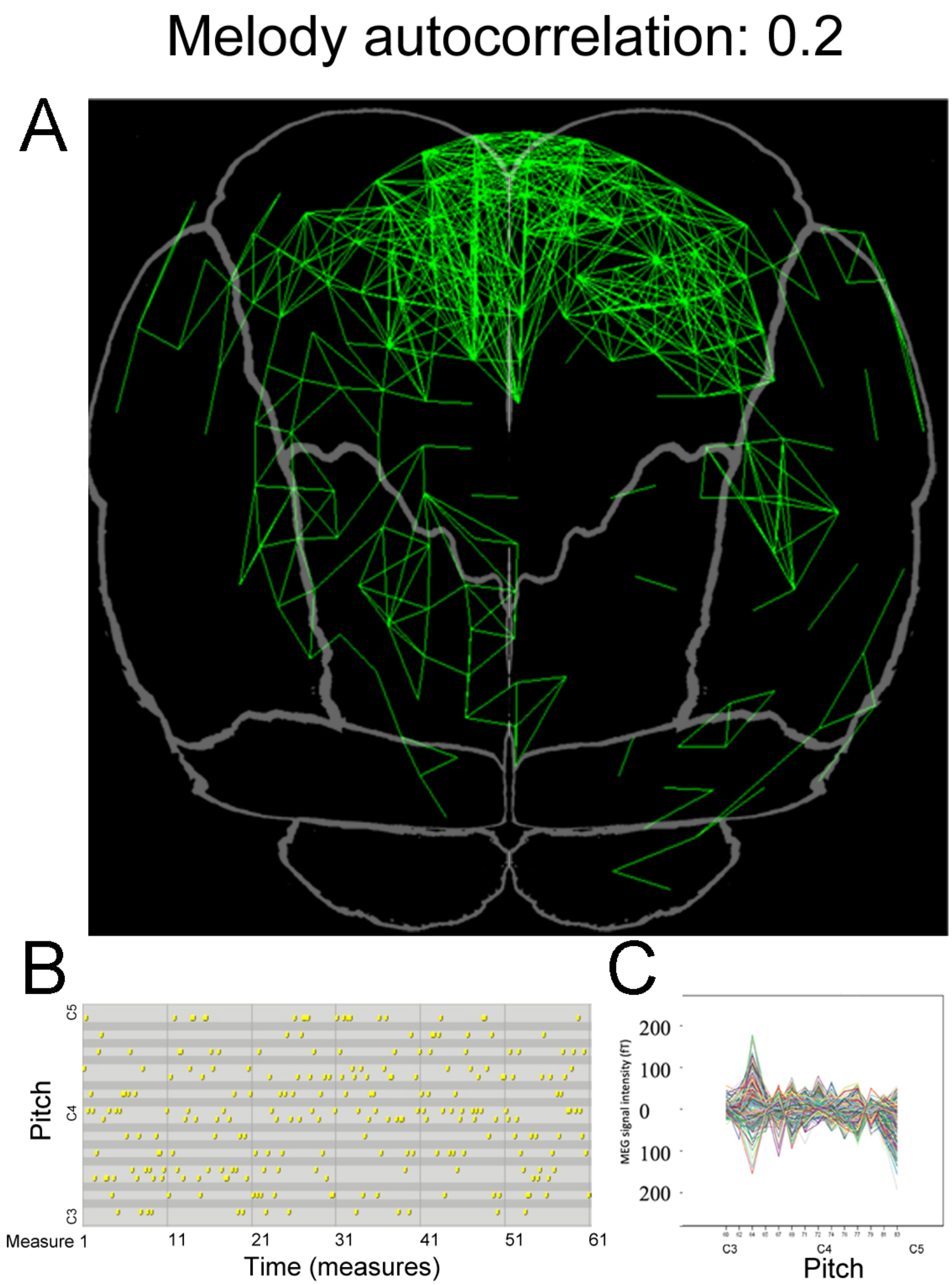

Figure 6-3. Plots for melody autocorrelation of 0.2. a) Positively correlated MEG sensors/AC across subjects. b) Piano-roll representation of sample stimulus. c) Average ACPVs across subjects for all sensors.

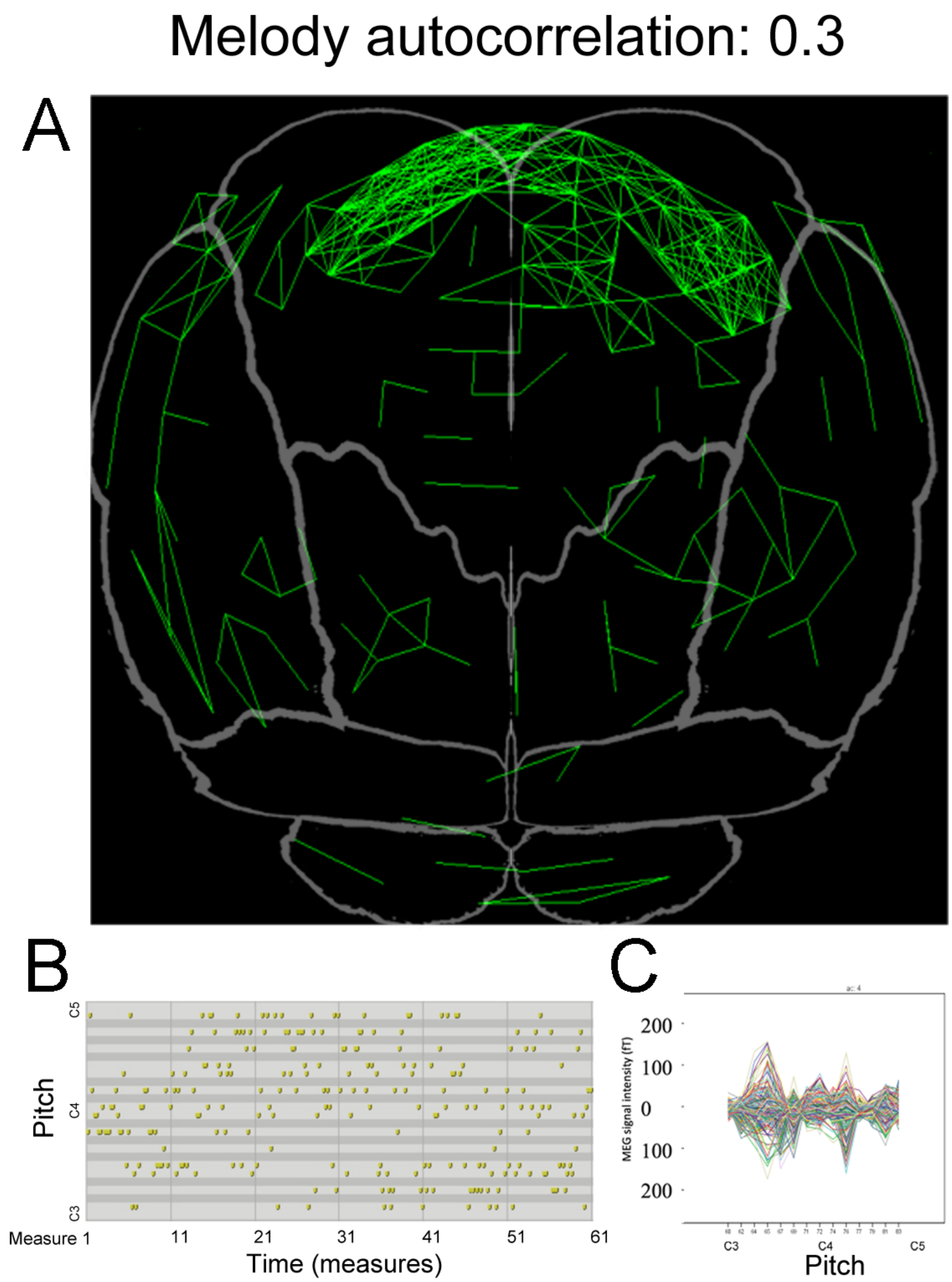

Figure 6-4. Plots for melody autocorrelation of 0.3. a) Positively correlated MEG sensors/AC across subjects. b) Piano-roll representation of sample stimulus. c) Average ACPVs across subjects for all sensors.

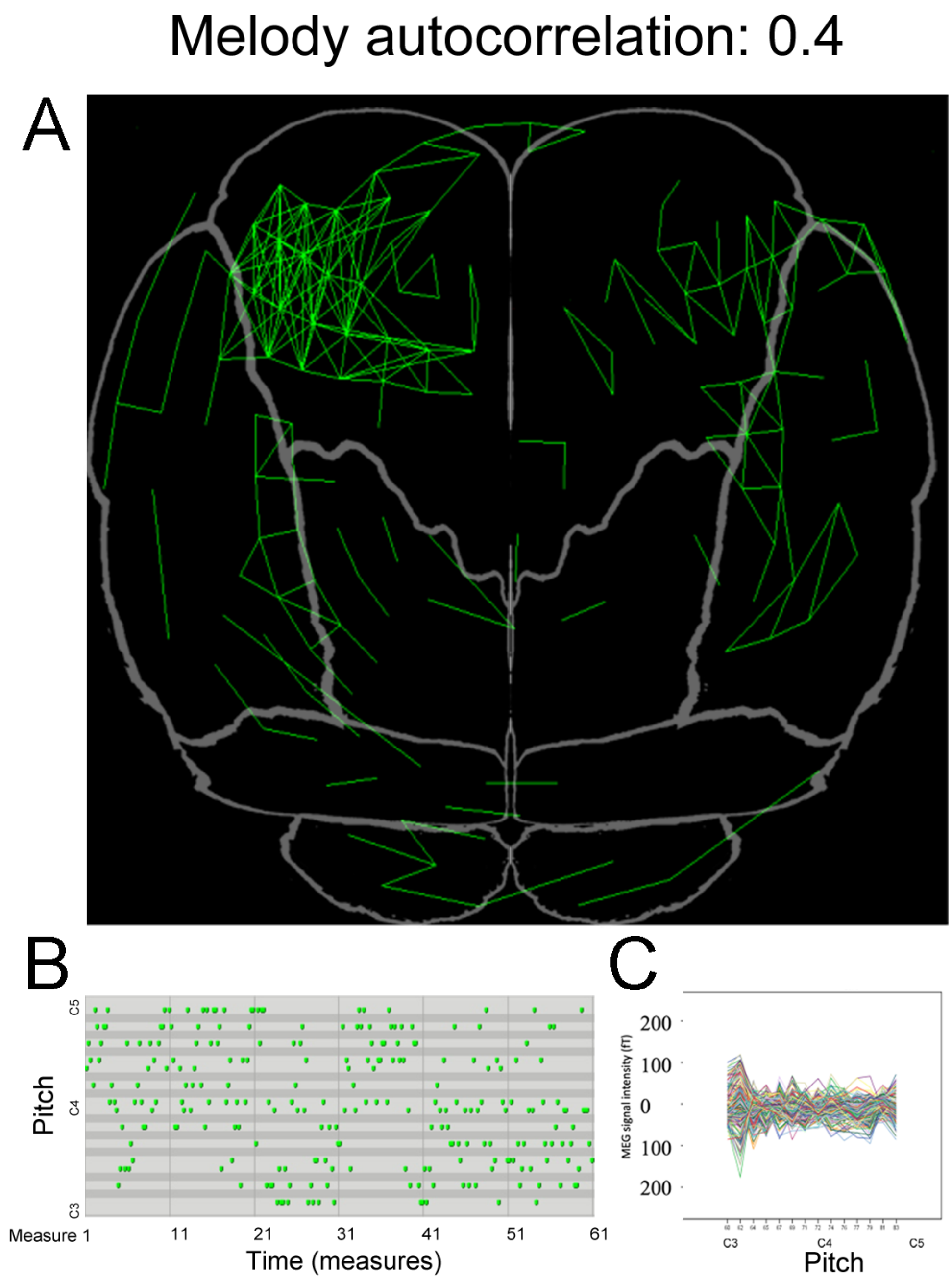

Figure 6-5. Plots for melody autocorrelation of 0.4. a) Positively correlated MEG sensors/AC across subjects. b) Piano-roll representation of sample stimulus. c) Average ACPVs across subjects for all sensors.

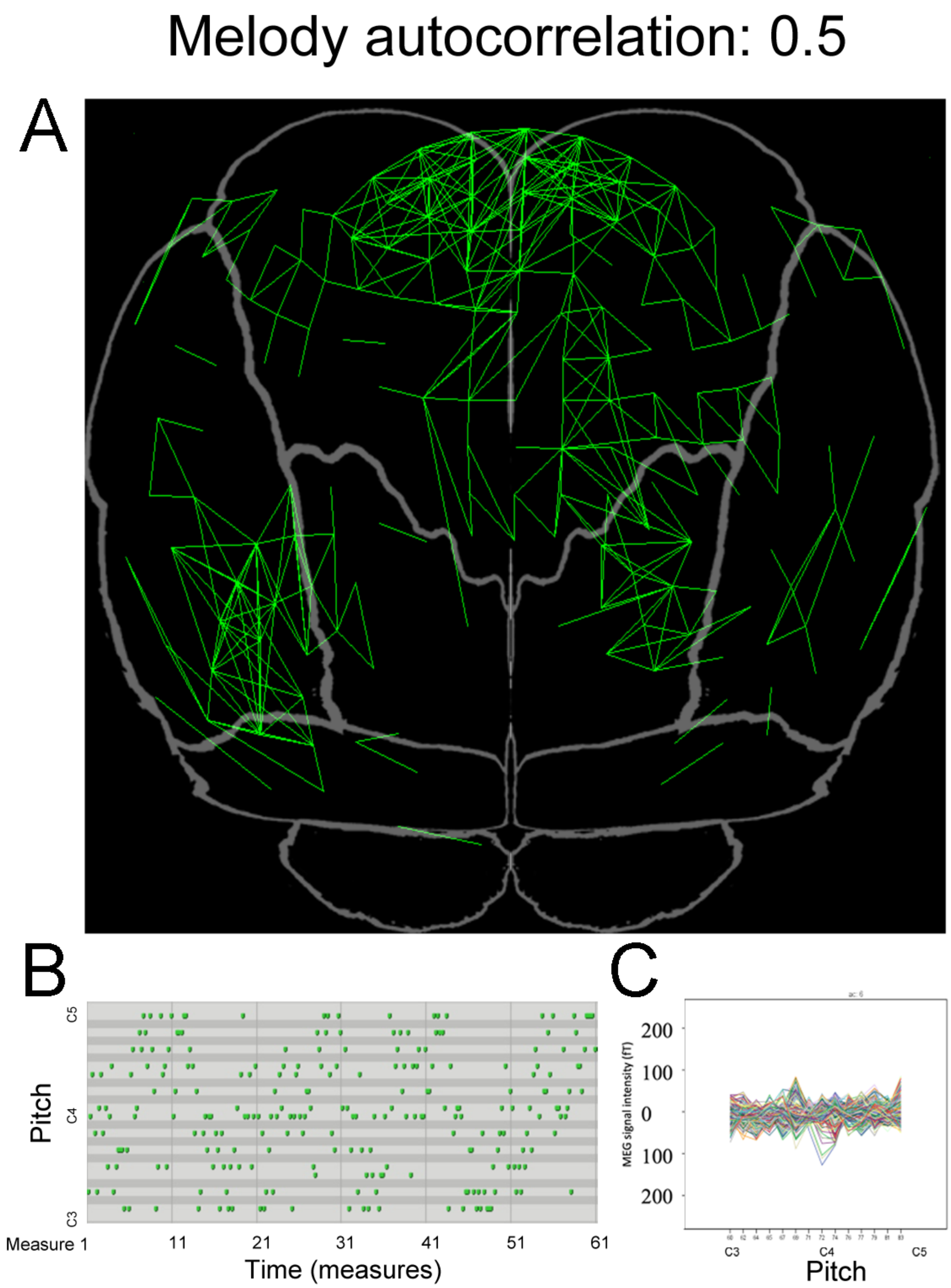

Figure 6-6. Plots for melody autocorrelation of 0.5. a) Positively correlated MEG sensors/AC across subjects. b) Piano-roll representation of sample stimulus. c) Average ACPVs across subjects for all sensors.

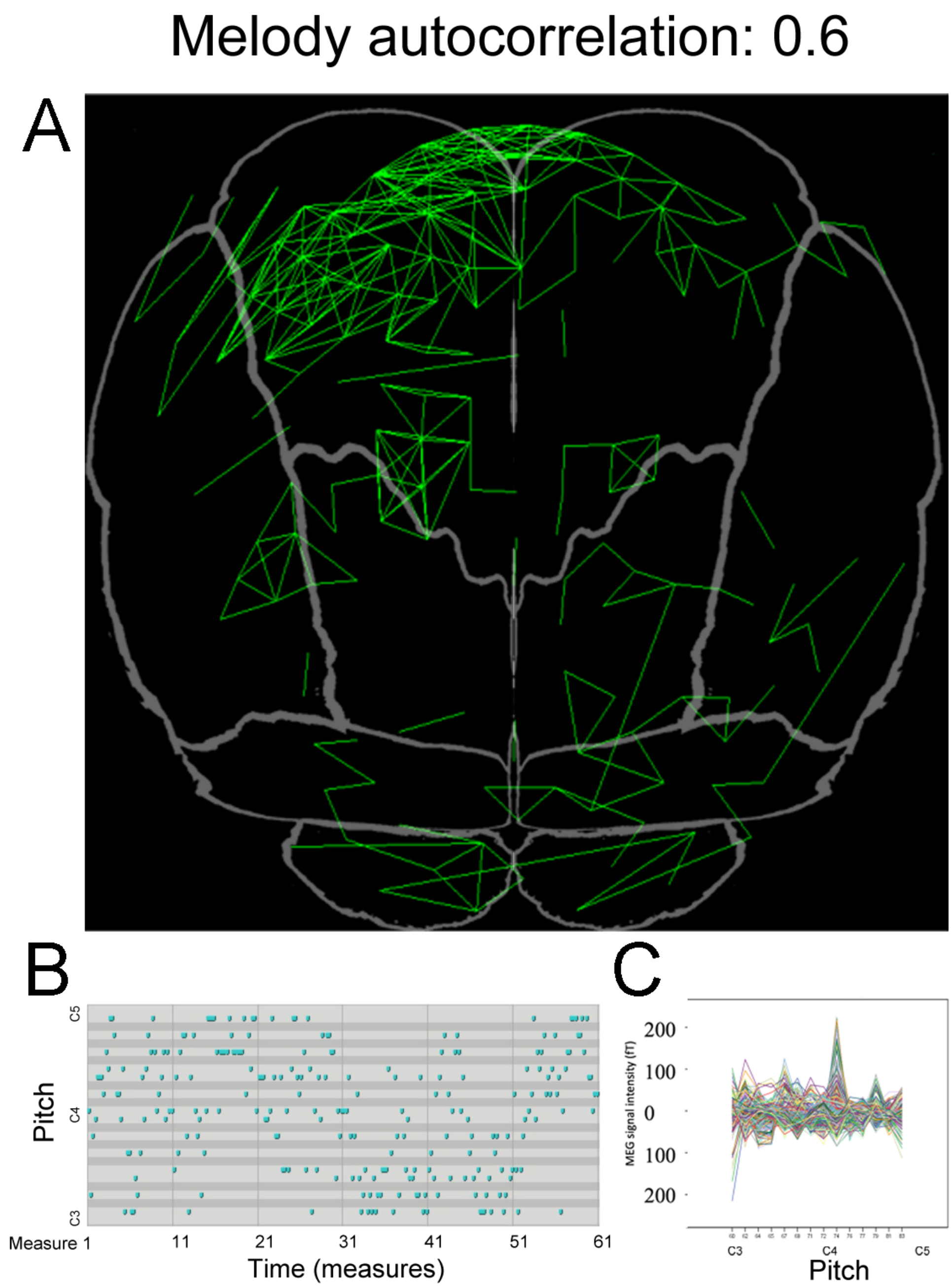

Figure 6-7. Plots for melody autocorrelation of 0.6. a) Positively correlated MEG sensors/AC across subjects. b) Piano-roll representation of sample stimulus. c) Average ACPVs across subjects for all sensors.

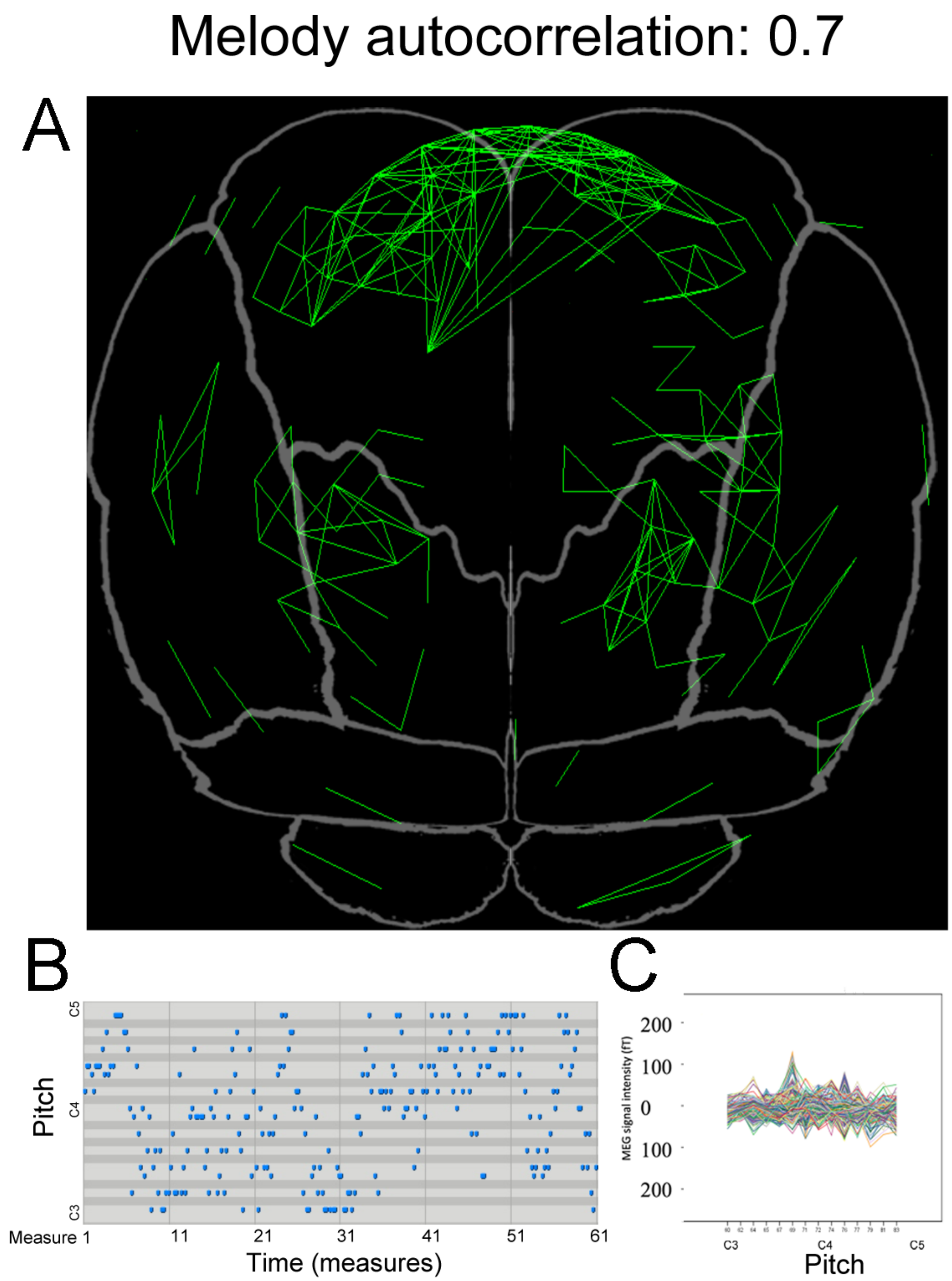

Figure 6-8. Plots for melody autocorrelation of 0.7. a) Positively correlated MEG sensors/AC across subjects. b) Piano-roll representation of sample stimulus. c) Average ACPVs across subjects for all sensors.

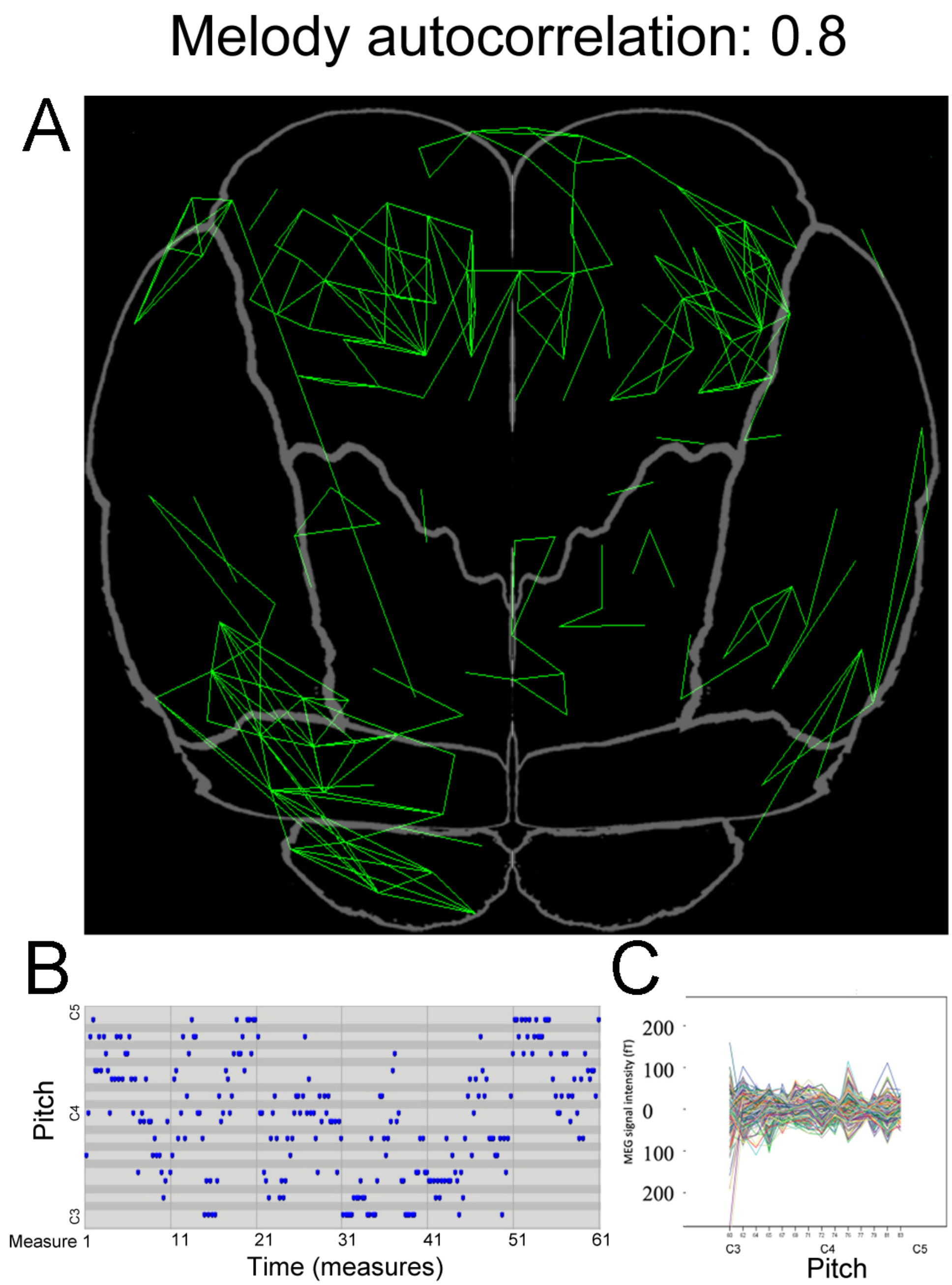

Figure 6-9. Plots for melody autocorrelation of 0.8. a) Positively correlated MEG sensors/AC across subjects. b) Piano-roll representation of sample stimulus. c) Average ACPVs across subjects for all sensors.

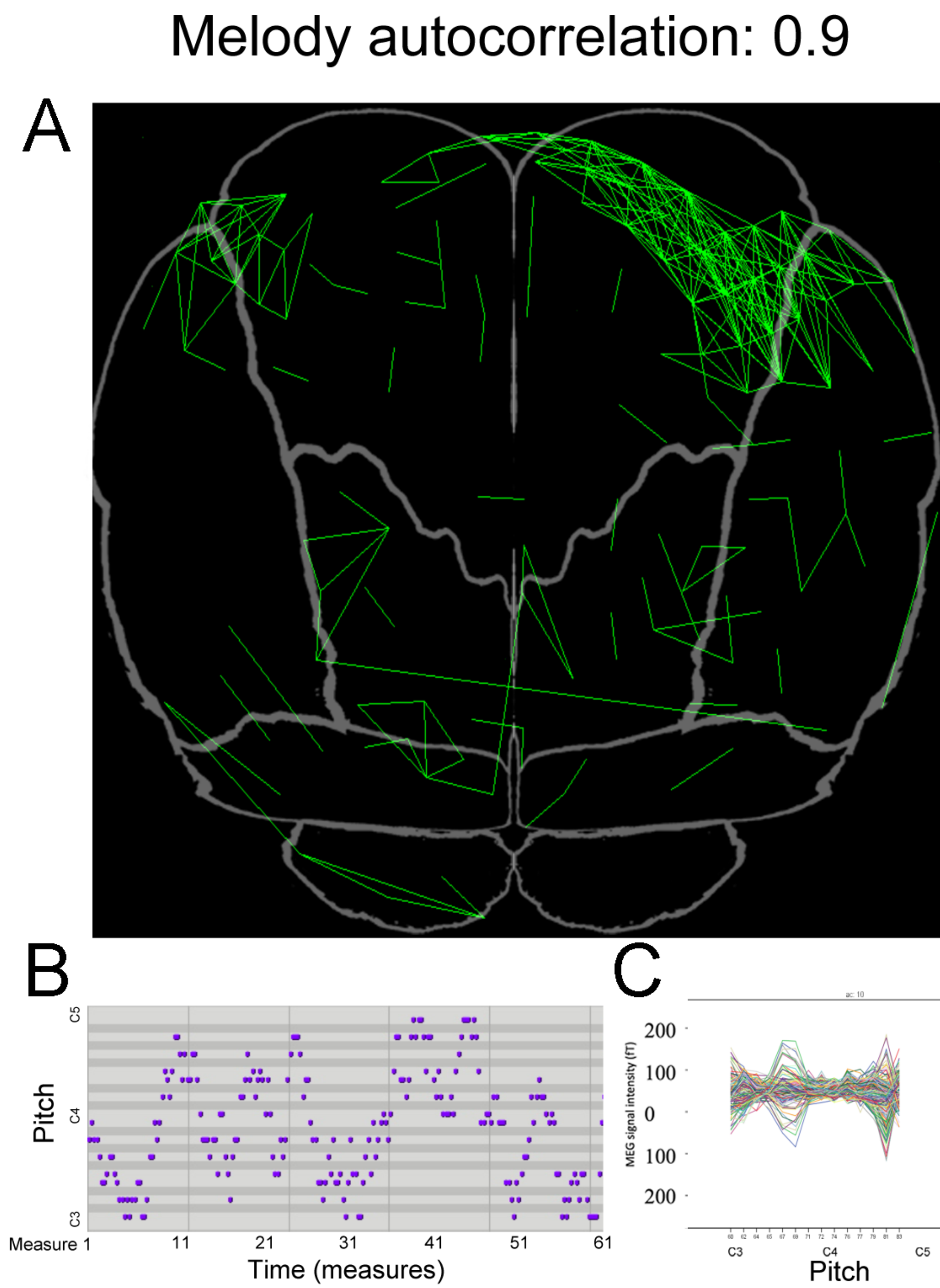

Figure 6-10. Plots for melody autocorrelation of 0.9. a) Positively correlated MEG sensors/AC across subjects. b) Piano-roll representation of sample stimulus. c) Average ACPVs across subjects for all sensors.

Appendix B: Experiment C MEG sensor plots

Tonal space #1: -log Frequency

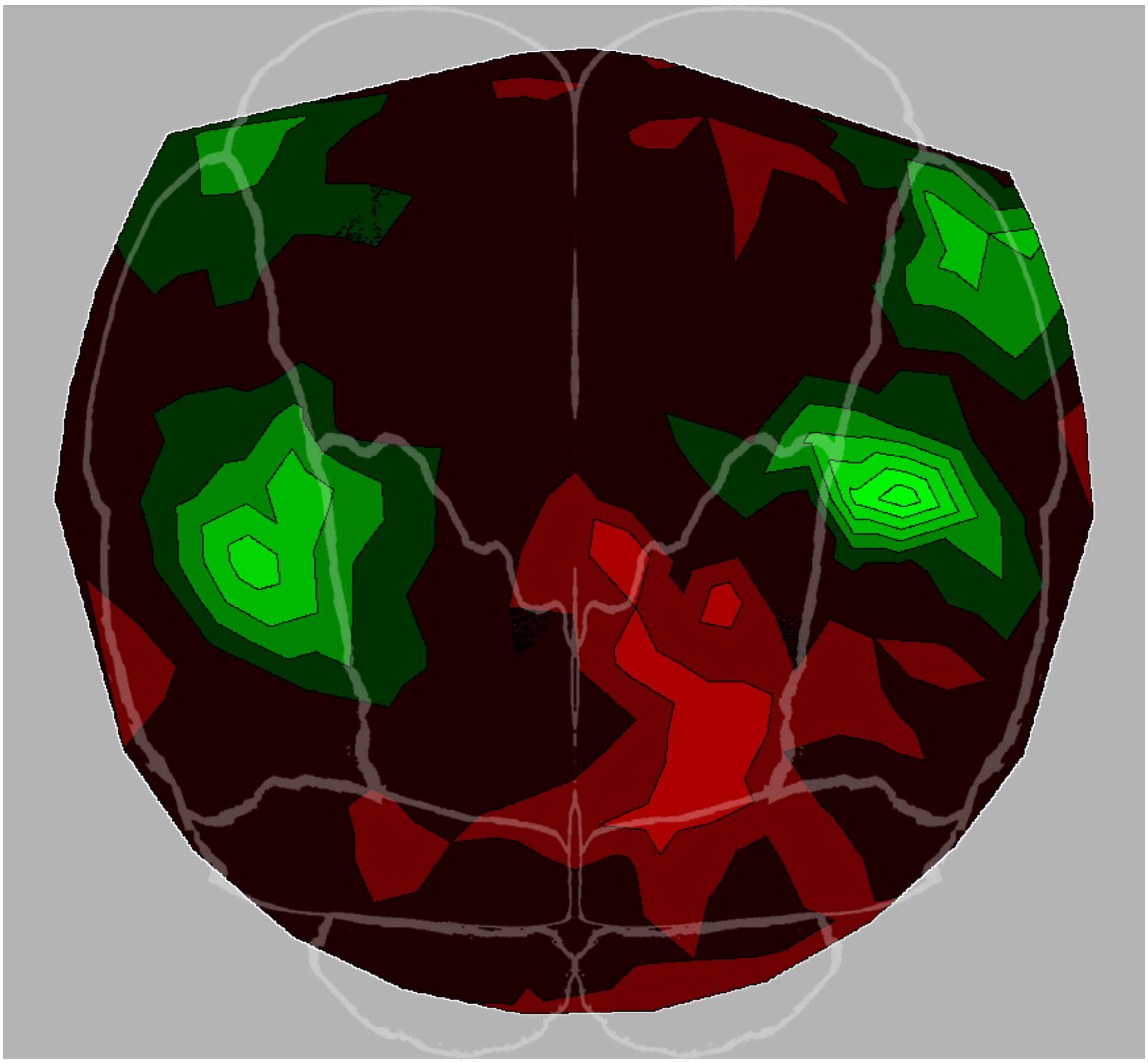

Figure 6-11. Neural-tonal map: -log frequency. Regression coefficient (b) significance [-ln(p), $p < 0.05$] per sensor across all stimuli and subjects. Green = positive relations, red = negative. Bright colors indicate higher significance.

Tonal space #2: Longuet-Higgins harmonic space

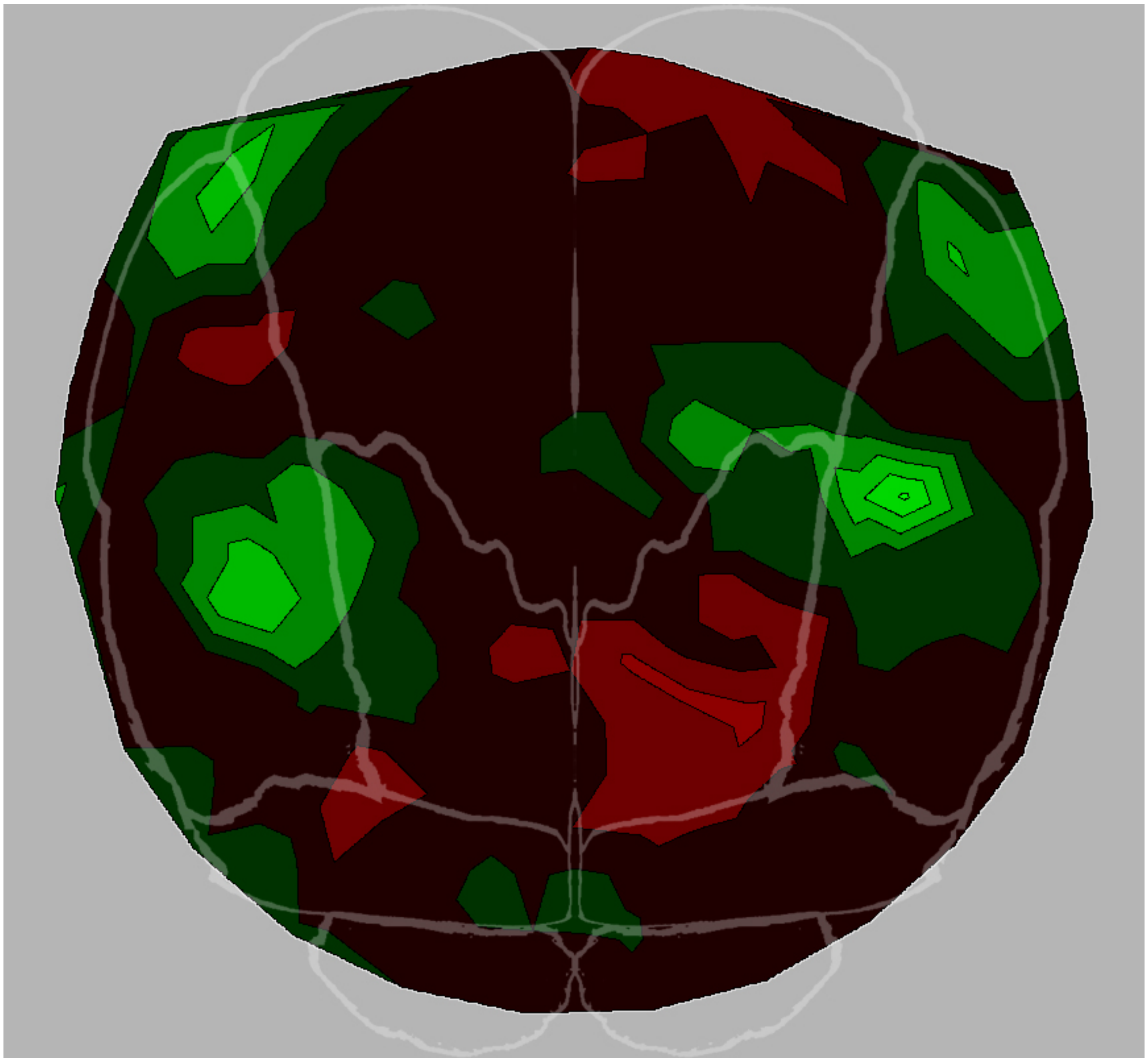

Figure 6-12. Neural-tonal map: Longuet-Higgins harmonic space. Regression coefficient (b) significance [-ln(p), $p < 0.05$] per sensor across all stimuli and subjects. Green = positive relations, red = negative. Bright colors indicate higher significance.

Tonal space #3: Dumas perfect 4th helix

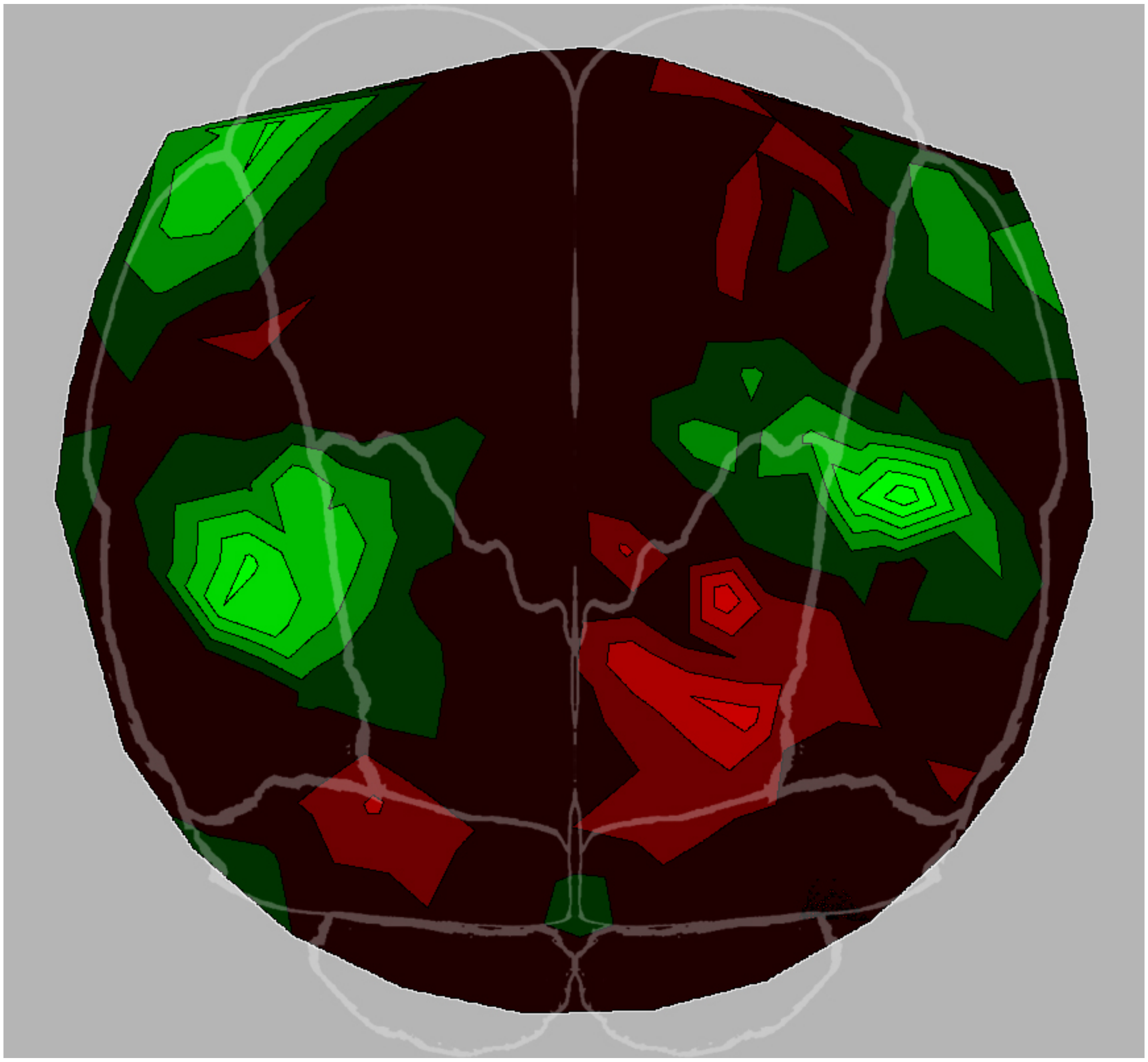

Figure 6-13. Neural-tonal map: Dumas perfect 4th helix. Regression coefficient (b) significance [-ln(p), $p < 0.05$] per sensor across all stimuli and subjects. Green = positive relations, red = negative. Bright colors indicate higher significance.

Tonal space #4: Krumhansl & Kessler probe tone profile

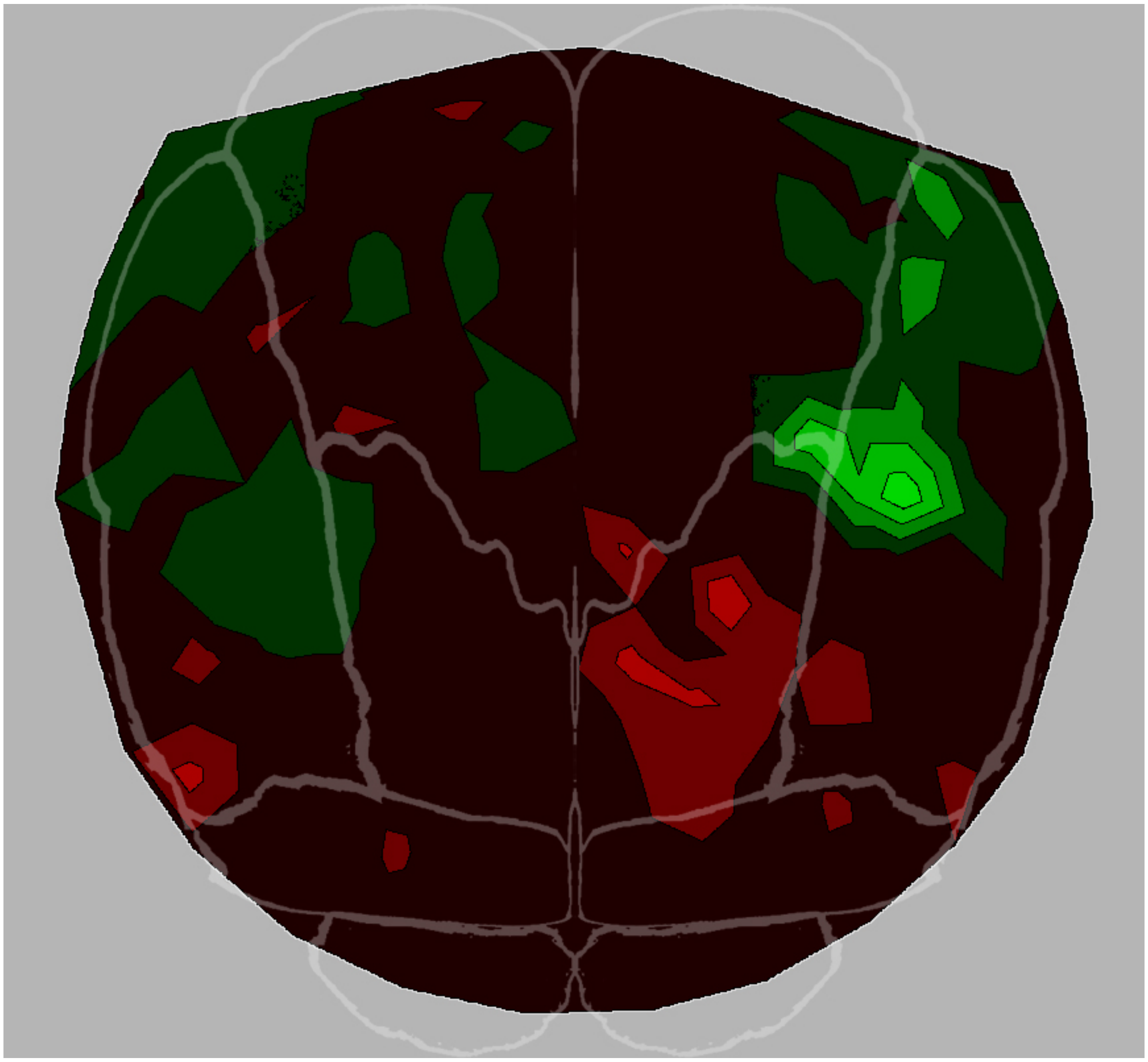

Figure 6-14. Neural-tonal map: Krumhansl & Kessler probe tone profile. Regression coefficient (b) significance [-ln(p), $p < 0.05$] per sensor across all stimuli and subjects. Green = positive relations, red = negative. Bright colors indicate higher significance.

Tonal space #5: Parncutt chroma salience profile

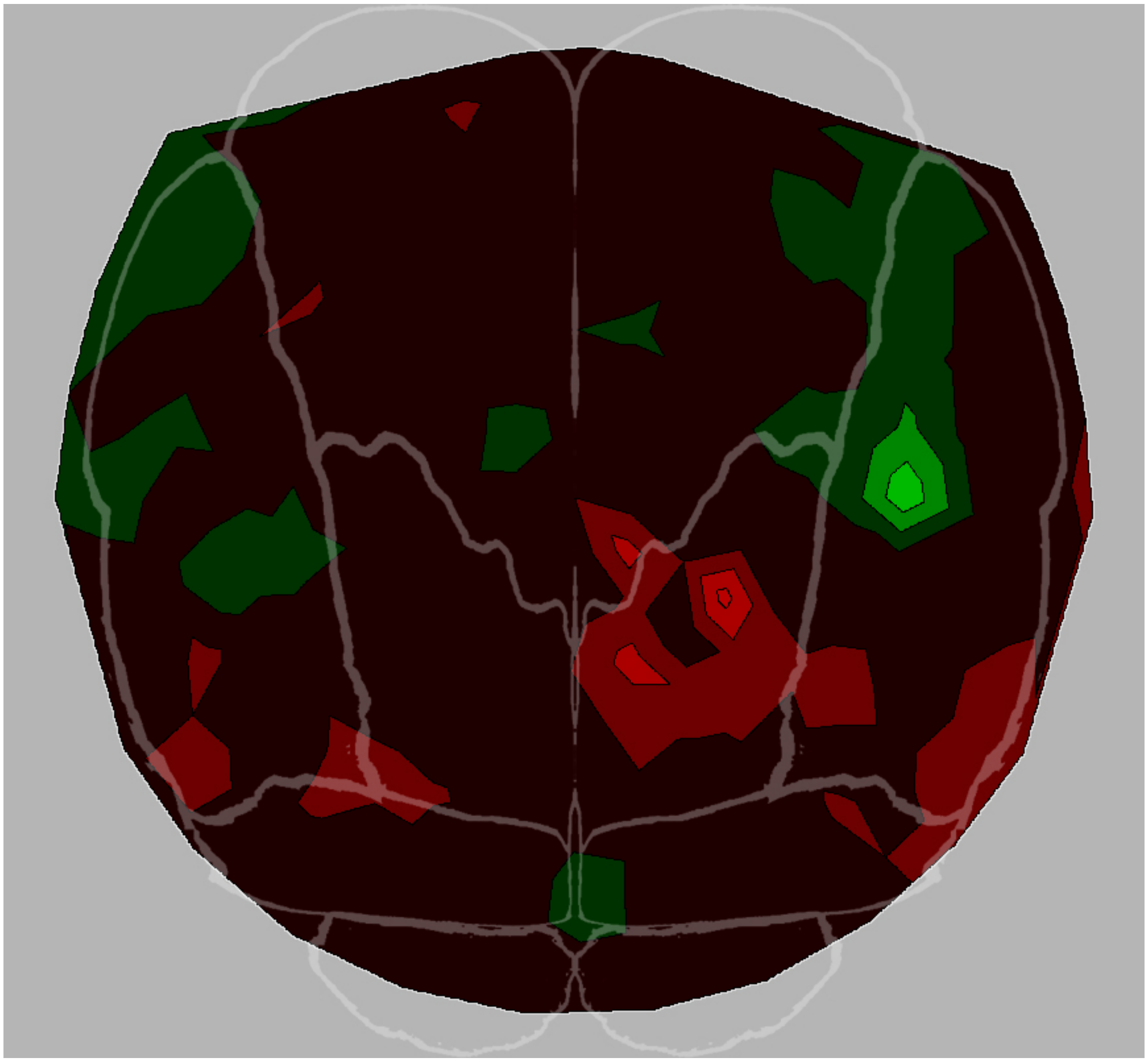

Figure 6-15. Neural-tonal map: Parncutt chroma salience profile. Regression coefficient (b) significance [-ln(p), $p < 0.05$] per sensor across all stimuli and subjects. Green = positive relations, red = negative. Bright colors indicate higher significance.

Tonal space #6: Chew spiral array model

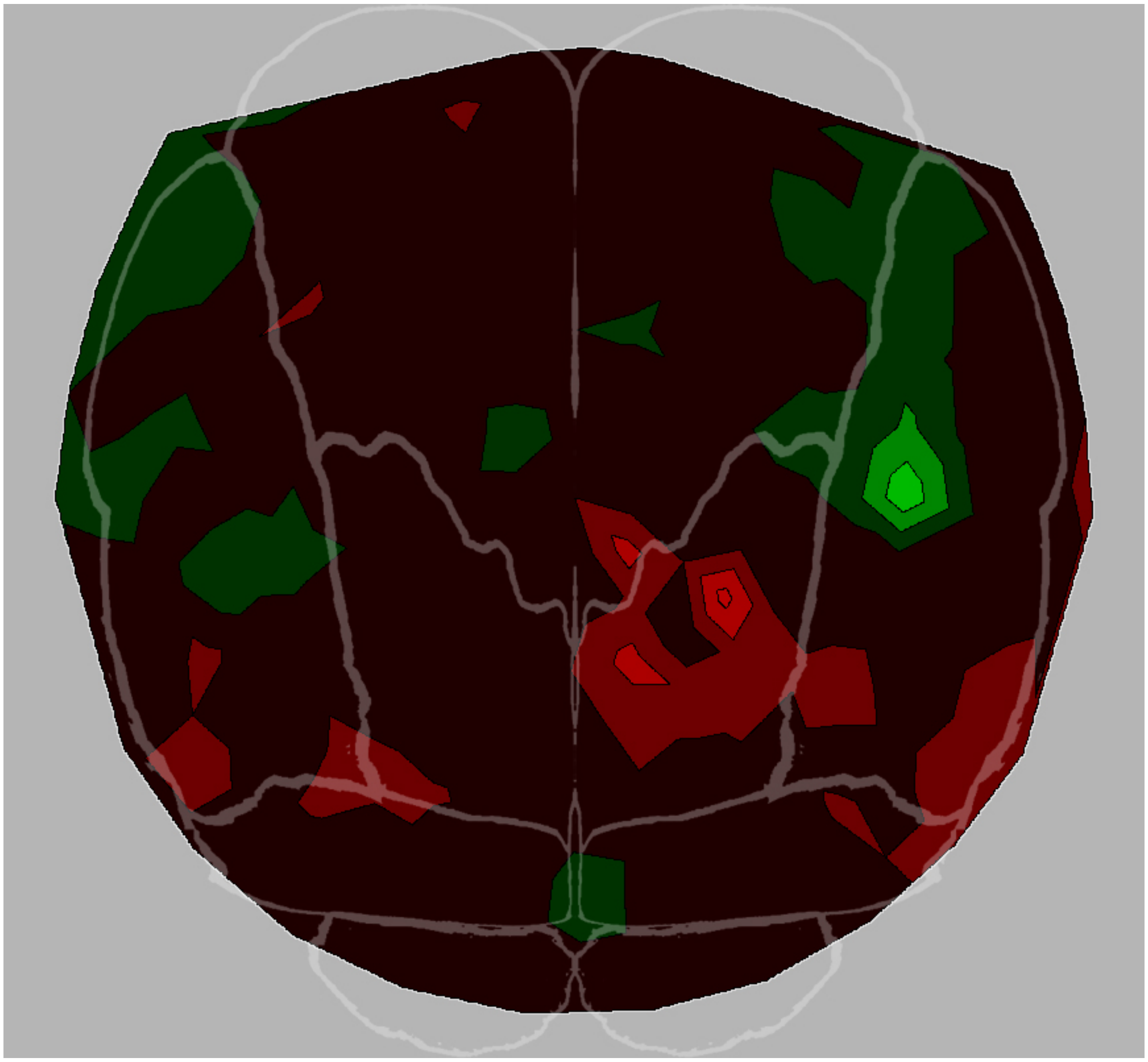

Figure 6-16. Neural-tonal map: Chew spiral array model. Regression coefficient (b) significance [-ln(p), $p < 0.05$] per sensor across all stimuli and subjects. Green = positive relations, red = negative. Bright colors indicate higher significance.